STUDIES OF PARAMETRIC EMISSIONS MONITORING AND DLN COMBUSTION NO_X FORMATION

by

RYAN A. KELLER

B.S., Kansas State University, 2002

A THESIS

submitted in partial fulfillment of the requirements for the degree

MASTER OF SCIENCE

Department of Mechanical and Nuclear Engineering
College of Engineering

KANSAS STATE UNIVERSITY
Manhattan, Kansas

2011

Approved by:

Major Professor
Kirby Chapman

Copyright

Abstract

The increased emissions monitoring requirements of industrial gas turbines have created a demand for less expensive emissions monitoring systems. Typically, emissions monitoring is performed with a Continuous Emissions Monitoring System (CEMS), which monitors emissions by direct sampling of the exhaust gas. An alternative to a CEMS is a system which predicts emissions using easily measured operating parameters. This system is referred to as a Parametric Emissions Monitoring System (PEMS). A review of the literature indicates there is no globally applicable PEMS. Because of this, a PEMS that is applicable to a variety of gas turbine manufacturers and models is desired.

The research presented herein includes a literature review of NO_x reduction techniques, NO_x production mechanisms, current PEMS research, and combustor modeling. Based on this preliminary research, a combustor model based on first-engineering principles was developed to describe the NO_x formation process and relate NO_x emissions to combustion turbine operating parameters. A review of available literature indicates that lean-premixed combustion is the most widely-used NO_x reduction design strategy, so the model is based on this type of combustion system. A review of the NO_x formation processes revealed four well-recognized NO_x formation mechanisms: the Zeldovich, prompt, nitrous oxide, and fuel-bound nitrogen mechanisms. In lean-premixed combustion, the Zeldovich and nitrous oxide mechanisms dominate the NO_x formation.

This research focuses on combustion modeling including the Zeldovich mechanism for NO_x formation. The combustor model is based on the Siemens SGT-200 combustion turbine and consists of a series of well-stirred reactors. Results show that the calculated NO_x is on the same order of magnitude, but less than the NO_x measured in field tests. These results are expected because the NO_x calculation was based only on the Zeldovich mechanism, and the literature shows that significant NO_x is formed through the nitrous oxide mechanism. The model also shows appropriate trends of NO_x with respect to various operating parameters including equivalence ratio, ambient temperature, humidity, and atmospheric pressure. Model refinements are suggested with the ultimate goal being integration of the model into a PEMS.

Table of Contents

List of Figures

List of Tables

Nomenclature

Variables

Symbol	Description	Units
[X]	Concentration of species X	$\mathrm{kmol/m^3}$
A	Area	$\mathrm{m^2}$
d	Diameter	m
f	Fuel-air ratio	none
ΔG°_{T}	Standard state Gibbs function change	kJ/kmol
$\overline{h}$	Specific molar enthalpy	kJ/kmol
$\overline{h}^{\circ}_{f}$	Enthalpy of formation	kJ/kmol
$\Delta\overline{h}_{s}$	Sensible enthalpy	kJ/kmol
h	Heat transfer coefficient	$\mathrm{W/m^2 \cdot K}$
h	Specific mass enthalpy	kJ/kg
k	Specific heat ratio	none
k_f	Forward kinetic rate coefficient	$\mathrm{m^3/kmol \cdot s}$
K_p	Equilibrium constant	none
l_b	Average beam length	m
LHV	Lower heating value	kJ/kg
$\dot{m}$	Mass flow rate	kg/s
MW	Molecular weight	kg/kmol
$\dot{n}_f$	Fuel molar flow rate	kmol/s
N	Number of moles	none

Nu_D	Nusselt number	none
p	Pressure	kPa
P	Perimeter	m
P°	Standard state pressure	kPa
PR	Compressor pressure ratio	none
q	Heat transfer rate	kJ/s
q''	Heat flux	$kJ/s \cdot m^2$
Re_D	Reynolds number	none
$\overline{R}$	Universal gas constant	$kJ/kmol \cdot K$
RH	Relative humidity	none
t	Thickness	m
T	Temperature	K
V	Volume	m^3
$\overline{V}$	Average velocity	m/s

Greek Symbols

ε	Emissivity	none
η	Efficiency	none
ϕ	Equivalence ratio	none
σ	Stefan-Boltzmann constant	$W/m^2 \cdot K^4$
τ	Residence time	s
μ	Dynamic viscosity	$kg/m \cdot s$

Subscripts

a	Air
act	Actual
atm	Atmospheric
c	Cooling air
comba	Combustion air
combp	Combustion products
comp	Compressor
conv	Convective
coola,e	Cooling air exit
e	Exit
f	Fuel
g	Gas
h	Hydraulic
i	Inlet
p	Products
r	Reactants
rad	Radiative
s	Isentropic
sat	Saturated
stoi	Stoichiometric
turb	Turbine

tot	Total
w	Wall
xs	Cross-section

CHAPTER 1 - Introduction

Oxides of Nitrogen (NO_x), including nitrogen monoxide (NO) and nitrogen dioxide (NO_2), have long been identified as harmful atmospheric pollutants. These compounds, which are formed during the combustion of fossil fuels, are detrimental to the atmosphere in numerous ways, including:

- Environmental acidification – NO_x mixes with rain water and acidifies it, creating nitric acid (HNO_3). This acid rain can kill vegetation and fish as it falls onto plants and into streams. In addition, acid rain accelerates the decay of man-made outdoor structures such as buildings and statues. (Environmental Protection Agency, 2011)
- Stratospheric ozone depletion – NO_x reacts with ozone and free oxygen in the atmosphere to destroy upper-level ozone, which is an ultraviolet light-blocking compound. This chemical mechanism is depicted in Figure 1.1.

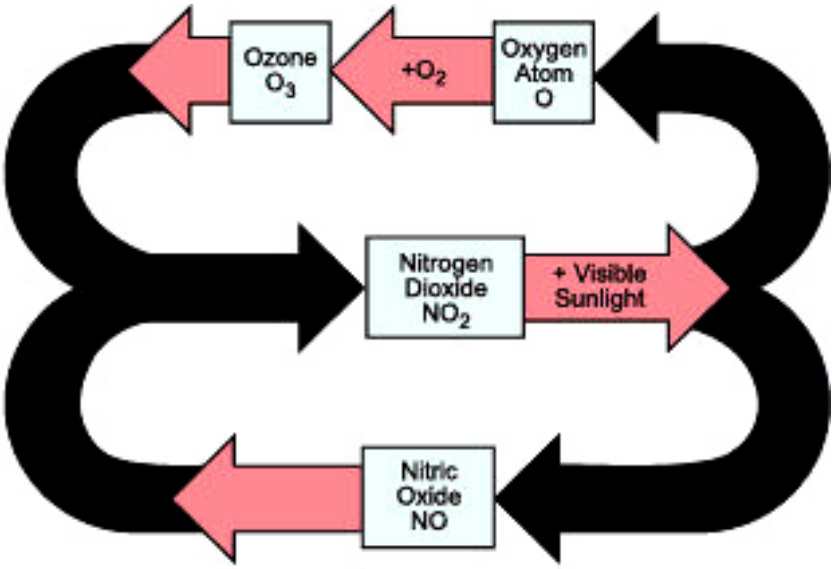

Figure 1.1 NO_x Ozone Depletion Chemical Mechanism (National Institute of Environmental Health Sciences, 2011)

- Respiratory problems - NO_x is harmful to the respiratory system in three ways. Firstly, it can react with ammonia, moisture, and other compounds to form small particles. These small particles can get into the lungs and create or worsen respiratory complications

including airway inflammation in healthy people or increased symptoms in people with asthma, emphysema, and bronchitis. Secondly, NO_x reacts with atmospheric oxygen to produce ground level ozone that contributes to respiratory problems through the oxidation of lung tissue. Thirdly, NO_2 itself has been deemed toxic from indoor exposure studies (Environmental Protection Agency, 2011).

Because of these harmful effects, various government agencies place restrictions on NO_x emissions. These restrictions are enforced through the Clean Air Act Amendments (CAAA) of 1990, which established upper-limit standards for a number of atmospheric pollutants, including NO_x. In order to prove compliance with these standards, combustion turbine operators must implement continuous NO_x monitoring (Hung, 1995). The restriction on NO_x emissions has led to combustion turbine technology enhancements for NO_x control, while the associated requirement for continuous monitoring has lead to the demand for less expensive, more efficient emissions monitoring technologies.

Monitoring NO_x from gas turbines is typically done with a complex and costly Continuous Emissions Monitoring System (CEMS). This system monitors NO_x and other emissions through direct sampling of the exhaust gas. In addition to the initial cost of a CEMS, there are significant annual costs for calibration and maintenance. The typical interior of a CEMS cabinet is shown in Figure 1.2.

Figure 1.2 Typical CEMS Configuration (AirNova, 2011)

A less expensive and thus more desirable approach is to calculate NO_x using easily measured parameters. These parameters can include ambient conditions, combustion pressure, fuel-air ratio, and gas-generator turbine exit temperature. A package consisting of the appropriate sensors, hardware, and incorporated algorithms used to calculate emissions is referred to as a Parametric Emissions Monitoring System (PEMS). A PEMS is less complex, does not require periodic calibration using costly calibration gases, and can be incorporated into existing gas turbine monitoring systems which already measure most of the appropriate parameters. Significant work has been done to develop a PEMS. However, a review of the literature indicates that the PEMS previously developed are primarily statistical based and specific to particular combustion turbine models. PEMS which are more broadly applicable do not exist.

The goal of the present research was to develop a combustion turbine model which could be used to generate correlations between NO_x and appropriate operating parameters. Such a model could be applied to develop a broadly-applicable PEMS for use on a wide range of gas turbine models from multiple manufacturers. The combustor modeling techniques were based on first-engineering principles, with model inputs from a gas turbine manufacturer. The model was validated by comparing its outputs to gathered field data including gas turbine operating

parameters and NO_x emissions. The development of this model required a detailed understanding of NO_x formation and gas turbine combustion processes.

A thorough literature review was performed to gain an understanding of PEMS technology, NO_x reduction techniques, NO_x formation processes, and combustor modeling techniques. This knowledge base was necessary to establish the necessity of this research and to develop an appropriate path forward for the combustor modeling. This thesis will present a description of the work done including a description of the combustor model, a presentation of the model capabilities, and suggestions for future refinements.

CHAPTER 2 - Literature Review

The primary goal of the present research is to develop a combustor model based on first-engineering principles for calculating NO_x emissions based on combustion turbine operating parameters. This type of model could ultimately be used in a PEMS. To begin this journey, an investigation of the available literature was performed to review the current PEMS technology and to develop an appropriate path for the combustor modeling.

Current PEMS Technology

The literature review of current PEMS technologies revealed a significant amount of work that has been done to develop gas-turbine PEMS. The bulk of this work was done by W.S.Y. Hung for Solar. The previously developed PEMS were primarily based on statistical analysis of CEMS data, not fundamental engineering principles.

PEMS Development by W.S.Y. Hung

Most of the work published on NO_x prediction technology is by W.S.Y. Hung. In 1975, he first published a description of an analytical model used to determine NO_x emissions for a specific family of conventional gas turbine combustors (Hung, 1975). Shortly after, he published a description of modifications made to the model to include the effects of water injection, operation at reduced air/fuel ratio, primary air leaning, fuel with low flame temperatures, and fuel/air premixing (Hung, 1975). Because the main feature of this model was the way in which the diffusion process was modeled, it was later referred to as the diffusion-limited mixing model. The model showed good agreement with laboratory and field data, but at that time it was only used as a design tool for NO_x reduction in combustors.

Beginning in 1991, Hung published work on a PEMS in which the diffusion-limited mixing model was referenced, but not directly used (Hung, 1991). Instead, the PEMS was based on a performance and emissions program that was developed for various gas turbine models using field data on NO_x emissions. The program was basically developed by gathering NO_x data, correcting it to ISO (e.g. 20°F, 14.73 psia) conditions (using either EPA correlations or special expressions developed by Hung), and establishing the ISO corrected NO_x as functions of fuel/air ratio and water/fuel ratio (if applicable) (Hung, 1995). User inputs of fuel type, duct

losses, elevation, combustion system, humidity, and water injection schedule are used to calculate the ISO corrected NO_x as a function of ambient temperature and either power turbine inlet temperature (T_5) or gas producer speed. These two functions are stored in the PEMS and used to calculate NO_x based on inputs of those two parameters from the gas turbine control system. The calculated NO_x is corrected to ambient pressure and humidity using the same correlations used in the development of the performance and emissions program. The diffusion-limited mixing model was used to verify the performance and emissions program, but no results of this verification were provided (Hung, 1995).

At the end of 1994, Hung reported that 36 PEMS were installed on various Solar gas turbines using conventional combustion, water injection, and "SoLoNO$_x$" (Solar's version of lean-premixed) combustion. The relative accuracy ranged from about 2 to 12% when compared to CEMS measurements (Hung, 1995). However, because of problems with the correlations, the end-users removed most, if not all, of these PEMS.

Other PEMS Development

A paper on PEMS development was published by Marshall and Bautista (1997). The goal of their project was to develop CO and NO_x emission algorithms for small (<20 MW) stationary gas turbines used in natural gas pipeline compression stations. The general forms of the NO_x and CO predictive algorithms were said to be based on first engineering principles, but the forms of these algorithms were said to be proprietary and no details of how these algorithms were developed were described in the paper. The coefficients for these algorithms were determined based on regression analysis of data gathered with a CEMS.

The analysis was completed on data from GE Frame 3 and Rolls Royce Avon turbines so that the technique employed could be validated on engines representing old (Frame 3) and recent (Avon) technologies. The data was taken over a wide range of operating conditions and divided into a development subset and a validation subset. The coefficients and applicable operating parameters for the predictive algorithms were determined by using regression analysis on the development subset. The algorithms used parameters such as humidity, ambient temperature, exhaust gas temperature, and gas generator speed, which are all routinely monitored for process control. These applicable operating parameters were then used from the development subset to

generate NO_x and CO data to be compared to the validation subset. Relative accuracy for the NO_x data varied between 3 and 5%.

While the results of this work are promising, neither additional publications referencing the continued development of this technique, nor publications describing the application of these algorithms to a field-installed PEMS could be found.

A pure statistical based PEMS was developed by CMC Solutions and the result of their work was published in 2003. Their PEMS uses historical CEMS data to generate predicted emission rates. The PEMS was installed on two GE Frame 7 gas turbines which are operated in a power plant. One of the turbines was a peaking unit burning natural gas and utilizing a DLN (dry low-NO_x) combustor, while the other was a base-load unit firing natural gas and/or fuel oil and utilizing steam injection for NO_x reduction. The PEMS algorithm was generated using an initial 40 or 60 hours of data gathered by a CEMS. Details of the algorithm development were not provided. The final PEMS algorithm was based on an additional 720 hours of data that was gathered during the demonstration period. This type of PEMS differs from the work presented in this report in that the models are not based on the fundamental physical processes controlling NO_x production.

In addition to the direct PEMS development, a number of semi-analytical expressions have been developed to determine NO_x emissions from gas turbines. In 1981, Lewis published the following expression for NO_x prediction from experimental flame data published by NASA:

$$NO_x = 7.50 \times 10^{-6} e^{8.28 \times 10^{-3} T} \quad (1)$$

This expression is a function of only flame temperature, but there are accompanying expressions for correcting this temperature based on humidity, fuel type, power, and water injection. Lewis notes that these correlations are only useful as a design tool (Lewis, 1981).

In 1994, Becker and Perkavec published a summary of four equations for NO_x emission prediction. All of these equations make use of a different set of parameters and constants that were found by fitting curves to experimental or field data. The parameters include fuel/air ratio (or equivalence ratio), combustion pressure, combustion temperature, humidity, and air mass flow rate. The authors state that the four equations are limited to the gas turbine model, operating conditions, and type of fuel used at the time of the equation development. Because of these limitations, a new semi-analytical equation was developed with a minimum number of constants that need to be determined for each combustor and environment it is applicable to. The

expression is semi-analytical because it is based on a combustor energy balance used to calculate the flame temperature, but the dependence on NO_x is still found by statistically analyzing the test data. The published comparison between the expression and experimental data is very good for some combustors and fuels, while not so good for others. Although it was concluded that the developed expression is effective, there are no published results of an actual PEMS installation using the correlation.

A similar paper was published in 1995 by Bakken and Skogly. Two previously developed correlations are presented, along with the following new correlation:

$$NO_x = 62 p_3^{0.5} f^{1.4} \exp\left(-635/T_4\right) \tag{2}$$

In this equation, T_4 is the combustor discharge temperature, f is the fuel-air ratio, and p_3 is the compressor discharge pressure. The new correlation was developed to include the effects of component degradation. Based on their statistical analysis, the effects of component degradation can be captured by measuring only the compressor discharge pressure, fuel/air ratio, and combustor discharge temperature. The correlation presented was implemented in the condition monitoring system of a Sleipner A installation, but the results of this effort were never published.

NO_x Reduction Techniques

There are many widely-differing techniques for NO_x reduction, all of which employ various types of combustion. Because the combustor designs involved with these various types of combustion vary greatly, the literature was reviewed to select the most common technique to be employed in the combustor model used in the present research.

A conventional combustion turbine combustor burns fuel using a diffusion flame. In this type of flame, the pure fuel and pure air combust stoichiometrically through the flame boundary. Stoichiometric combustion creates the highest peak combustion temperatures. Because NO_x emissions increase exponentially with temperature, stoichiometric combustion also produces the highest concentrations of NO_x (Lewis, 1981). The primary method for NO_x reduction in gas turbines is to reduce peak temperatures within the combustor. Gas turbine manufacturers have developed a number of methods for doing this. The primary methods are water injection, rich burn – quick quench – lean burn (RQL) combustion, catalytic combustion, and lean-premixed combustion. Additional methods, selective catalytic combustion (SCR) and selective non-

catalytic reduction (SNCR), use chemical reactions in the post-turbine exhaust gas to convert the NO_x into less-harmful compounds.

Water Injection

The concept behind water injection is simple: Liquid water or steam is injected into the combustor to act as a heat sink, drawing heat away from the hottest combustion products to lower their temperature and mitigate NO_x formation. This procedure is very effective, offering NO_x reductions up to 60 percent in natural gas burning combustors (Hilt, 1984). However, water injection has significant drawbacks. There are increased capital costs from the water injection equipment which usually includes a water treatment facility to produce the required demineralized water. The operating costs can also increase due to the additional fuel consumption necessary to heat the water to combustion temperatures, the water treatment maintenance requirements, and the additional combustion turbine maintenance requirements due to the accelerated combustor corrosion. Water injection has also been shown to increase CO (carbon monoxide) emissions, UHC (unburned hydrocarbon) emissions, and combustion pressure pulsations (Lefebvre, 1999).

Rich Burn – Quick Quench – Lean Burn (RQL) Combustion

RQL combustors rely on the principal that combustion temperatures, and therefore NO_x production, are lower at rich and lean conditions than at stoichiometric conditions. Combustion begins in a fuel-rich primary zone followed by quenching with dilution air and further burning in a lean zone. The effectiveness of this complex process is limited by the rate at which the dilution air can quench the rich combustion products (Correa, 1991). During the transition from rich to lean combustion, the complete avoidance of brief stoichiometric conditions, and therefore high NO_x production rates, is not possible.

Catalytic Combustion

Catalytic combustion employs various catalysts inside the combustion chamber to allow the fuel to be oxidized at temperatures and equivalence ratios below the normal lean flammability limit of the fuel-air mixture. Combustion at such low temperatures dramatically reduces NO_x emissions. However, the temperatures are still high enough to approach the stability limits of most catalyst substrate materials. This shortens the catalyst life and makes the

combustor unreliable. The effectiveness of the system (NO_x concentrations <5 ppm) provides incentive for researchers to overcome the durability issues of the catalytic combustor, but it has yet to become widely-used technology (Lefebvre, 1999).

Lean-Premixed Combustion

In a conventional diffusion-flame combustor, the hot combustion products are diluted and cooled to meet the material-limited temperature requirements of the compressor-drive turbine inlet temperature. The dilution is accomplished using excess air from the gas turbine compressor. In lean-premixed combustion, the excess air available for dilution is instead used to premix the air and fuel at a low equivalence ratio (fuel-lean) prior to combustion. This lean mixture burns at a lower temperature, thus reducing NO_x emissions. Because the theoretical cycle efficiency depends only on the compressor-drive turbine inlet temperature, the point of dilution with excess air should not affect efficiency when compared to an equivalent diffusion-flame combustor.

NO_x emission levels below 10 ppm have been demonstrated with lean-premixed combustion (Correa, 1991). Gas turbines using this type of combustion have difficulty operating at partial loads, but this is often overcome by operating the combustor in a diffusion flame mode during these periods, thus creating a high temperature – high NO_x environment. Since partial loads in industrial gas turbines are typically only experienced during startups and transients, lean-premixed combustion is overall a highly effective NO_x reduction strategy.

The concept of lean-premixed combustion (also called dry low-NO_x combustion because low NO_x is achieved without water injection), is used in some form by nearly every gas turbine manufacturer (Lefebvre, 1999). It is currently the most widely-used combustor design method for reducing NO_x emissions from gas turbines.

Selective Catalytic Reduction (SCR) and Selective Non-Catalytic Reduction (SNCR)

In the SCR and SNCR technologies, NO_x is converted to nitrogen and water by injecting a nitrogen-containing additive (usually ammonia) into the exhaust gas. The SCR system uses a catalyst to aid the reaction, while SNCR does not. The process is effective over a limited temperature range, so it is restricted to gas turbines that exhaust to a heat recovery device. The catalytic process has been shown to reduce NO_x emissions to concentrations below 10 ppm when

combined with water injection. Major drawbacks of SCR and SNCR are the size and cost of the equipment, the performance degradation associated with the additional turbine exhaust pressure losses from the catalyst, and the complex control system with continuous monitoring required to adjust the ammonia flow based on load as excess unreacted ammonia which passes to the atmosphere is undesirable. In large-scale applications such as combined-cycle power plants, the effectiveness of these systems typically outweighs the drawbacks, making them viable NO_x reduction methods. However, for smaller gas turbine applications with no heat recovery device, other methods are typically used.

NO_x Formation Processes

"NO_x" refers to the sum of NO (nitric oxide) and NO_2 (nitrogen dioxide). The formation of NO_2 results only from the subsequent oxidation of NO, so the total NO_x (NO + NO_2) is not affected by the amount of NO_2 formed (Turns, 2000). Therefore, the calculation of NO is sufficient for determining total NO_x and the literature review of NO_x formation processes focused only on NO formation.

There are four well-recognized chemical mechanisms for NO formation. These include the Zeldovich, prompt, nitrous oxide, and fuel-bound nitrogen mechanism. The following sections provide a description of these four NO-producing chemical pathways.

Zeldovich Mechanism

The Zeldovich Mechanism produces NO by the reaction of atmospheric oxygen and nitrogen at elevated temperatures. The mechanism consists of two chain reactions:

$$O + N_2 \rightleftharpoons NO + N \tag{3}$$

$$N + O_2 \rightleftharpoons NO + O \tag{4}$$

These reactions can be further extended by adding the reaction:

$$N + OH \rightleftharpoons NO + H \tag{5}$$

This three-reaction set is known as the Extended Zeldovich Mechanism. The NO formed through the Zeldovich mechanism is commonly referred to as thermal NO because the formation rates are only significant at high temperatures (~1800+ K). This set of reactions is a widely-used and recognized mechanism for NO formation (Turns, 2000).

Prompt Mechanism

The prompt, or Fenimore mechanism, was first proposed by Fenimore in 1971 to account for NO formation that occurred very quickly in the primary reaction zone of the combustor (Fenimore, 1971). It was later found that the NO is formed from the reaction of hydrocarbon radicals present during the combustion process reacting with atmospheric nitrogen (Nicol, 1995). The primary initiating reaction is:

$$N_2 + CH \rightleftarrows HCN + N \tag{6}$$

The N atom becomes NO through the last two reactions in the Zeldovich mechanism. The HCN route to NO is complex, but the main path is through NCO, NH, N, and then finally to NO through the same Zeldovich N atom reactions.

Nitrous Oxide Mechanism

The nitrous oxide (N_2O) mechanism was recognized by Malte and Pratt in 1974 as an important NO pathway (Corr, 1991). It is regarded as being most important in fuel-lean ($\phi <$ 0.8), low-temperature conditions, such as those experienced in lean-premixed combustion (Turns, 2000). The three main steps of this mechanism are:

$$O + N_2 + M \rightleftarrows N_2O + M \tag{7}$$

$$H + N_2O \rightleftarrows NO + NH \tag{8}$$

$$O + N_2O \rightleftarrows NO + NO \tag{9}$$

Fuel-Bound Nitrogen Mechanism

Combustors burning fuel which contains nitrogen show an increase in NO production (Toof, 1985). This increase in NO results from the conversion of the organically-bound nitrogen in the fuel to NO. The mechanism begins with the pyrolysis of the nitrogen containing fuel to HCN. The HCN then follows the same pathway to NO as the prompt mechanism. Because of this, the fuel and prompt NO are considered linked processes (Toof, 1985). This mechanism is obviously unimportant in fuels containing no nitrogen, such as natural gas, but contributes significantly when burning nitrogen containing fuels such as coal. Because the present research

focuses on gas turbine combustion with fuels containing negligible nitrogen, this mechanism is not further considered.

Relative Contributions of Each Mechanism

There are several publications by various authors that analyze the relative contribution of each NO_x mechanism for different fuels, conditions, and combustion types. Many of these studies involve the analysis of lean-premixed combustion because of its popularity as a NO_x reduction strategy.

Correa and Smooke (1990) performed a number of experiments and numerical simulations to determine the relative contributions of the thermal, nitrous oxide, and prompt NO mechanisms. An early study used experimental NO_x data taken from turbulent, premixed methane-air flames using a perforated-plate burner and compared this data to results from a numerical modeling study which used a well-stirred reactor (WSR) followed by a plug flow reactor (PFR) combined with a kinetic scheme including the Zeldovich and prompt mechanisms. The results of the study showed that the prompt mechanism dominates below a flame temperature of about 1800K (Leonard, 1990). The study also concluded that NO varies as the square-root of pressure in near-stoichiometric premixed flames, but is independent of pressure in flames below an equivalence ratio of about 0.75. Another pure numerical study was performed for premixed laminar methane-air flames under various conditions (Correa, 1990). This study used the Miller-Bowman mechanism for methane combustion and NO formation, which includes the Zeldovich, prompt, and now also the nitrous oxide NO mechanisms (Miller, 1989). The study also concluded that thermal NO_x dominated in the near-stoichiometric flames, but that the nitrous oxide mechanism is predominant in lean-premixed, laminar flames. The absence of pressure dependence in very lean flames was also confirmed.

Corr et al. (1991) presented results from experiments conducted at the University of Washington using a jet-stirred reactor operating at atmospheric pressure that was fired with ethylene and methane using premixed and non-premixed flames. Both NO and NO_2 were measured, and the contribution of each mechanism was deduced from the calculated free radical concentration that would be required to produce the measured NO_x. Both the Zeldovich and nitrous oxide mechanisms rely on the O atom radical for initiation of the reactions, while the prompt mechanism requires the CH radical. The study concluded that unreasonable O atom

concentrations would be necessary for the NO_x to be formed by either the Zeldovich or nitrous oxide mechanisms, but that the CH concentrations were reasonable based on an accompanying numerical study which used select reactions from the Miller-Bowman mechanism. Because of these findings, it was concluded that the prompt NO mechanism was dominant (Corr, 1991).

Later work done by Nicol et al. (1995), also at the University of Washington, indicates that the nitrous oxide and Zeldovich mechanisms are equally important in high-pressure lean-premixed methane combustion, while the prompt mechanism is practically negligible. Modeling was performed using a WSR to represent the flame zone and a PFR for the post-flame zone. Three different kinetic mechanisms were used, including the previously mentioned Miller-Bowman scheme, and all showed similar trends. The modeling efforts were verified from porous-plate burner experiments. The result also indicates that for temperatures, pressures, and equivalence ratios capable of producing NO less than 10 ppmv, the relative contribution of the nitrous oxide mechanism increases steeply and approaches 100 percent. However, for atmospheric combustion, all three pathways contribute similar amounts, and none can be dismissed.

These conclusions differ from the earlier ones of Corr et al. (1991) which determined that the prompt mechanism was most dominant. The discrepancy was likely because the Corr study used only select reactions from the Miller-Bowman mechanism which caused the scheme to neglect the super-equilibrium concentration possibilities for the O and OH atoms. These super-equilibrium concentrations can exist at up to 1000 times the equilibrium concentrations in flame regions, and this high concentration possibility could perhaps accommodate the high O atom requirement calculated in their study to produce the measured NO_x from the Zeldovich or nitrous oxide mechanisms. This type of NO formation is sometimes linked to the prompt mechanism because it takes place early in the flame front, but the pathway is still that of the Zeldovich mechanism (Turns, 2000).

Conclusion of Literature Review

Based on this review of the current PEMS technology it is clear that the objective of the present research is warranted. There have been sporadic PEMS developments but none have become accepted in the gas turbine industry. Industry feedback indicates that the few PEMS predictive algorithms developed are not reliable. The premise for the research presented herein

is that the failure of the existing algorithms is because they were developed primarily using statistical CEMS and operating data, not fundamental principles. The fundamental-principle based correlations should be more reliable as they would account for unforeseen variations in operating parameters and/or turbine degradation that could not be captured during the relatively brief operating periods when the statistical-based PEMS correlations were developed.

Based on the literature review of NO_x reduction techniques, lean-premixed combustion is the most widely used combustor-based technology. Because of this, the combustion model developed as part of this research was based on lean-premixed combustion. Although selective catalytic reduction is also used, it is applied external to the combustion process making it irrelevant to this research.

The conclusion drawn from the review of the studies to determine the relative contributions of the NO_x chemical mechanisms is that the Zeldovich and nitrous oxide mechanisms are the most important for lean-premixed combustion at gas turbine operating conditions, while the prompt mechanism makes insignificant contributions. These results are largely based on combustor modeling using the most accepted chemical kinetic mechanisms available. In addition, the most accurate method for NO calculation should use a complete kinetic scheme that models both the combustion process and nitric oxide formation. The lean-premixed combustor model selected will employ the Zeldovich mechanism for NO prediction. The remainder of this thesis focuses on the development of a combustor model, the validation of this model using field test data, and parametric studies of data generated from the model.

CHAPTER 3 - Combustor Model Development

Based on the literature review of NO_x reduction technology and NO formation processes, the combustor process modeled was lean-premixed combustion with NO formation modeled by the extended Zeldovich mechanism. This chapter focuses on describing the detailed design of the combustor model including all engineering principles used.

Combustor Model Arrangements

The previously discussed study by Nicol et al. (1995) at the University of Washington described modeling combustion with a WSR for flame stabilization, followed by a PFR. A WSR (well-stirred reactor, sometimes called PSR or perfectly stirred reactor) is a one-dimensional control volume in which perfect instantaneous mixing of all species is assumed. The control volume is also assumed to have uniform temperature and pressure, and the gaseous species are assumed to behave as ideal gases. A PFR (plug-flow reactor) represents an ideal reactor in steady-state, with steady-flow. It is also assumed that there is no mixing in the axial (or flow) direction, and that the mixture properties are uniform in the radial direction. Ideal frictionless flow, and ideal gas behavior is also assumed.

The modeling method used by Nicol et al. is one of many potential ideal-reactor schemes for modeling an axial-flow combustor. Some other arrangements are shown in Figure 3.1.

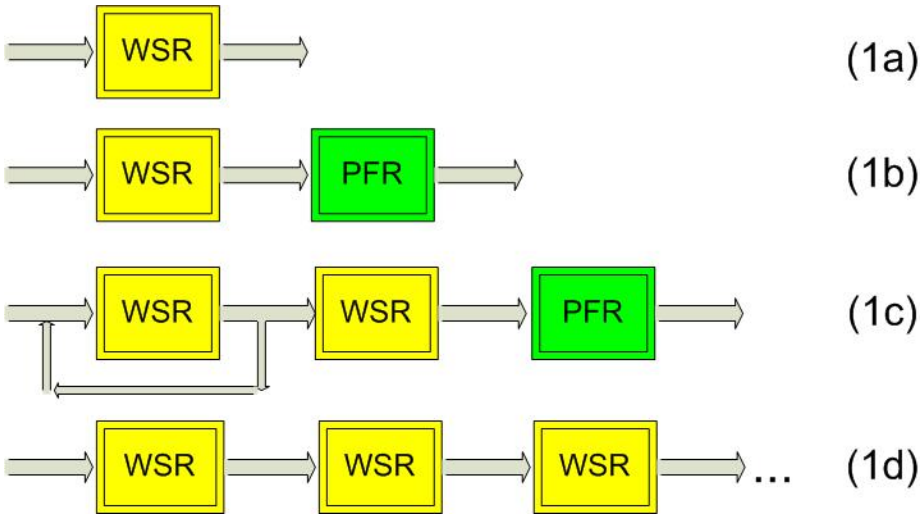

Figure 3.1 Ideal Reactor Arrangement Examples for Combustor Modeling

Arrangement 1a shows the simplest combustor model, which is a lone WSR. This model is very limited in that only one temperature, pressure, and species concentration can be calculated. Because of the temperature gradients, a single WSR is not conducive for representing the conditions of a real combustor. Arrangement 1b shows the combination of reactors that were previously mentioned, the WSR followed by a PFR. This combination better represents the actual combustion, in that combustion takes place in the WSR followed by a PFR for modeling the kinetics of the combustion products, which is where much of the NO is formed. A temperature profile to better match actual combustor conditions can be achieved with this arrangement, since a result of the PFR model is the distribution of temperature with respect to axial distance. An even better arrangement is shown in Arrangement 1c. This model has a second WSR to model the secondary combustion zone, and a recycle path on the first WSR to model the recirculation flow path that occurs in combustors for flame stabilization. The last possibility shown in Arrangement 1d is a series of WSR's. This arrangement is very flexible because the number, size, flow paths, and properties of the WSR's can be adjusted to fit various combustor types. More complex arrangements of parallel reactors are proposed by Rizk and Mongia (1993) to include radial effects within the combustion zone.

Description of Developed Combustor Model

The present research focuses on modeling the Siemens SGT-200 (formerly known as the Tornado DLE) gas-turbine combustor. This combustor uses a lean-premixed combustion system burning natural gas. Siemens refers to their lean-premixed combustion system as "dry-low emission" (DLE). The turbine is a single-shaft industrial gas turbine which uses twelve (12) of the DLE combustors in a can arrangement. The unit is capable of 7.7 MW of power when used as a mechanical drive (Siemens, 2011). Sketches of the SGT-200 and a typical combustor can arrangement are shown in is shown in Figure 3.2 and Figure 3.3.

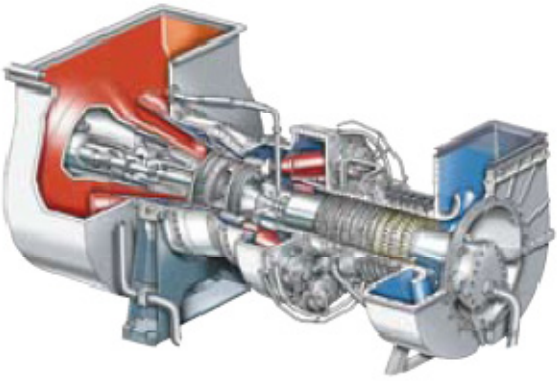

Figure 3.2 Siemens SGT-200 Industrial Gas Turbine (Siemens, 2011)

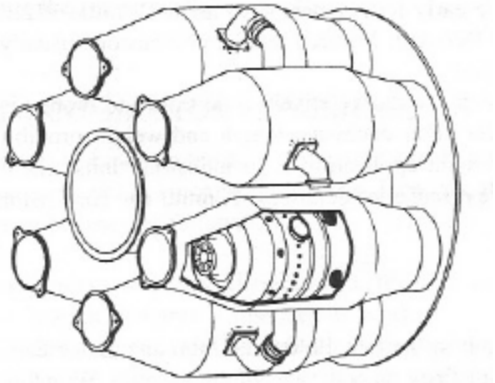

Figure 3.3 Combustion Turbine Combustors in Can Arrangement (Lefebvre, 1999)

Although the can arrangement consists of multiple combustors per engine, only one combustor was modeled in the program. This is acceptable for NO calculations, because each combustor can should produce the same emissions concentration. If an emissions mass flow calculation was performed then the calculated number would need to be multiplied by the number of combustor cans.

Figure 3.4 illustrates a model of a single can that is developed with a series of WSR's to represent the combustion zone. Outside and concentric to this is another series of WSR's that represent the combustion liner cooling air. The modeling is done with the aid of information from Siemens regarding the ratio of combustion air to cooling air, velocities through the

combustor, geometry of the combustor, and the combustor temperature profile. The series of WSR's method of combustor modeling was chosen for its previously mentioned flexibility and the ease of calculation when compared to PFR's. The additional capability of velocity calculation that is provided from a PFR calculation is not necessary since this information is already known. The solution of the mathematics representing the physics of the combustion process is accomplished using a developed FORTRAN program. A graphical representation of the model is shown in Figure 3.4.

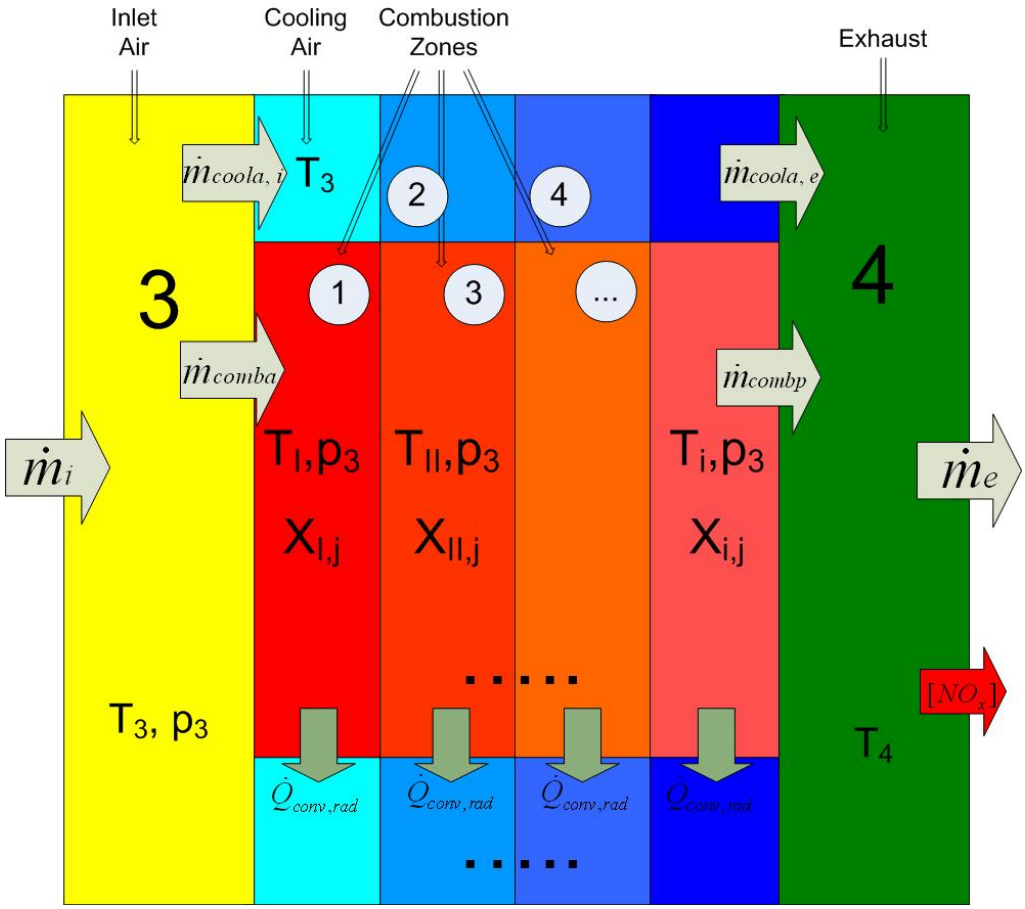

Figure 3.4 Combustor Model Diagram

Air/Fuel Chemistry Calculations

The turbine inlet air is assumed to be composed of oxygen, nitrogen, and water vapor. The amount of water vapor initially present is based on the user input of relative humidity. The fuel, which is pure methane, is allowed to partially react in each zone. This leads to the following stoichiometric chemical relationship for each combustion zone:

$$\begin{aligned} & z_r \mathrm{CH_4} + a\mathrm{O_2} + a_1\mathrm{N_2} + a_2\mathrm{H_2O} + a_3\mathrm{CO_2} \\ & \longrightarrow b\mathrm{CO_2} + c\mathrm{H_2O} + d\mathrm{N_2} + e\mathrm{O_2} + z_p\mathrm{CH_4} \end{aligned} \tag{10}$$

The coefficient z_r, which varies between 0 and 1, represents the fraction of the total amount of reactant fuel that is oxidized in the given zone. These fractions are an input to the combustor model for each region. The corresponding value of z_p is the remaining fuel fraction in the combustion zone products. The initial value of a is found from the equivalence ratio by:

$$a = \frac{MW_f}{4.76\phi f_{stoi} MW_a} \tag{11}$$

The initial a_1 is found from the known molar concentration of air by:

$$a_1 = 3.76a \tag{12}$$

Now a_2 is found using the ambient relative humidity and corresponding water vapor pressure:

$$a_2 = a\left\{1.608 \times \left(\frac{0.622 P_{sat} RH}{P_{atm}}\right)\right\} \tag{13}$$

The carbon dioxide coefficient, a_3, is initially zero. The coefficients z_r, a, a_2, and a_3 vary throughout the downstream combustor zones as the fuel and oxygen is consumed and converted to carbon dioxide and water. With z_p known from user input, the remaining product coefficients are found by balancing the C, O, H, and N atoms. The results of this are as follows:

$$b = z_r + a_3 - z_p \tag{14}$$

$$c = 2z_r + a_2 - 2z_p \tag{15}$$

$$d = a_1 \tag{16}$$

$$e = \frac{2a + a_2 + 2a_3 - 2b - c}{2} \tag{17}$$

Since all product coefficients are known, the mole fractions of all five product species (CO_2, H_2O, N_2, O_2, and CH_4) can be calculated for each zone. These values are used for later temperature and NO_x formation calculations. Finally, the products are carried over as reactants to the subsequent zone so the atom balancing and mole fraction determinations can be repeated until the values are known for all reactor zones.

Temperature and Pressure Calculations

Figure 3.5 represents the standard gas turbine numbering convention which will be used to designate conditions at the corresponding locations.

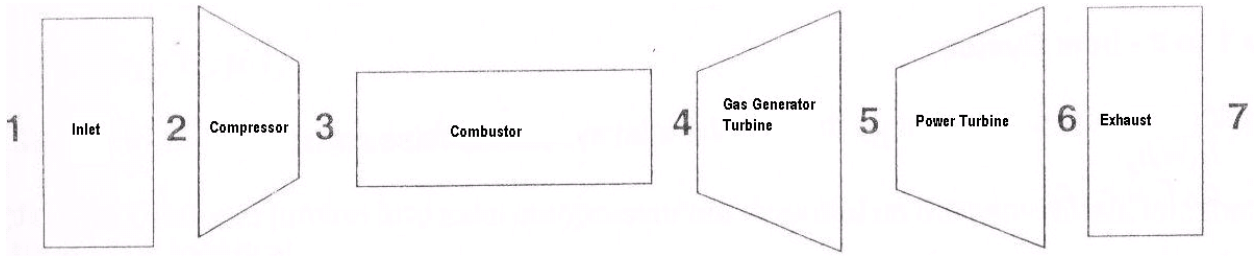

Figure 3.5 Gas Turbine Temperature Numbering Convention

Compressor Discharge

Region 3 represents the compressor discharge conditions. The pressure and temperature for region 3 are calculated based on the ambient conditions, compressor pressure ratio, and compressor isentropic efficiency. The compressor discharge pressure is given by:

$$p_3 = PR(p_2) \tag{18}$$

To calculate the compressor discharge temperature, the isentropic temperature T_{3s} is first calculated:

$$T_{3s} = T_2 \left(PR\right)^{k-1/k} \tag{19}$$

The actual temperature T_3 is determined from the isentropic efficiency relationship:

$$T_3 = \frac{T_{3s} - T_1}{\eta_{comp}} + T_1 \tag{20}$$

Combustor Discharge

The combustor is assumed to incur no pressure loss, so the combustor discharge pressure equals the compressor discharge pressure.

$$p_4 = p_3 \tag{21}$$

To determine the temperature of the combustor discharge, the temperatures of the combustion and cooling air zones must solved iteratively along the entire length of combustor. The temperatures of the combustion and cooling air zones are designated in Figure 3.4. To solve for these temperatures, an energy balance is applied to each zone. For each zone (cooling air or combustion), the energy balance is:

$$\frac{q_{conv,rad}}{\dot{n}_f} = \overline{h}_p - \overline{h}_r \tag{22}$$

In this equation, $q_{conv,rad}$ represents the heat transfer from the combustion zone as shown in Figure 3.4. The molar fuel flowrate is based on the fuel-air ratio and the mass flow rate of air. This term can be solved explicitly based on known parameters and is given by:

$$\dot{n}_f = \frac{\left(\frac{p_c MW_a}{R_u T}\right)\overline{V} A f_{act}}{MW_f} \tag{23}$$

The right hand side of equation (22) represents the energy entering and leaving a zone, while the left hand side represents the heat transfer to or from the zone. More specifically, the right hand side is the reactant (incoming) and product (exiting) specific molar enthalpies. For a cooling air zone, the reactant and product enthalpies simply represent the inlet and outlet conditions of a cooling air region, since there are no chemical reactions taking place. For a combustion zone, the absolute enthalpies of the incoming reactants and outgoing products are calculated from the enthalpy of formation and sensible enthalpy of each chemical species:

$$\overline{h} = \overline{h}_f^{\circ} + \Delta\overline{h}_s(T_i) \tag{24}$$

The sensible enthalpy is calculated by integrating the specific heat over the temperature range between the reference temperature, and the actual temperature:

$$\Delta\overline{h}_s(T_i) = \int_{T_{ref}}^{T_i} \overline{C}_p dT \tag{25}$$

The relationship for $\overline{C}_p$, from Moran and Shapiro (1999), is generically given as:

$$\overline{C}_p = \overline{R}(\alpha + \beta T + \gamma T^2 + \delta T^3 + \varepsilon T^4) \tag{26}$$

The values of the Greek constants are available for various chemical species.

Summing the absolute enthalpies for all products and reactants completes the right side of equation (22). However, as noted in equation (24), the enthalpy of formation is dependent on a known reference temperature, while the sensible enthalpy is a function of the species temperature. The reactant species temperature is assumed to be that of the preceding zone (or T_3 for the initial zones), while the product species temperature (which is also assumed to be the temperature of the current zone) is unknown. To solve for this unknown temperature, the heat transfer to and from the zone, which is also a function of the product species temperature, must be analyzed.

The heat transfer term on the left hand side of equation (22) designates the radiative and convective heat transfers from a combustion zone. This term can be broken down further as the separate radiative and convective fluxes multiplied by the segmental area over which the heat transfer takes place:

$$q_{conv,rad} = A\left(q_{conv}'' + q_{rad}''\right) \tag{27}$$

The area, *A*, is the area of the combustion chamber liner section for a given combustion zone. These areas are calculated based on the user-chosen segmentation of the overall combustor and the manufacturer-provided combustor diameter. Because the heat transfer from a combustion zone flows into a cooling air zone, the entire thermal resistance from the combustion zone, through the liner wall, and into the cooling air zone must be considered to get an accurate temperature for the combustion zone. In addition, heat transfer from the cooling air zone to the ambient is considered to ensure that the temperature of the cooling air zone remains accurate as the cooling air flows down the length of the combustor. The following sections will describe the analysis of these heat transfer modes through the combustor.

Heat Transfer from Combustion Gases to Cooling Air

Heat transfer from a combustion zone to a cooling air zone is modeled in three parts (see Figure 3.6):

1. Heat transfer from combustion products to combustor liner inner wall
    - Radiation ($q_{rad,1}$)
    - Convection ($q_{conv,1}$)
2. Heat transfer through liner wall ($q_{cond,12}$)
3. Heat transfer from combustion liner outer wall to cooling air
    - Radiation ($q_{rad,2}$)
    - Convection ($q_{conv,2}$)

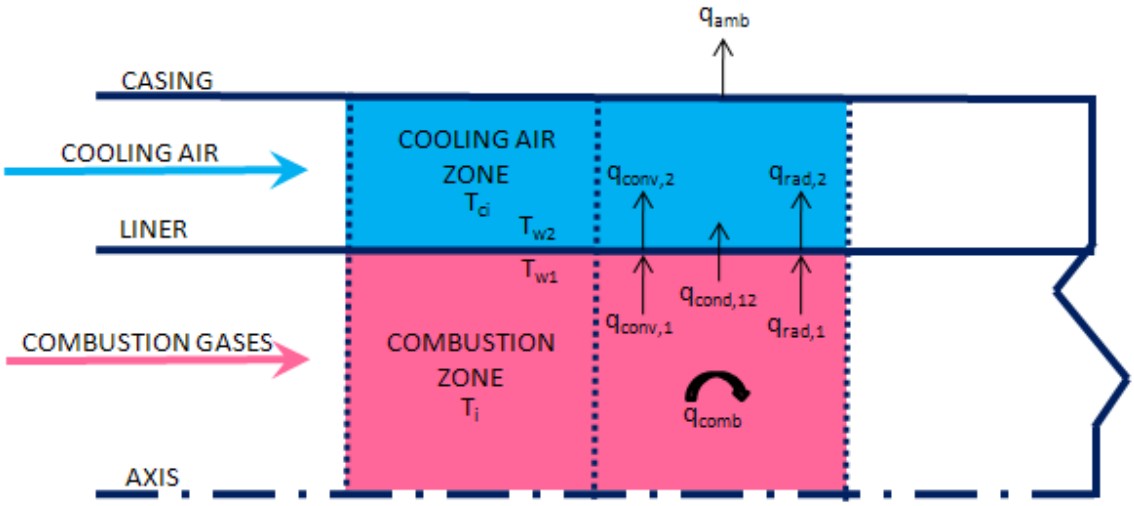

Figure 3.6 Combustor Heat Transfer Arrangement

Heat Transfer from Combustion Gases to Combustor Liner Inner Wall, Radiation

The radiation from the combustion products to the combustor liner wall is calculated using the method outlined in Lefebvre's *Gas Turbine Combustion* book, which considers the combustion products as non-luminous gases (Lefebvre, 1999). The radiative flux is calculated as:

$$q_{rad,1}'' = 0.5\sigma\left(1+\varepsilon_w\right)\varepsilon_g T_i^{1.5}\left(T_i^{2.5} - T_{w1}^{2.5}\right) \tag{28}$$

The parameter σ is the Stefan-Boltzman constant, ε_w is the emissivity of the wall, ε_g is the emissivity of the gas, T_i is the temperature of the gas in the zone being considered, and T_{w1} is the inner liner-wall temperature.

An expression for the emissivity of the gas is also provided:

$$\varepsilon_g = 1 - \exp\left[-290\, p\left(l_b f\right)^{0.5} T_i^{-1.5} L\right] \tag{29}$$

Where p is the gas pressure in kPa, l_b is the average beam length in meters, f is the fuel/air ratio by mass, and L is a unitless luminosity factor to account for the luminosity of the soot particles formed during hydrocarbon fuel combustion. Many different expressions exist for the luminosity factor, but Lefebvre recommends the following expression:

$$L = 336 / H^2 \tag{30}$$

In this expression, H is the percentage of hydrogen by mass in the fuel. Lastly, the average beam length for tubular systems is given by:

$$l_b = 3.4 \times V / A \tag{31}$$

Heat Transfer from Combustion Gases to Combustor Liner Wall, Convection

For the purposes of calculating the convective heat flux, the combustor liner is treated as a straight pipe. There are many expressions used to calculate convective heat transfer within a cylindrical pipe, but Lefebvre recommends the following expression, which is based on a turbulent Reynolds number:

$$q_{conv,1}'' = 0.020 \frac{k_g}{d_h^{0.2}} \left(\frac{\dot{m}_g}{A_L \mu_g}\right)^{0.8} \left(T_i - T_{w1}\right) \tag{32}$$

In this expression, $\dot{m}_g$ is the mass flow rate of the combustion gases, A_L is the cross-sectional area of the liner, k_g is the thermal conductivity of the combustion gases given by:

$$k = \frac{2.495 \times 10^{-3} T^{1.5}}{T + 194} \tag{33}$$

The dynamic viscosity of the gas, μ_g, in units of Pa-s, is given by:

$$\mu_g = 47.88\left\{2.27\times10^{-8}\left[\frac{1.8T^{1.5}}{1.8T+198.6}\right]\right\} \tag{34}$$

The temperature used in this equation is again in Kelvin. The final parameter, d_h, is the hydraulic diameter given by:

$$d_h = 4\frac{A_L}{P_{wetted}} \tag{35}$$

The constant in equation (32) is lowered from 0.020 to 0.017 in the first zone calculations to account for the gas flow reversal (to stabilize the flame) and the greatly reduced gas temperature near the liner wall.

Heat Transfer Through Liner Wall

Heat transfer through the liner wall is modeled as one-dimensional conduction and is given by:

$$q_{cond,12}'' = \frac{k_w}{t_w}(T_{w1} - T_{w2}) \tag{36}$$

The thermal conductivity of the liner wall material is given by k_w with t_w as the wall thickness.

Heat Transfer from Combustion Liner Outer Wall to Cooling Air, Radiation

The heat transfer from the combustion liner outer wall to the cooling air can be expressed as:

$$q_{rad,2}'' = 0.6\sigma({T_{w2}}^4 - {T_{ci}}^4) \tag{37}$$

Here, T_{ci} is the cooling air zone temperature. This equation assumes the following:

- Cooling air temperature equals temperature of outer casing.
- Radiative shape factor equal to unity.
- Ratio of liner wall area to casing surface area equals 0.8.

Heat Transfer from Combustion Liner Outer Wall to Cooling Air, Convection

Convection between the hot liner outer wall and the cooling air in the annulus air space between the liner and the casing is modeled assuming fully turbulent flow. The equation is:

$$q_{conv,2}'' = 0.020 \frac{k_c}{d_h^{0.2}} \left(\frac{\dot{m}_c}{A_L \mu_c} \right)^{0.8} \left(T_{ci} - T_{w2} \right) \tag{38}$$

Overall Heat Transfer

All parameters in the energy balance, equation (22), are known except for T_i and $\bar{h}_p$, which is a function of T_i, T_{ci}, T_{w1}, and T_{w2}. Rewriting equation (22) to show the temperature dependencies gives:

$$\frac{q_{conv,rad}\left(T_i, T_{ci}, T_{w1}, T_{w2}\right)}{\dot{n}_f} = \bar{h}_p\left(T_i\right) - \bar{h}_r \tag{39}$$

Equation (39) represents the four unknowns in a specific zone, while Table 3.1 outlines these unknowns and the sets of equations solved to calculate them.

Table 3.1 Combustor Model Unknowns and Equations

UNKNOWNS	PRIMARY EQUATIONS	DESCRIPTION
T_i	(22), (28), (32)	COMBUSTION ZONE ENERGY BALANCE
T_{ci}	(22), (37), (38)	COOLING AIR ZONE ENERGY BALANCE
T_{w1}	(10)	COMBUSTION CHEMISTRY
T_{w2}	(36)	COMBUSTION AND COOLING AIR ZONE INTERFACE

These primary equations and the relevant secondary equations are solved numerically for the four unknown temperatures. The previous section outlined how to calculate a single set of temperatures for one pair of combustion/cooling air zones. The following section describes how the combustion and cooling air zones are iterated in the calculation scheme to find all of the unknown temperatures along the entire length of the combustor.

Combustion and Cooling Air Zone Temperature Calculation Scheme

The first cooling air zone and the reactant temperatures in the first combustion zone are assumed to be the same temperature as the compressor discharge, T_3 (see Figure 3.4). This is the starting point for the combustion and cooling air zone temperature calculations.

The combustion zone reactant enthalpies (h_r term, equation (22)) for the first zone are calculated using the compressor discharge temperature, T_3. The product temperatures are solved iteratively using the equations for the dissipated heat transfer through the liner wall to the cooling air zone, as well as the product enthalpy term in the energy balance (h_p term, equation (22)).

The heat transfer calculated from the combustion zone is assumed to be transferred to the subsequent cooling air zone. The incoming "reactant" enthalpy in a cooling air zone is calculated using the temperature of the previous cooling air zone. Using this heat transfer, the ambient heat transfer and "product" enthalpy is solved iteratively to find the temperature of the cooling air zone. The temperature is iterated in increments which can be specified by the user, with a default of 0.1 deg. K.

The calculation scheme progresses to the next combustion zone using the most recently calculated cooling air zone temperature as the heat transfer medium. This is continued through the length of the combustor until all zone temperatures are calculated. The calculation sequence described above is indicated by the numbered circles on Figure 3.4.

Combustor Discharge Temperature Calculation

The previous section described the temperature calculations for the individual combustion and cooling air zones. After exiting the combustion chamber, the combustion gases are mixed with the cooling air. The temperature of this mixture is T_4, the combustor discharge temperature. This temperature is calculated from an energy balance on the combustor exit including the cooling air and combustion air:

$$\dot{m}_e h_4 = \dot{m}_{c,e} h_{c,e} + \dot{m}_{combp} h_{combp} \tag{40}$$

A parameter *r*, which is provided from the combustor manufacturer, is defined as the ratio of combustion air to cooling air:

$$r \equiv \frac{\dot{m}_{comba}}{\dot{m}_{c,i}} \tag{41}$$

Substituting this expression, along with $\dot{m}_{c,e} = \dot{m}_{c,i}$, gives the result:

$$r h_{combp} + h_c = (r+1) h_4 \tag{42}$$

The combustor exit enthalpy, h_4, is a function of the temperature T_4. This equation can also be solved iteratively using Newton's method until the converged T_4 is determined.

Gas Generator Turbine Discharge

The temperature T_5 (gas-generator turbine outlet temperature) is determined based on using a coupled compressor-turbine such that the compressor work equals the gas-generator turbine work. If the gas-generator turbine operates isentropically, the energy balance expression for this coupled arrangement reduces to:

$$h_3 - h_2 = (1+f)(h_4 - h_{5s}) \tag{43}$$

In this expression, the only unknown is h_{5s}. This is the enthalpy that would occur if the gas-generator turbine operated isentropically. To find the actual enthalpy, h_5, the gas-generator turbine isentropic efficiency is used:

$$h_5 = h_4 - \eta_{turb}(h_4 - h_{5s}) \tag{44}$$

The temperature T_5 can now be calculated from the known h_5.

NO_x Concentration Calculation

The equations to calculate the temperature profile of the gas turbine, including the segmented combustor, have now been developed. However, in order to calculate the NO concentration, a relationship between the combustion temperature and species concentrations must be used.

NO Relationship

In Chapter 2 it was concluded that the Extended Zeldovich Mechanism is the dominant chemical process for NO formation in lean-premixed combustion. Again, this chemical mechanism consists of three reactions; equations (3), (4), and (5).

With certain assumptions, the first two reactions (generally considered the most important) can be used to create a simple expression for the rate of NO formation. Reaction 2 has a much faster reaction rate than reaction 1, so the N atom can be assumed to be in steady state. In addition, the NO formation process is assumed to be much slower than the combustion process; this allows the assumption that the elements affecting the formation of NO are in their equilibrium concentrations during the NO formation process (Turns, 2000). With these assumptions, the rate of NO formation can be expressed by (Heywood, 1988):

$$\frac{\mathrm{d}[\mathrm{NO}]}{\mathrm{dt}} = \frac{2R_1\left\{1-\left([\mathrm{NO}]/[\mathrm{NO}]_e\right)^2\right\}}{1+\left([\mathrm{NO}]/[\mathrm{NO}]_e\right)R_1/\left(R_2+R_3\right)} \tag{45}$$

The R parameters are based on the forward kinetic reaction rate constants for the three reactions in the Extended Zeldovich Mechanism and the equilibrium concentrations of the applicable species:

$$R_1 = k_{f,1}{}^{+}[\mathrm{O}]_e[\mathrm{N}_2]_e \tag{46}$$

$$R_2 = k_{f,2}{}^{+}[\mathrm{N}]_e[\mathrm{O}_2]_e \tag{47}$$

$$R_3 = k_{f,3}{}^{+}[\mathrm{N}]_e[\mathrm{OH}]_e \tag{48}$$

The kinetic rate constants are based on the temperature of the reacting mixture and are readily available for each reaction.

Determination of Equilibrium Subspecies

Because the equilibrium concentrations of the combustion sub-species are not part of the global combustion reaction (equation (10)) used to calculate zone temperatures, a separate combustion equilibrium subroutine is necessary to calculate these concentrations. This subroutine was extracted from software that was provided with the textbook *An Introduction to Combustion* (Turns, 2000). The software calculates the equilibrium products of combustion for a

fuel composed of C, H, O, and N atoms using the method of equilibrium constants, along with six gas-phase equilibrium reactions. Eleven species are considered in the products of combustion: H, O, N, H_2, OH, CO, NO, O_2, H_2O, CO_2, and N_2. Included in these species are those necessary for the determination of the NO formation rate in equation (45). The routine requires an input of fuel composition (model input), temperature (previously calculated), pressure (assumed constant from compressor), gas enthalpy (calculated from known temperature and bulk species composition), and equivalence ratio (model input).

The subroutine just described is written assuming complete combustion. As described previously, the combustor model is divided into a series of WSR's with partial combustion taking place in the initial zones until all fuel is consumed. The method of calculating combustion equilibrium with equilibrium constants is not conducive to this type of arrangement. However, based on preliminary model runs in comparison to Siemens' CFD analysis of the SGT-200 combustor (See Figure 3.7), it was determined that most (> 90%) of the fuel must be consumed in the first zone. This allows for the assumption that the mole fractions of the species affecting NO formation are constant through the remaining zones. The concentrations are still allowed to vary based on temperature differences.

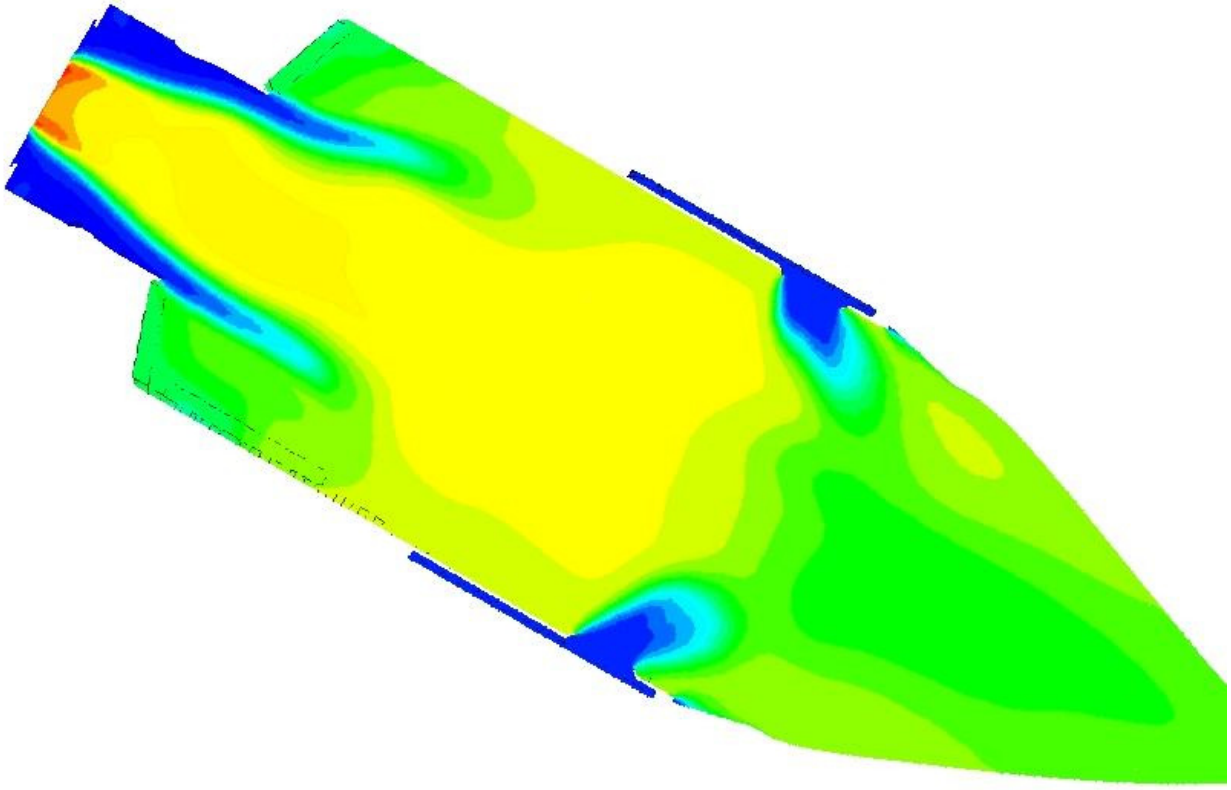

Figure 3.7 SGT-200 Combustor CFD Temperature Profile (Boyns, M., 2004)

Implementation of the NO Relationship

Equation (45) is a relatively simple expression that can be used to calculate the NO formation rate when the temperature and equilibrium concentrations of the applicable species are known. Using this formation rate, concentration of NO can be determined in each zone.

To translate from a NO formation rate to a NO concentration, a residence time is calculated for each zone based on the gas velocity and cross-sectional area:

$$\tau = \frac{A_{xs}}{\bar{V}} \tag{49}$$

This residence time allows for the calculation of the change in NO concentration for each zone:

$$\Delta[\mathrm{NO}] = \left\{ \frac{2R_1 \left\{ 1 - \left([\mathrm{NO}]/[\mathrm{NO}]_e \right)^2 \right\}}{1 + \left([\mathrm{NO}]/[\mathrm{NO}]_e \right) R_1/(R_2 + R_3)} \right\} \tau \tag{50}$$

Again, this calculation assumes that the combustion process is not coupled with the NO formation process. Summing the changes in NO concentration for each zone results in a total NO concentration in the final combustion zone.

NO Mole Fraction Calculation

Using equation (50) the NO concentration is calculated in a mole per volume basis. To convert this to a mole fraction, the following equation based on the ideal gas law is used.

$$\chi_{NO,combp} = \frac{[\mathrm{NO}]\bar{R}T_{combp}}{p} \tag{51}$$

This mole fraction of NO is typically multiplied by 10^6 and denoted as "ppmvw". This is meant to indicate "parts per million by volume, wet". Using parts per million allows the emissions to be reported in easily communicable numbers, while the "by volume" notation is typical for gaseous concentrations, and is equivalent to mole fractions. In addition, the concentrations may be expressed on a wet or dry basis depending on whether water is accounted for in the combustion products. The natural combustion process produces water vapor in the combustion products, thus the NO concentration in the exhaust stream is a wet basis by default. However, CEMS analyzers require dry samples, so they typically report emission concentrations with a dry basis.

Equation (51) gives the NO concentration in the final combustion zone. To calculate the NO concentration at the combustor discharge, the dilution of the cooling air must be accounted for. The total NO concentration, after dilution of cooling air, can be written as:

$$\chi_{\mathrm{NO},tot} = \frac{\dot{n}_{\mathrm{NO},combp} + \dot{n}_{\mathrm{NO},c}}{\dot{n}_{combp} + \dot{n}_c + \dot{n}_f} \tag{52}$$

Using the defined ratio of combustion air to cooling air (equation (41)), the fuel-air ratio, and the fact that there is zero NO in the cooling air, equation (52) becomes:

$$\chi_{\mathrm{NO},tot} = \frac{\dot{n}_{\mathrm{NO},combp}}{\dot{n}_{combp}\left(1+\frac{1}{r}+\frac{MW_{air}f}{MW_{fuel}}\right)} \tag{53}$$

The NO concentration in the combustion products, equation (51), can also be defined as:

$$\chi_{\mathrm{NO},combp} = \frac{\dot{n}_{\mathrm{NO},combp}}{\dot{n}_{combp}} \tag{54}$$

Substituting into equation (53) yields:

$$\chi_{\mathrm{NO},tot} = \frac{\chi_{\mathrm{NO},combp}}{\left(1+\frac{1}{r}+\frac{MW_{a}f}{MW_{f}}\right)} \tag{55}$$

Equation (55) allows the conversion from NO concentration in the combustion products to the overall NO concentration after dilution by the cooling air.

NO Concentration Conversion to Reference Values

To provide a consistent reference point to account for varying dilution and pressures, NO_x concentrations are typically corrected to specific oxygen levels. The general equation for this conversion from one oxygen level to another is as follows:

$$\chi_{\mathrm{NO},\mathrm{O}_2,2} = \chi_{\mathrm{NO},\mathrm{O}_2,1}\frac{N_{\mathrm{mix},\mathrm{O}_2,1}}{N_{\mathrm{mix},\mathrm{O}_2,2}} \tag{56}$$

Where N, the total number of moles in the combustion product mixture, can be calculated by:

$$N_{\mathrm{mix}} = 4.76\left[\frac{b+\left(1+\chi_{\mathrm{O}_2}\right)}{1-4.76\chi_{\mathrm{O}_2}}\right]+1 \tag{57}$$

The "*b*" term is the CO_2 molar product coefficient from the combustion reaction equation (10). The O_2 mole fraction is calculated using the coefficients from this same equation and can be calculated on a wet or dry basis:

$$\chi_{O_2,wet} = \frac{e_{tot}}{b_{tot} + c_{tot} + d_{tot} + e_{tot}} \tag{58}$$

$$\chi_{O_2,dry} = \frac{e_{tot}}{b_{tot} + d_{tot} + e_{tot}} \tag{59}$$

The "tot" subscripts are necessary because the combustion product coefficients must be reevaluated for this analysis to account for the cooling air dilution. This is done by calculating a total fuel-air ratio:

$$f_{tot} = f\left(1 + r\right) \tag{60}$$

Equation (11), the reacting oxygen molar coefficient, can now be rewritten as:

$$a_{tot} = \frac{MW_f}{4.76 f_{tot} MW_a} \tag{61}$$

The subsequent reactant and product coefficients can be calculated using the method described by equations (12) through (17). Finally, to convert between wet and dry concentrations:

$$\chi_{O_2,dry} = \chi_{O_2,wet} \frac{N_{mix,wet}}{N_{mix,dry}} \tag{62}$$

This set of equations allows the NO calculations performed in the combustion modeling program to be converted to industry-standard measurement references.

Modeling Program Description

The subsequent sections outlined the equations and methods used to develop the combustor model. Implementing these equations and methods into an executable computer program was done concurrently in steps of increasing complexity. The combustor modeling computer program was named Kombust. Table 3.2 summarizes the revision notes for the Kombust program.

Table 3.2 Kombust Revision Notes

Kombust Version	Revision Notes
1.0	Original
1.1	Used Cp functions from Van Wylen and Sonntag (valid to 3500K) instead of Moran and Shapiro (valid to 1000K).
1.2	Added ambient humidity into combustion chemical reaction.
2.0	Incorporated specific component enthalpy change functions.
2.1	Developed multi-zone combustion.
2.2	Added heat transfer effects between combustion and cooling zones.
2.3	Added Carvalho NO_x Model.
3.0	Integrated TPEQUIL, equilibrium combustion routine from combustion book by Turns, replaced Carvalho NOx model with Heywood NOx model using equilibrium concentrations from TPEQUIL.
3.1	Use TPEQUIL equilibrium routine assuming cumulative radical concentrations in combusting zones and constant concentrations in non-combusting zones.
3.2	Added T_5 calculation.
3.3	Integrate heat transfer calculation from Lefebvre to include radiative heat tranfer. Correct T_5 calc to include isentropic turbine efficiency. Correct T_5 calc to use proper specific enthalpy (per mole vs. per mass). Fix area calc error in adflame subroutine. Update adflame Newton solving iteration scheme so loops exit when positive/negative increments stop.
4.0	Include external heat transfer with ambient. Update T_4 and T_5 Newton solving iteration schemes so loops exit when positive/negative increments stop. Calculate NO_x at 15% O2, wet and dry basis.
4.1	Update NO_x calc to account for cooling air dilution.
4.2	Incorporate external program loop for parametric studies.

Kombust was written in the FORTRAN programming language and consists of a main module which calls multiple subroutines and functions. In addition, there is an input file specifying ambient conditions, equivalence ratio, number of combustion regions, combustor geometry, gas velocity, fuel fraction oxidized in each region, compressor pressure ratio and isentropic efficiency, gas-generator turbine isentropic efficiency, mass flow ratio between the combustion and cooling air, and other various parameters. The code outputs a file containing NO_x concentration in ppmv (uncorrected and corrected to 15% O_2), temperature of each combustion and cooling air region, concentrations of species in each region, T_3, T_4, and T_5. The program subroutine logic flow diagram is shown in Figure 3.8, while Table 3.3 outlines a brief description for each subroutine. The complete program can be found in Appendix A, including the input file "komin.inp" which lists the complete set of program inputs.

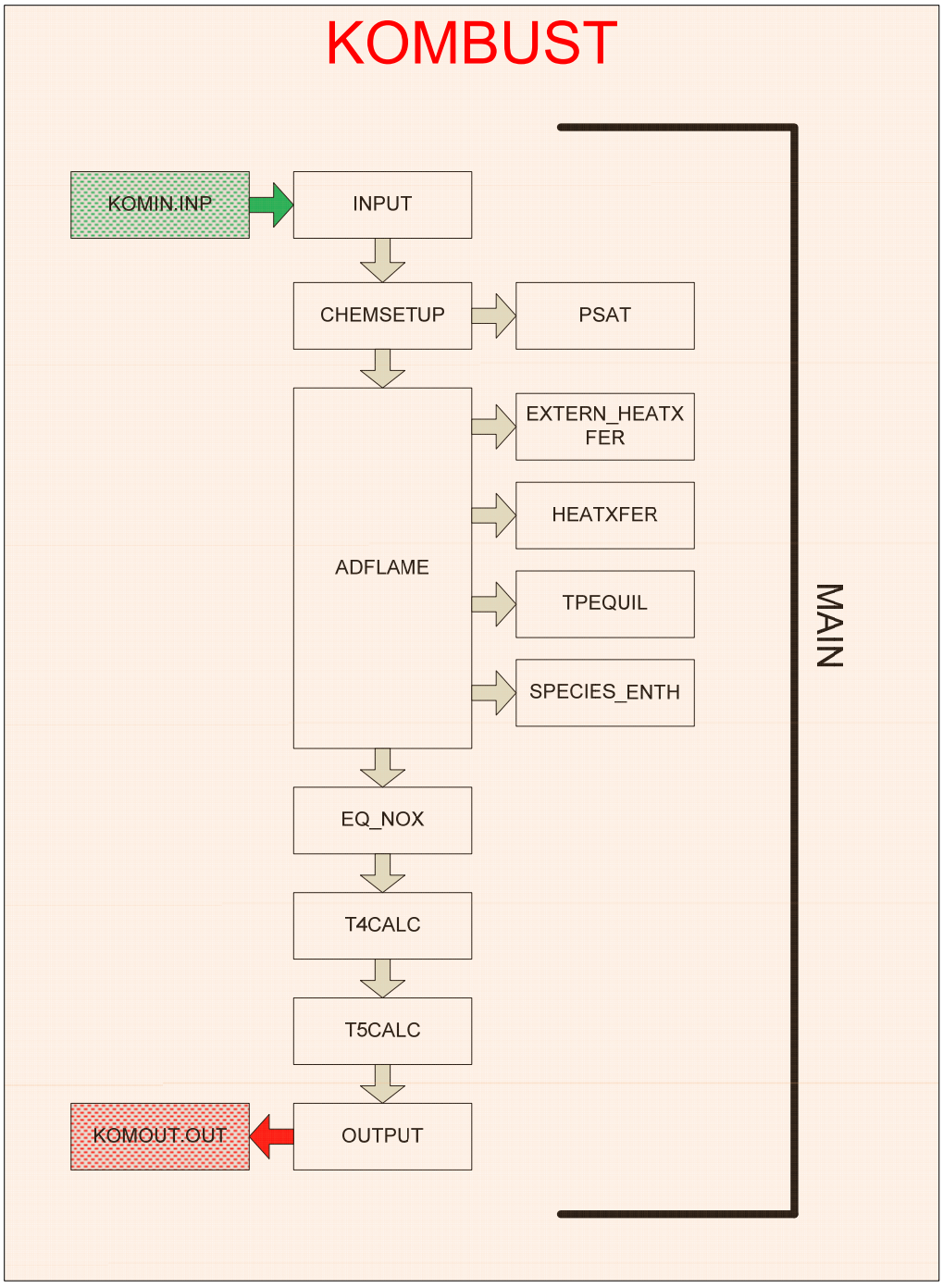

Figure 3.8 Kombust Program Subroutine Logic Flow Diagram

Table 3.3 Kombust Program Subroutine Descriptions

INPUT	Reads the input file and writes corresponding inputs to the command prompt window.
CHEMSETUP	Calculates the combustion chemistry properties for the combustor model including reactant/product molar coefficients and mole fractions.
PSAT	This is a single subroutine which is part of the larger set of subroutines, steam.f90 (Iowa State University, 2011). PSAT calculates the saturation pressure of air.
ADFLAME	This is the primary subroutine which calculates effects of the turbine compressor and iteratively solves for the combustion zone and cooling air zone temperatures,
EXTERN_HEATXFER	Determines the external convective heat transfer coefficient (from the casing to the ambient air).
HEAT XFER	Calculates the convective, conductive, and radiative heat transfer properties from the combustion zones to the cooling air zones. Also calculates the cooling air liner inner and outer wall temperatures.
TPEQUIL	This subroutine calculates the H, O, N, NO and OH, equilibrium concentrations for use in equation (50). This program accompanies the textbook *An Introduction to Combustion* (Turns, 2000).
SPECIES_ENTH	This is a set of functions written for enthalpy calculation calls from the ADFLAME subroutine. Allows enthalpy calculations for CH_4, O_2, N_2, H_2O, CO_2 and air.
EQ_NOX	A subroutine to calculate the NO concentration and corresponding dry and wet correct mole fractions.
T4CALC	T_4 (combustor exit) temperature calculation after mixing of cooling air.
T5CALC	T_5 (gas generator turbine) temperature calculation using calculated compressor power.
OUTPUT	The final subroutine writes pertinent data to an output file, komout.out.

After the development of the theory, equations, methods, and computer program of the combustor model, the next step was to review the validity of the model and develop parametric studies that could be the basis for implementation into a PEMS.

CHAPTER 4 - Combustor Model Validation

As previously discussed, the combustor model was based on a Siemens SGT-200 industrial gas turbine. This engine was selected primarily because of the field data gathered and provided by a corporate partner for this research, Advanced Engine Technologies Corporation (AETC), on this same engine. This field data was used for comparison to the model outputs to validate the Kombust program. Before this was done, however, a qualitative trend evaluation was performed and the optimal number of combustion regions to be analyzed was determined. This chapter discusses a review of the trend evaluation, the combustion region analysis, a general review of the AETC field data, and a comparison study of some Kombust output data to the field data.

General Combustor Model Trend Analysis

Before quantitative test data comparisons could be made, the model was first used to examine the trend of NO_x, T_4, and T_5 vs. equivalence ratio to qualitatively determine its validity. Ambient conditions were input as 25°C, 50% relative humidity, and barometric pressure of 101.325 kPa. Five combustion zones were used in the analysis.

It is expected that an increase in equivalence ratio will increase NO_x production exponentially, because temperature is increased with an increase in equivalence ratio (under lean conditions) and NO_x production increases exponentially with temperature (Turns, 2000). Figure 4.1 demonstrates this relationship:

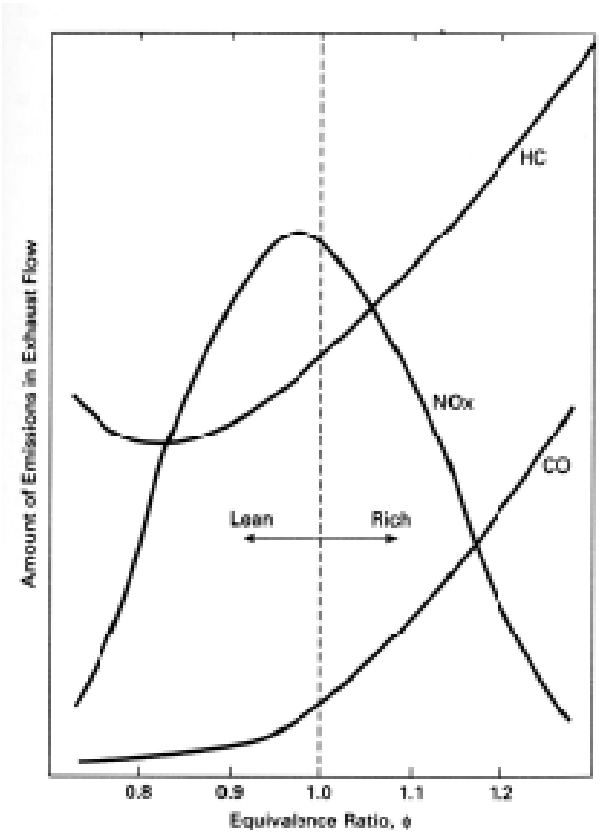

Figure 4.1 Dependence of Emissions on Eqivalence Ratio (Pulkrabek, 1997)

To validate this relationship, multiple runs of the Kombust program were executed with the equivalence ratio ranging from 0.6 to 1.0 in 0.05 increments. This represents an increase in the fuel flow rate to the engine with a constant air flow rate, i.e. an increase to the fuel-air ratio. Figure 4.2 shows the results of these calculations:

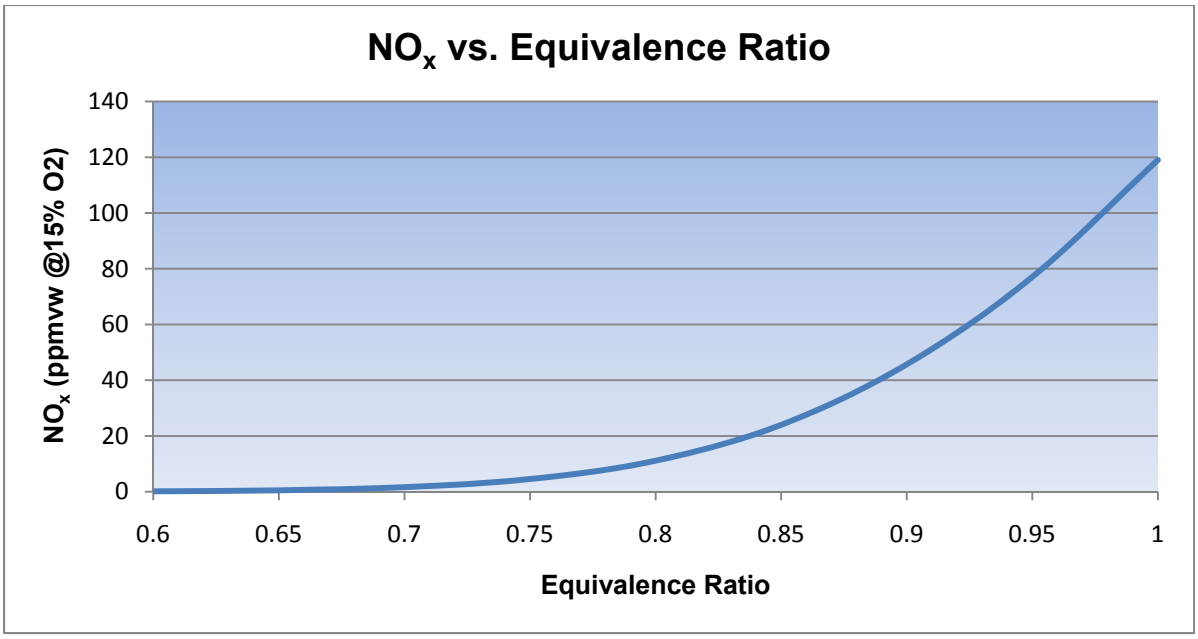

Figure 4.2 Kombust NO_x vs. Equivalence Ratio

Based on a general shape comparison of Figure 4.1 to Figure 4.2, the Kombust program combustor model correctly predicts the trend that is expected for the temperature-dependant Zeldovich NO_x mechanism.

Because the computational path through the Kombust program that is required to relate NO_x to equivalence ratio encompasses most of the program routines, this sensitivity analysis provides a general validation of most of the calculations performed, with the exception of the NO_x concentration adjustment calculations and downstream temperature calculations, including T_4 and T_5. The latter can be easily plotted from the same program outputs used on the initial analysis:

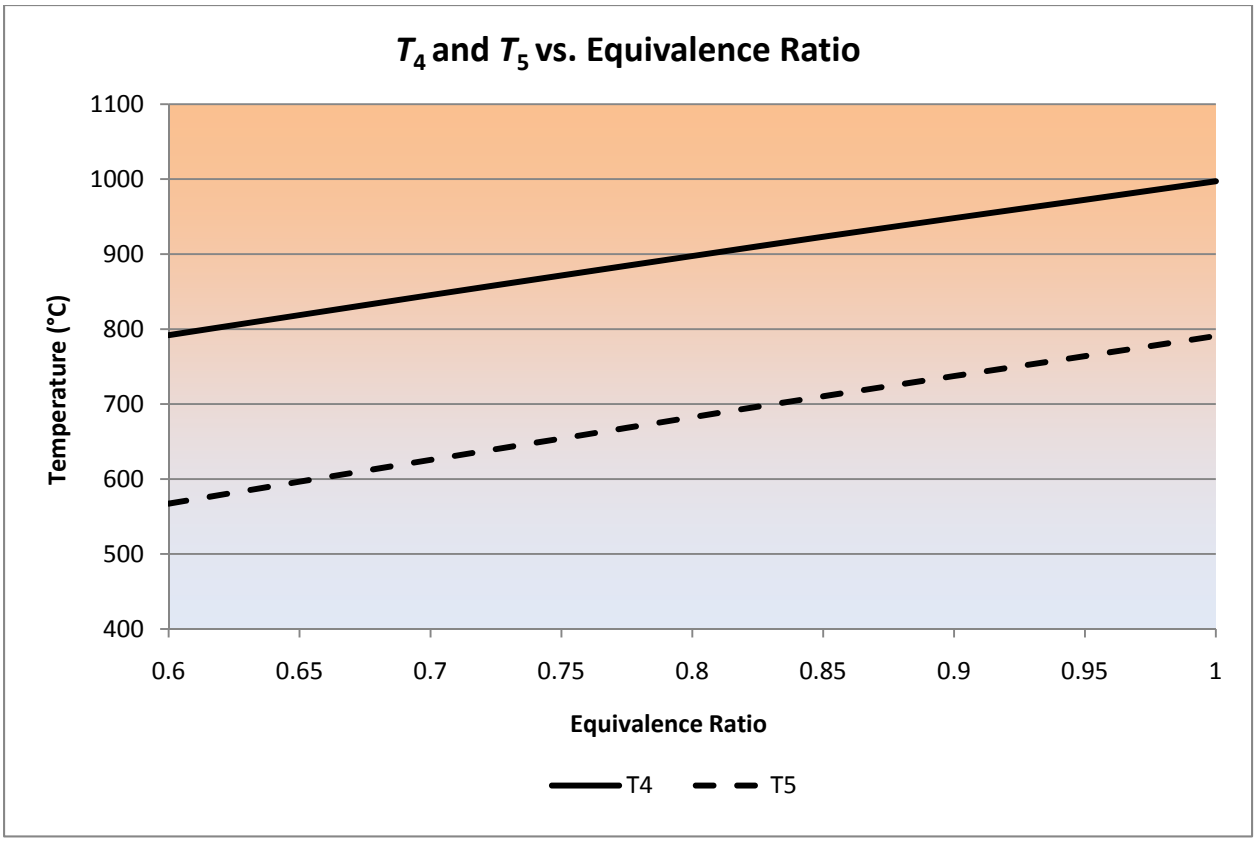

Figure 4.3 Kombust T_4 and T_5 vs. Equivalence Ratio

There are two things that can be highlighted from these results. Firstly, there is a nearly constant differential between T_4 and T_5. This temperature differential represents the power supplied by the gas-generator turbine to the compressor. The engine is modeled with a constant pressure ratio, and these Kombust program runs were performed with constant ambient conditions, so this constant differential between T_4 and T_5 is justified. Secondly, the relationship between equivalence ratio and both T_4 and T_5 is approximately linear. Increasing the equivalence ratio is the same as increasing the fuel-to-air ratio, or increasing the mass flow rate of fuel into the engine. By increasing the mass flow of fuel to the engine, the amount of energy supplied is increased by:

$$\Delta \dot{E} = \Delta \dot{m}_f (LHV) \tag{63}$$

Since the heating value is constant, the mass flow rate of fuel is directly and linearly related to the change in energy, so the linear relationship shown in Figure 4.3 is appropriate.

These two preliminary sensitivity studies indicate that the Kombust program is producing reasonable qualitative results, and thus the fundamental equations and methods used in the program are acceptable. The next step in the development of the model was to determine the proper number of combustion zones to be used in subsequent analyses.

Formulation of Proper Number of Combustor Zones

Before any useful data could be generated with the combustor modeling program, it had to be set up with an appropriate number of combustion regions and their corresponding dimensions.

In its simplest form, the combustor can be modeled in two regions:

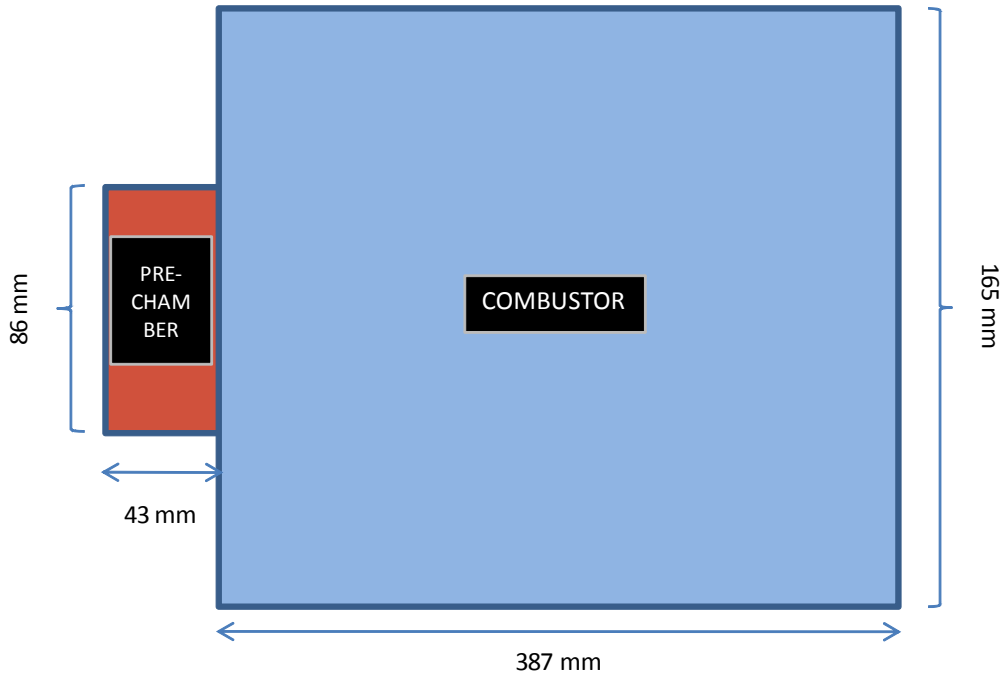

Figure 4.4 2-Combustion Region Model

The dimensions shown are typical for the SGT-200 DLN combustor, and were provided by Siemens. Running the Kombust program with this model arrangement produced the combustor zone temperature profile shown in Figure 4.5, with a T_5 of 625°C and a NO_x concentration of 165 ppmvw @ 15% O_2 at an equivalence ratio of 0.8.

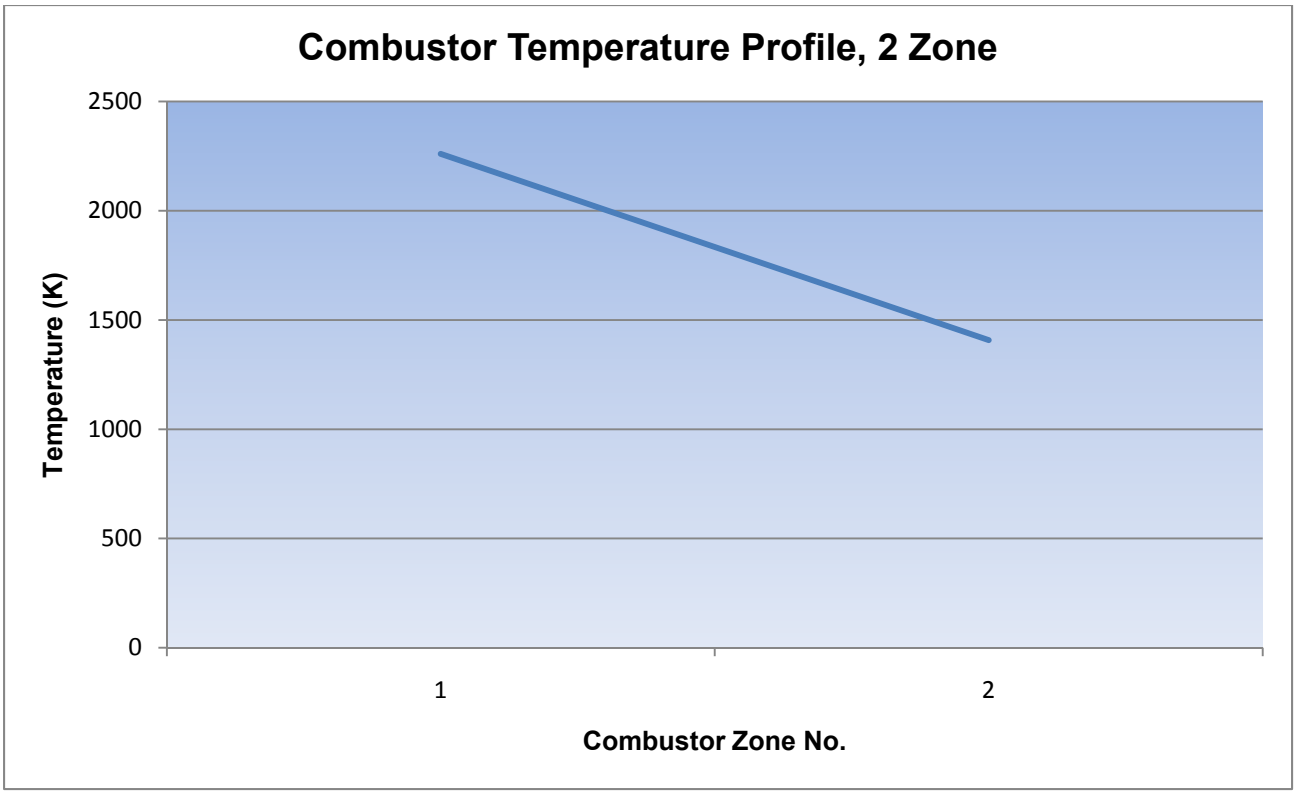

Figure 4.5 Combustor Temperature Profile, 2 Zone

It was anticipated that the discretization effect from the increase in combustion zone regions would refine the model to a more realistic scenario, similar to the techniques employed by finite element analysis (FEA) and computational fluid dynamics (CFD). To test this, the number of combustion zones was increased systematically by breaking the pre-chamber and combustor sections into multiple zones:

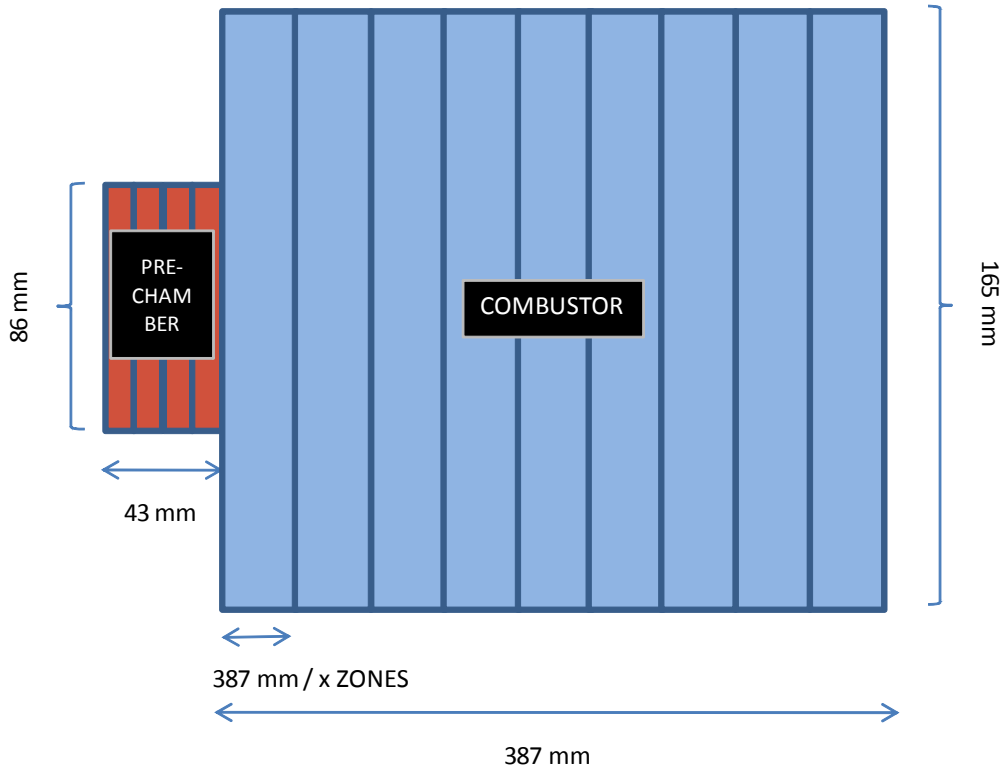

Figure 4.6 Multi-Combustion Region Model

Using 29 zones had the following effect on the combustor temperature profile:

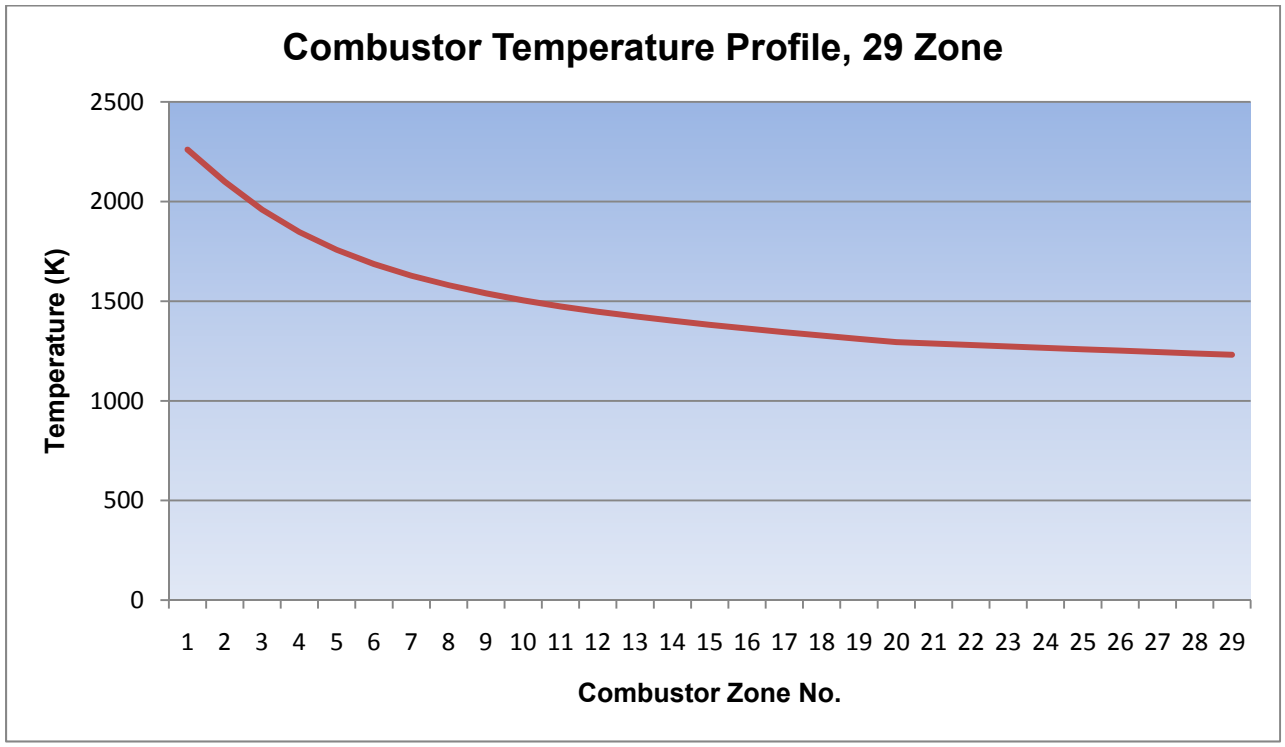

Figure 4.7 Combustor Temperature Profile, 29 Zone

This appears a valid trend as the combustion products to the cooling air temperature delta is reduced along the combustion chamber by the heat transfer. For this arrangement, T_5 was 460°C with a NO_x concentration of 26 ppmvw @ 15% O_2. Both of these parameters were decreased from the 2-zone run, and they continued to decrease asymptotically as the number of zones increased:

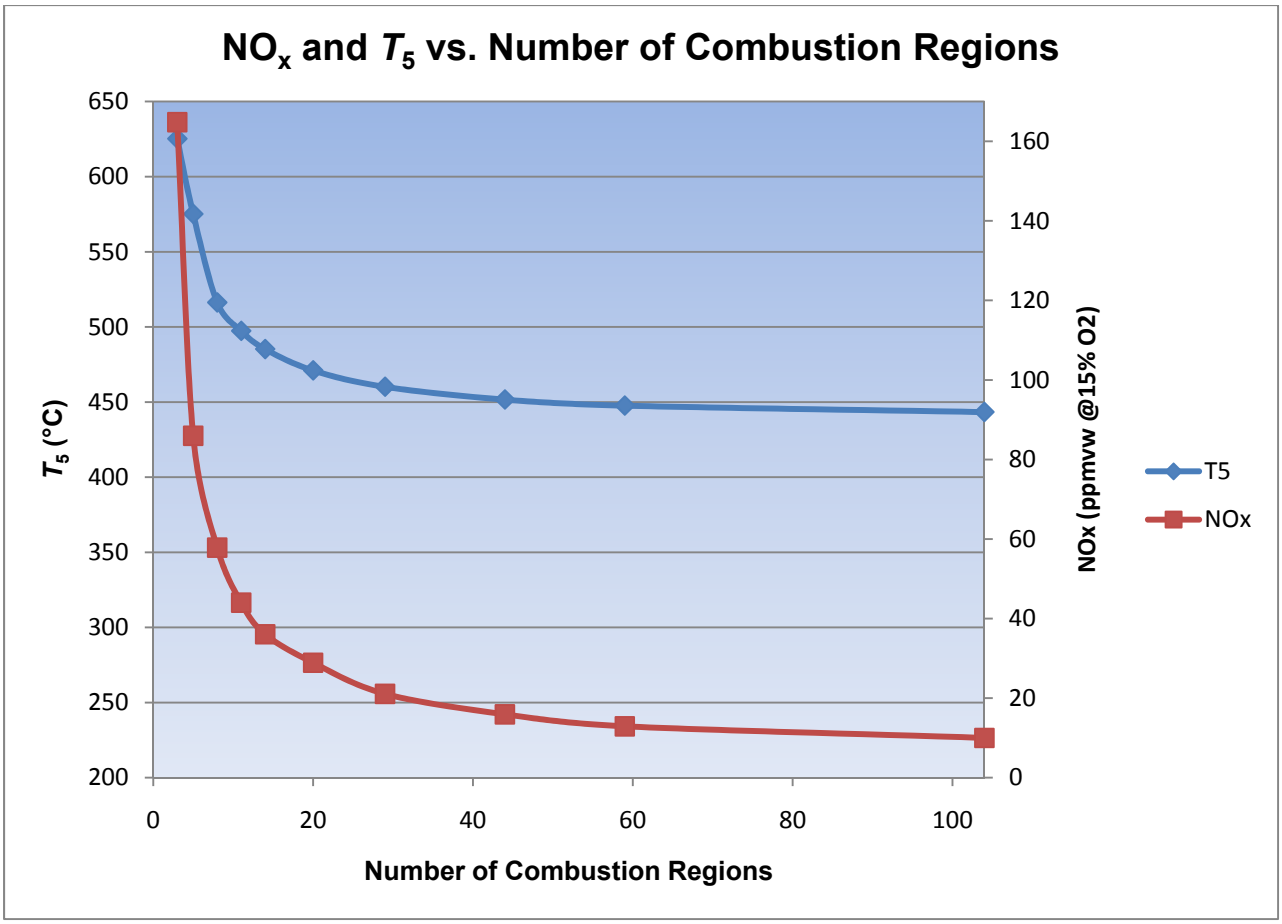

Figure 4.8 Number of Combustion Zone Analysis, Absolute Values

The asymptotic nature of this change can be seen more clearly if the data is plotted as a change in dependant variable per zone number increase:

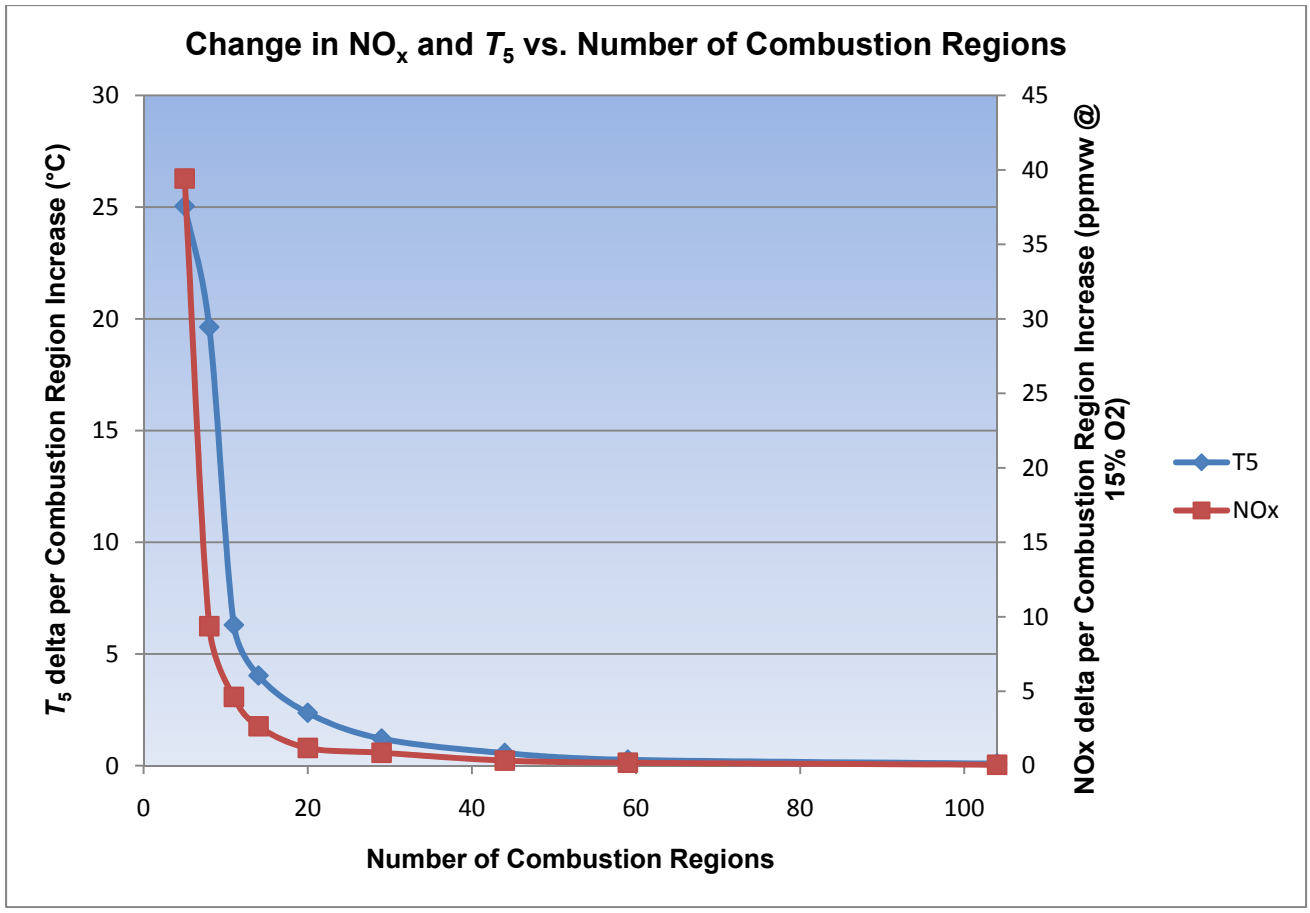

Figure 4.9 Number of Combustion Zone Analysis, Change per Zone Number Increase

As Figure 4.9 illustrates, the change in T_5 and NO_x per unit increase in the number of combustion regions approaches zero. The last data point was 104 zones which resulted in a variable change of 0.09°C/zone for T_5 and 0.06 ppm/zone for NO_x. These small variable changes per zone number increase were deemed insignificant enough to conclude that a further increase in the number of zones would not justify the increased computational demand required to converge the more complex simulation. Because of this, 104 zones were selected henceforth as the proper quantity to use in subsequent calculations.

With the number of combustion zones selected, the primary work of this chapter, which was to compare Kombust program outputs to the field-gathered operating data provided by AETC, could proceed. The first step in doing this was to review said data and determine the appropriate trends for comparison.

Combustion Turbine Operating Reference Data

The data used for comparison to the combustor model was from an SGT-200 test run and data collection by AETC on March 9, 2004. The combustion turbine is installed as a compressor drive on the Trans Canada Pipeline, station 148. Eighteen (18) test runs were performed over a two-day period. The data collected was extensive, with the primary parameters of interest for this research being NO_x concentration, T_1, T_3, T_5, and T_7. AETC also did extensive analysis on the data to develop trends and examine variable relationships. They showed that many parameters strongly correlated, including fuel flow and torque vs. power, as shown in Figure 4.10, as well as T_5 (gas generator turbine exit temperature) and T_7 (exhaust temperature) vs. power, as shown in Figure 4.11.

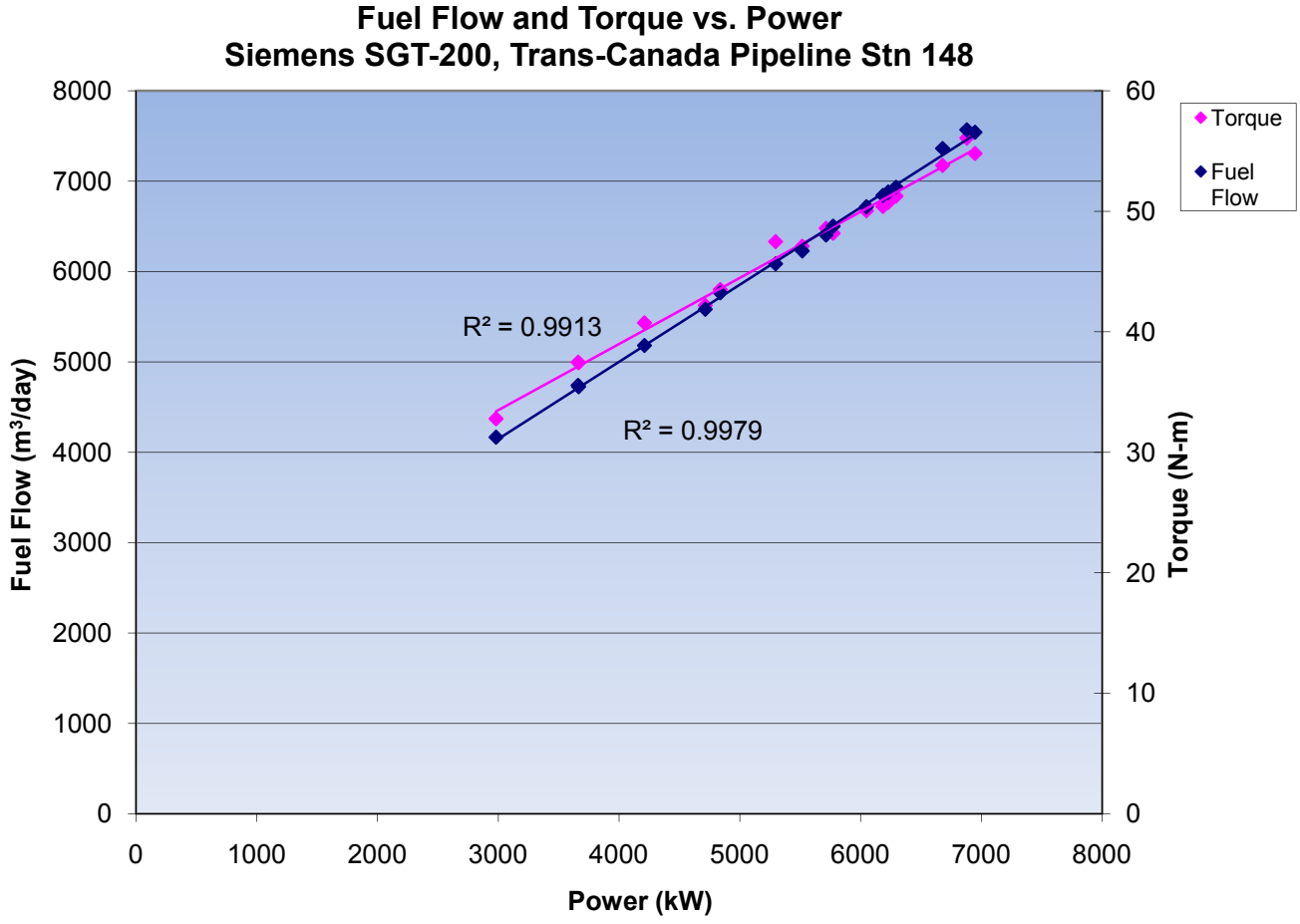

Figure 4.10 AETC Field Data Fuel Flow and Torque Curves

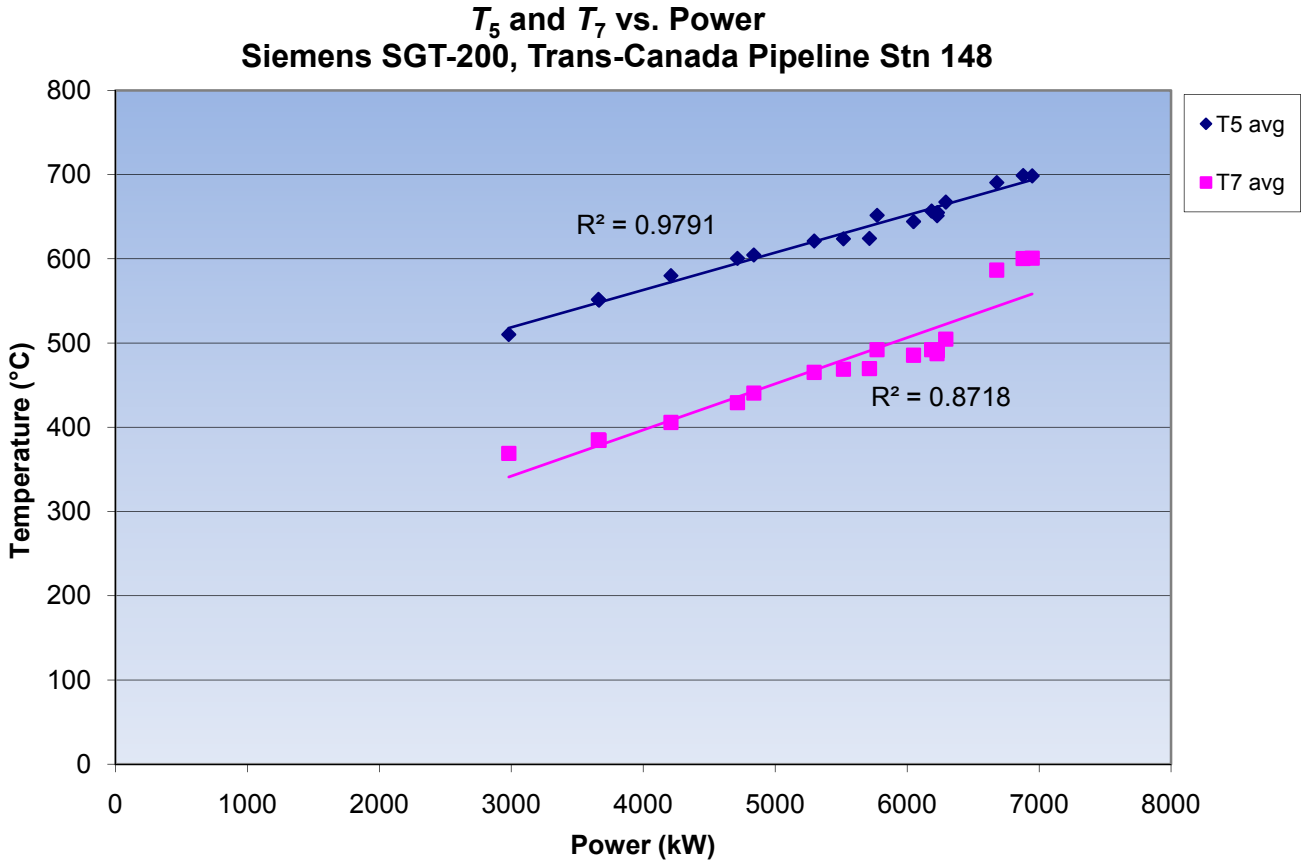

Figure 4.11 AETC Field Data T_5 and T_7 Curves

These relationships are expected as these parameters should relate almost directly to power with no additional strongly-correlating variables that would not be accounted for on these plots. Contrary to this, Figure 4.12 shows that NO_x, does not correlate well with power. This difference in parameter correlation alludes to the complexity of the NO_x formation process.

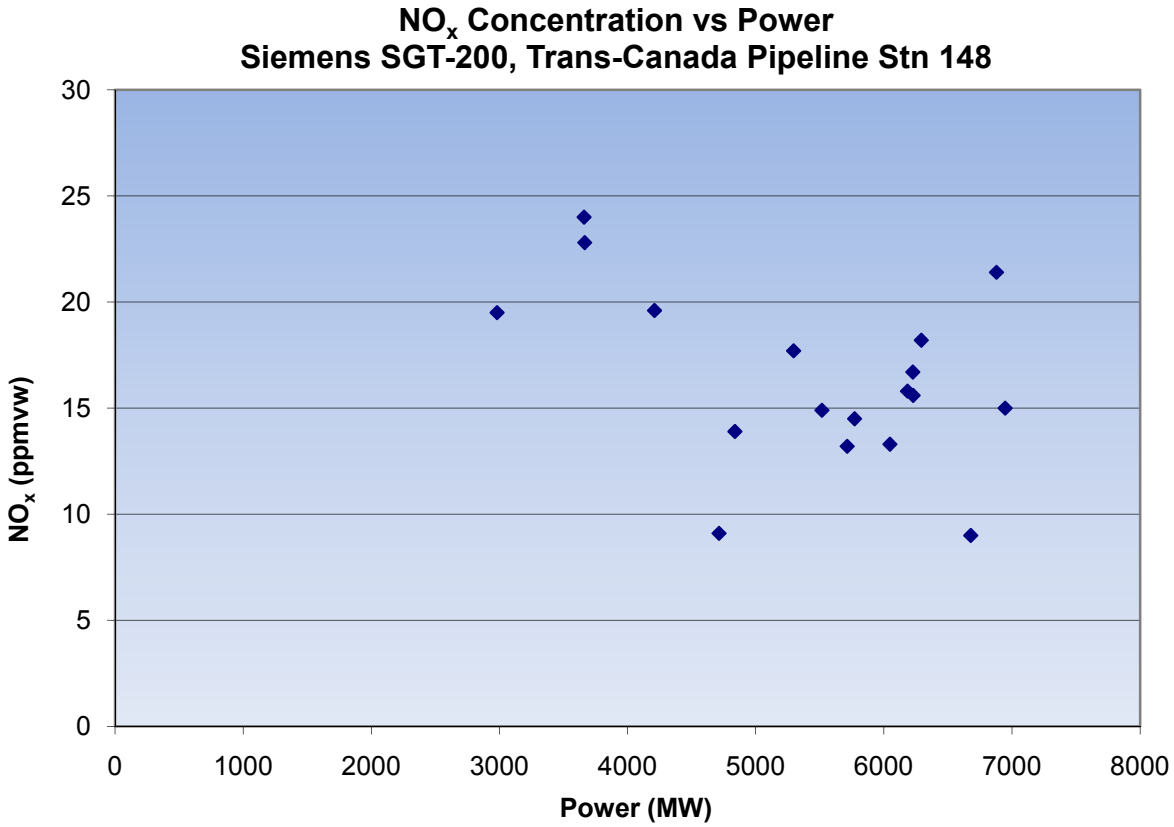

Figure 4.12 AETC Field Data NO_x vs. Power Plot

To find variable dependency with NO_x, more complex relationships must be investigated. AETC accomplished this by correlating various temperature differences with NO_x. These temperature differences were also grouped by load ranges to find dependencies. Figure 4.13 shows one such instance of this investigation, in which NO_x was correlated to T_5 minus T_3.

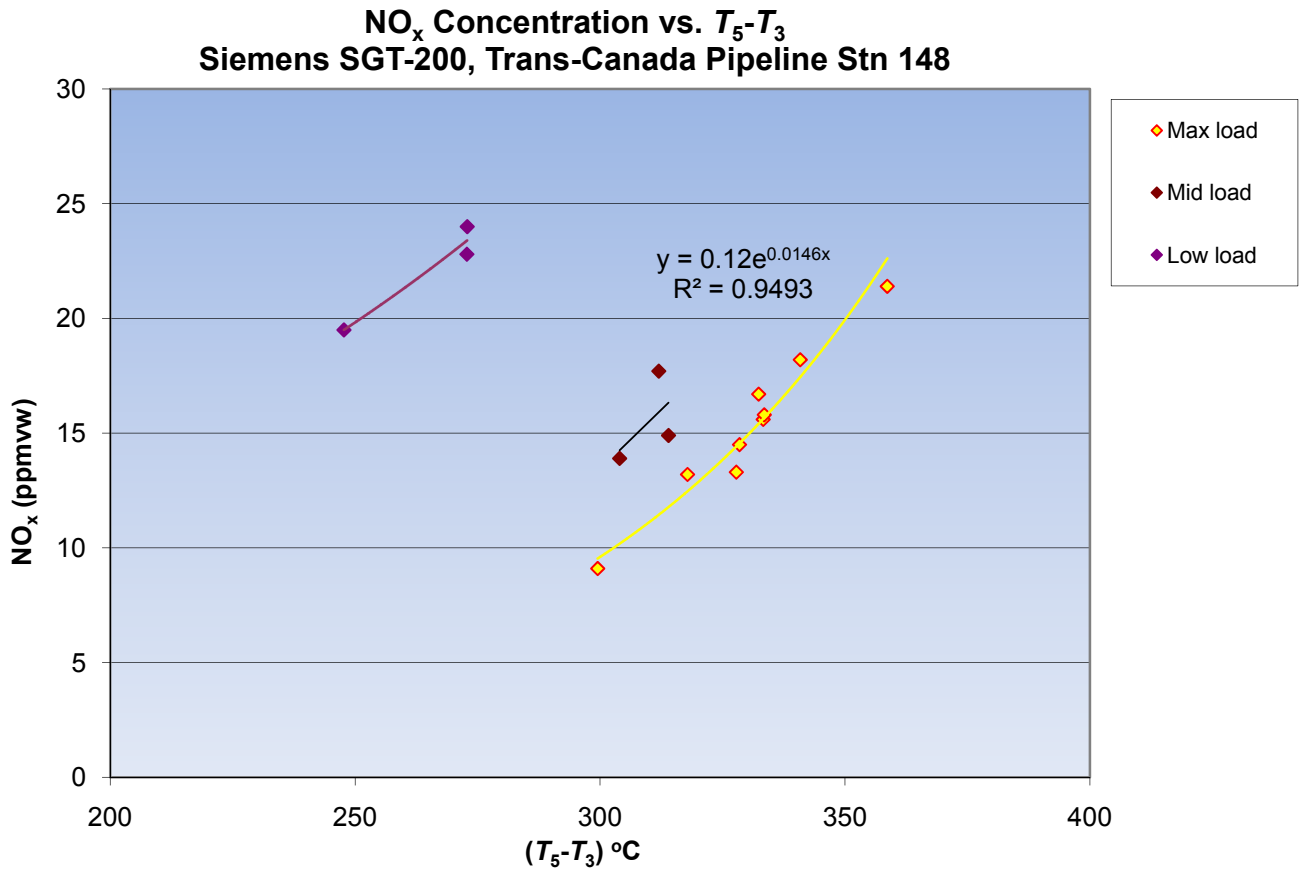

Figure 4.13 AETC Field Data NO_x vs. T_5-T_3 Plot

The data was grouped by load ranges for low, mid, and max loads. The general trend for all three of these load ranges is that NO_x directly correlates with an increase in the T_5 minus T_3 temperature difference. For the max load points, this correlation can be well-represented by an exponential curve fit.

Fundamentally speaking, T_4 minus T_3 should represent the heat input into the combustor. However, the high temperatures associated with T_4 are very difficult to measure. In addition, as discussed in the previous section and shown on Figure 4.3, the temperature difference across the gas-generator turbine, T_5 minus T_4, is constant. Therefore, using T_5 minus T_3 instead of T_4 minus T_3 is appropriate and should not affect the trend. The combustor model validation will focus on recreating this dependency as accurately as possible.

Kombust Model Comparison to Field Data

As previously mentioned, the goal of the model validation was to recreate the T_5 minus T_3 NO_x relationship for the max load conditions shown in the AETC field data and plotted in Figure 4.13. To recreate this relationship, values of equivalence ratio were selected that correspond to an equal range of NO_x outputs that were seen in the AETC field data points, about 9 to 22 ppmvw. This corresponds to a Kombust program equivalence ratio of 0.73 to 0.79. Note that this is slightly less than the values that would be selected from Figure 4.2 because the field data is absolute NO_x while the data plotted in Figure 4.2 is corrected to 15% O_2. The Kombust program was rerun through this range of equivalence ratio in 0.01 increments. The data from these runs were reconciled and plotted on Figure 4.14 below, along with the AETC field data.

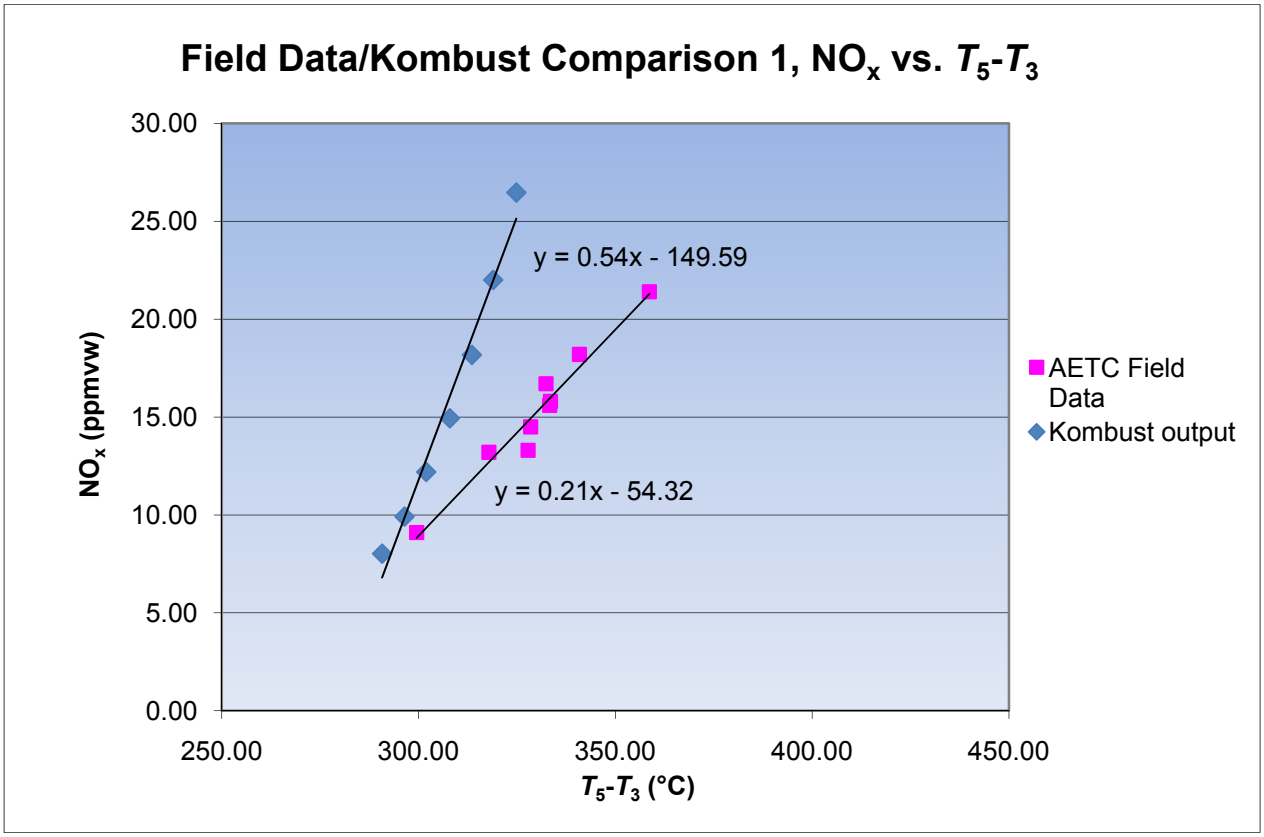

Figure 4.14 AETC Field Data/Kombust Comparison 1

The results show that the Kombust-generated values of T_5 minus T_3 are approximately 20°C to 50°C than less the AETC field data, for a given concentration of NO_x. The range of the temperature offset is because the slopes, ppmv/°C, are also different.

The previous analysis assumes that the equivalence ratio range used to match the NO_x output of the field data is appropriate, i.e. the Kombust model will calculate all the NO_x measured in the field data. However, there are three items which may contribute to this being an incorrect assumption:

1. It is anticipated that the modeled NO_x will be less than the actual NO_x because the model is only calculating the thermal NO_x contributed from the Zeldovich chemical mechanism, while the literature review deemed that the nitrous oxide mechanism is also prevalent for lean-premixed combustion.
2. The SGT-200 DLE combustion system uses a pilot flame configuration that would operate with a diffusion flame at a near-stoichiometric fuel-air ratio. This would produce a maximum temperature combustion region thus producing additional thermal NO_x not accounted for in this analysis.
3. In discussions with Siemens it was also determined that the SGT-200 typically operates at an equivalence ratio of about 0.67.

The slopes of the trend lines fit to the modeled and tested NO_x vs. T_5-T_3 are 0.54 ppmvw/°C and 0.21 ppmvw/°C respectively. Because the NO_x vs. equivalence ratio relationship presented in Figure 4.2 is an exponential one, the slope, or derivative, decreases with decreasing equivalence ratio. Thus in order to produce data more resembling the slope of the field data it is necessary to decrease the range of equivalence ratios analyzed, which would also decrease the NO_x range of the outputs. This methodology agrees with the three items above.

To determine the proper range of equivalence ratios necessary to reproduce the slope of the field data, a plot of the NO_x vs. T_5-T_3 derivative vs. equivalence ratio was created and the vertical axis ranged for the slope values seen on Figure 4.14.

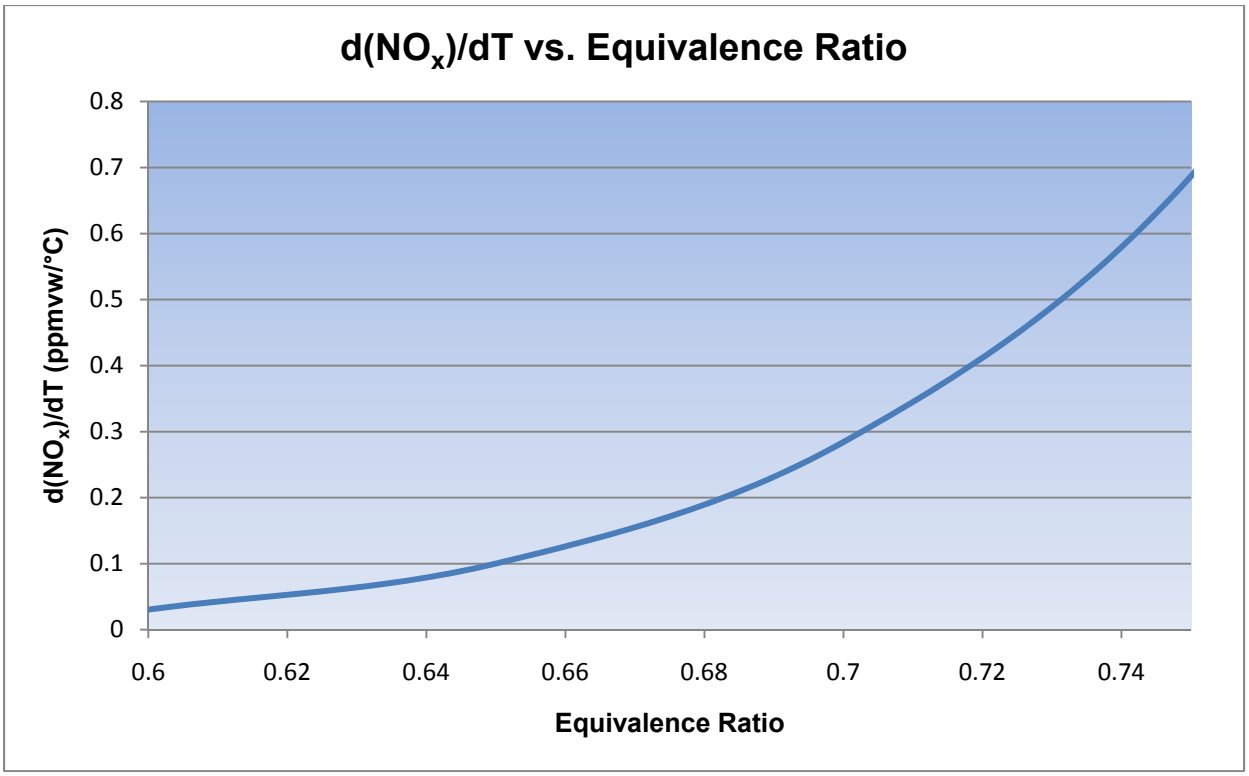

Figure 4.15 NO_x Derivative vs. Equivalence Ratio

This plot shows the 0.73 beginning range of equivalence ratio used in the previous analysis corresponding to 0.54 ppmvw/°C slope. To reach the 0.21 ppmvw/°C slope of the field data, the Kombust model equivalence ratio should be reduced to about 0.69. This value was straddled in the next set of Kombust model runs, ranging from 0.66 to 0.72.

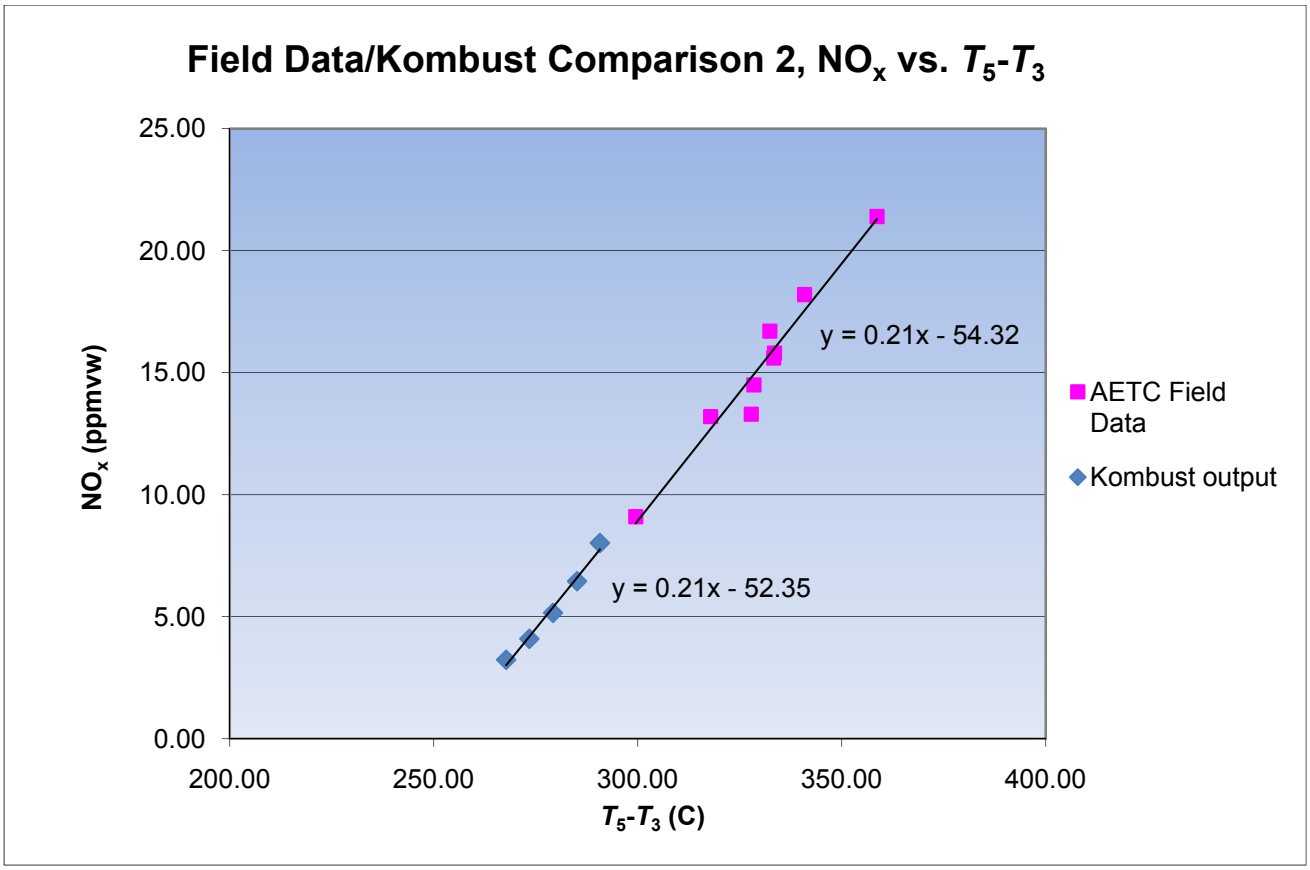

Figure 4.16 AETC Field Data/Kombust Comparison 2

This set of Kombust runs demonstrates that the model creates a nearly equal slope of the AETC field data for NO_x vs. T_5-T_3, albeit with lesser values of NO_x and T_5-T_3. The lesser values of NO_x are expected per the above three discussion points, but the lower T_5-T_3 values are a different story. There are a number of factors that may contribute to this discrepancy including:

- Inaccurate modeling of the heat transfer – Obviously the heat transfer involved in a combustion turbine is a very complex process, especially due to the extremely high temperatures and temperature gradients which make the complex radiative heat transfer process so important. While the goal of this research was to model the heat transfer process as accurately as possible by accounting for all modes of heat transfer including conductive, convective, and radiative mechanisms, in judging Figure 4.16 it would appear that the calculated heat transfer was excessive.

- Fuel – The Kombust model uses pure methane as the fuel, while the field turbine was burning natural gas with an unknown heating value.
- Compressor and turbine efficiencies – The compressor and gas-generator turbine efficiencies used in the Kombust model were typical values of 0.85. Differences in the actual efficiencies will affect the accuracy of the calculated temperatures.

While the model validation exercise revealed potential for future enhancements, the model comparison to the field data was deemed sufficient for the purpose of this research. The following chapter will focus on creating additional sensitivity studies and a review of the potential incorporation of the Kombust program into a PEMS.

CHAPTER 5 - Parametric Studies and PEMS Implementation

The preceding chapters reviewed the necessity of this research, determined the appropriate path forward including the general type of combustor model to be developed, reviewed the development of the model through fundamental chemistry, thermodynamic, and heat transfer principles, and validated the model both qualitatively and quantitatively. The present chapter will focus on additional sensitivity studies.

Parametric Studies

The goal of this chapter is to review some additional parametric studies to further validate the Kombust program and gain an understanding of some of the variable dependencies. The parameter studies reviewed are as follows:

1. NO_x vs. Ambient Temperature
2. NO_x vs. Ambient Relative Humidity
3. NO_x vs. Ambient Atmospheric Pressure
4. NO_x vs. Combustion to Cooling Air Ratio
5. NO_x vs. Compressor Pressure Ratio

To review the effects of changing these parameters on combustion temperature, all plots will also include T_5. In addition, to review the relative contribution of a change in combustion temperature vs. other effects to the change in NO_x concentration, a new parameter, $dT_5/d[NO_x]$, will be calculated and reviewed for each study.

NO_x vs. Ambient Temperature

The first parametric study reviewed was NO_x vs. ambient temperature. For this study, all program input parameters were held constant while the ambient temperature (dry bulb) was adjusted from -30°C to 50°C in 10 degree increments. The relative humidity was 50% with an equivalence ratio of 0.7. The results of this are shown in Figure 5.1.

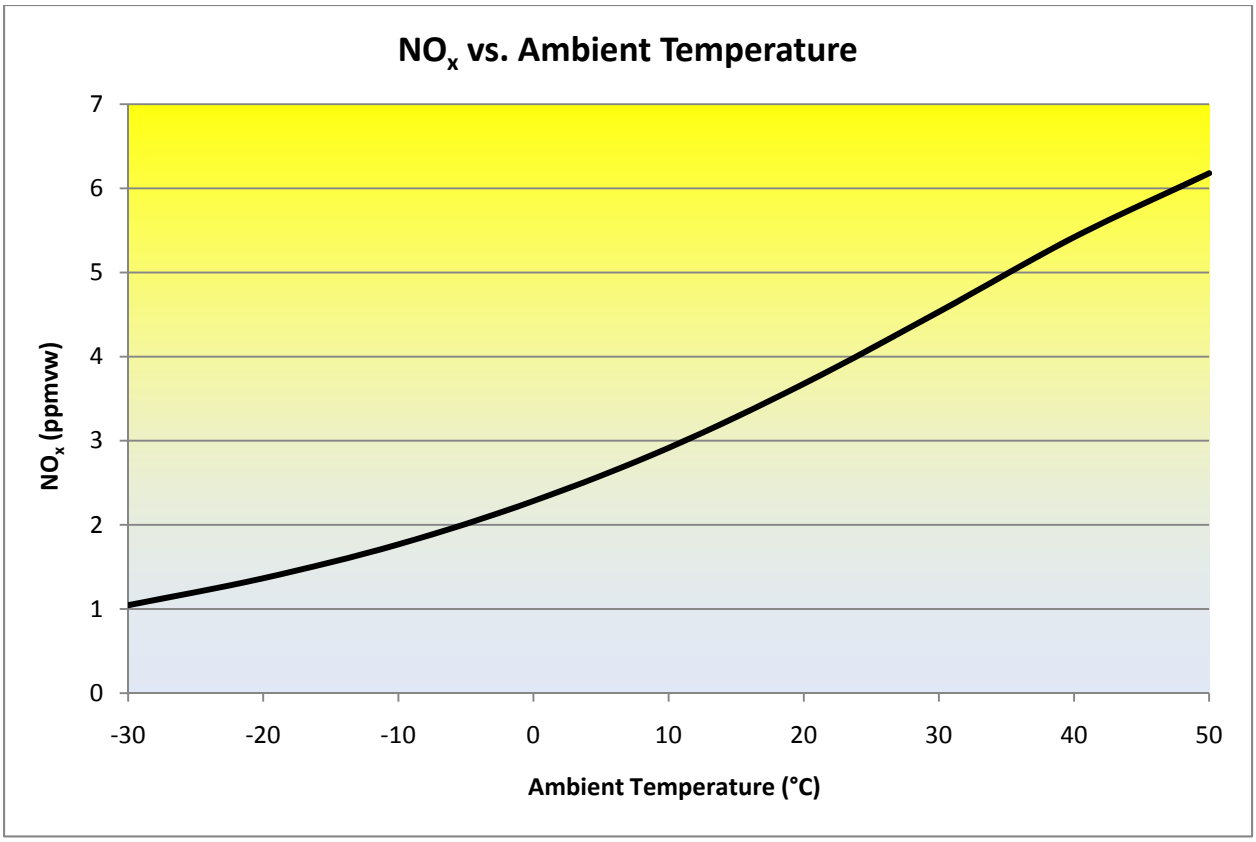

Figure 5.1 Kombust NO_x vs. Ambient Temperature

The plot shows a direct relationship between the ambient temperature change and NO_x output, with an increase of about six-fold in the NO_x output over the analyzed temperature range. If T_5 is added to this same plot it alludes to the reason for this increase in NO_x. Because thermal NO_x is modeled with the Kombust program, the increase in NO_x should be a direct result of the increase in combustion temperature. This is represented by a similar rise in T_5 relative to NO_x shown in Figure 5.2.

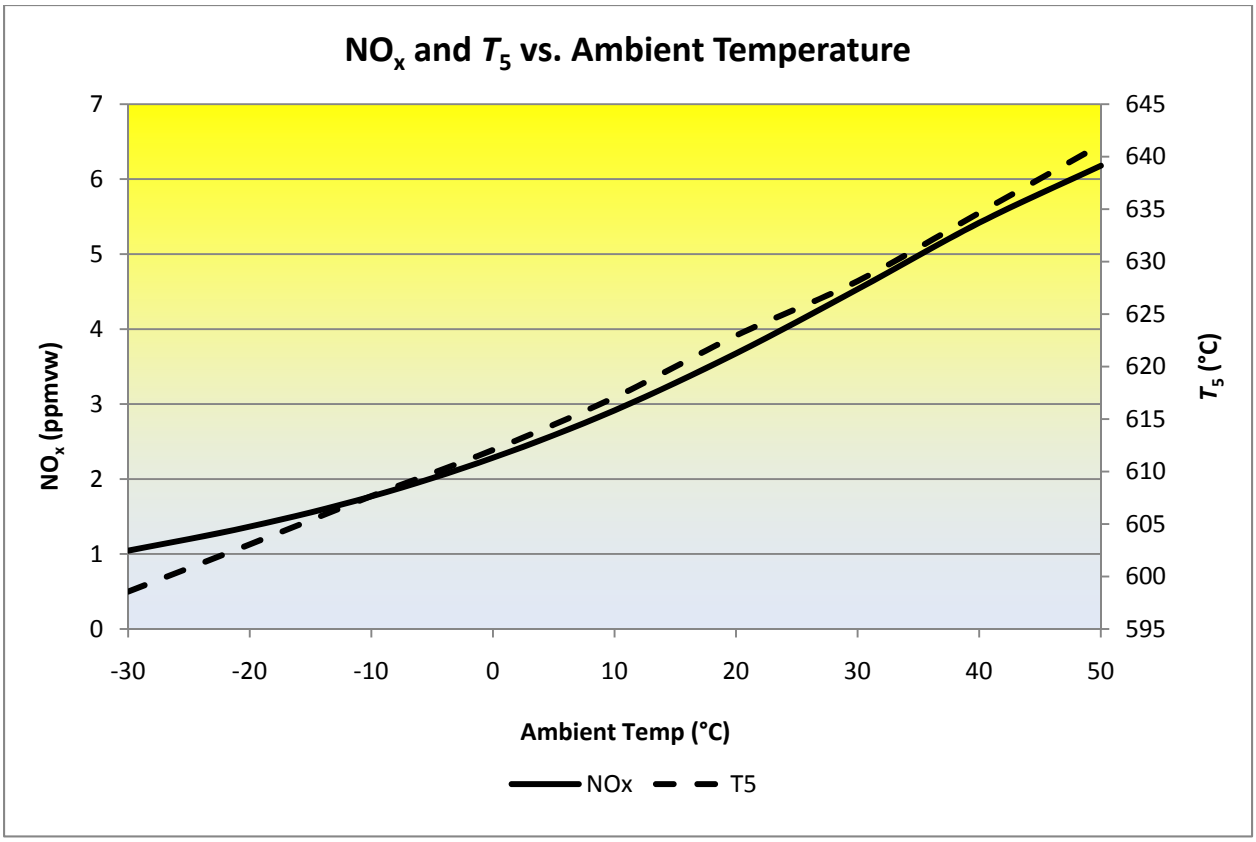

Figure 5.2 Kombust NO_x and T_5 vs. Ambient Temperature

NO_x vs. Ambient Relative Humidity

The next parameter reviewed was the ambient relative humidity vs. NO_x. For this curve, the ambient temperature was held at 25°C with the relative humidity varying from 20% to 100% in 10% increments with an equivalence ratio of 0.7. The results of this are shown in Figure 5.3 along with a plot of T_5.

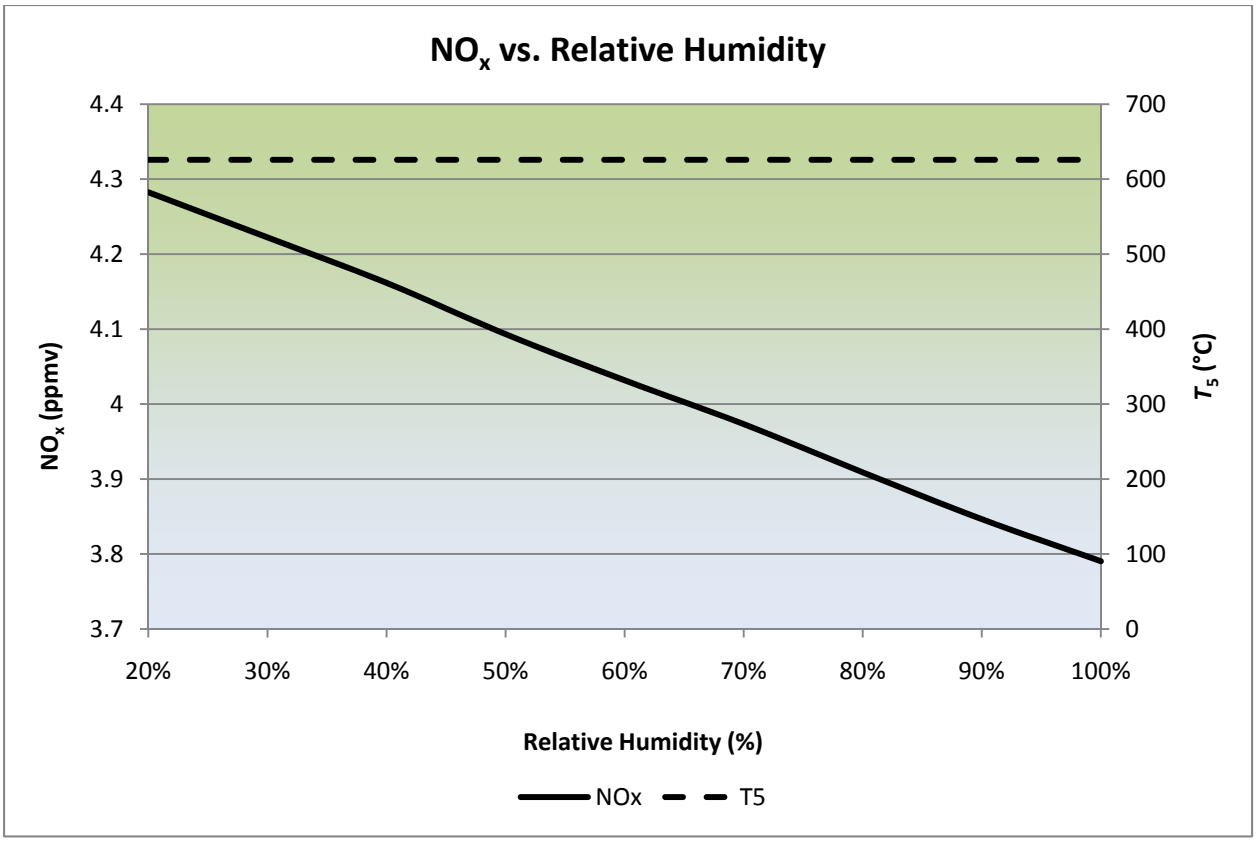

Figure 5.3 Kombust NO_x and T_5 vs. Relative Humidity

The plot shows a rather strong inverse linear correlation for NO_x while T_5 remains nearly constant. This difference in correlation is not expected, because as discussed for the ambient temperature graph, the thermal NO_x model should only be affected by combustion temperatures. After reviewing the calculations it was revealed that the decrease in NO_x concentration is actually a result of the dilution effects of the increased humidity, meaning the humidity has little effect on the combustion temperatures but a larger effect on the mass flow through the engine.

Referring again to equation (45), the NO_x formation rate equation, and the associated equations of its parameters, it is apparent that a change in the equilibrium concentration of the combustion species will affect the rate of NO_x formation. To confirm the downward trend in NO_x with increasing relative humidity, two points were checked manually (by debugging the program) to prove the reduced NO_x formation rate. The results of this are shown in Table 5.1 which shows the slight difference in the rate of NO_x formation, assuming an initial NO concentration of 1.

Table 5.1 Relative Humidity Effect on NO_x Formation Rate Parameters

Relative Humidity 0.5	
R_1	$1.86x10^{-4}$
R_2	$1.54x10^{-7}$
R_3	$7.37x10^{-5}$
$[NO]_e$	$3.22x10^{-4}$
d[NO]/dt	**0.459**
Relative Humidity 0.9	
R_1	$1.84x10^{-4}$
R_2	$1.52x10^{-7}$
R_3	$7.29x10^{-5}$
$[NO]_e$	$3.21x10^{-4}$
d[NO]/dt	**0.454**

The results show that there is a lower NO formation rate for a higher humidity. This indicates that the NO_x concentration change is due to the increase in water vapor concentration diluting the remaining exhaust gas constituents.

NO_x vs. Ambient Atmospheric Pressure

The NO_x vs. ambient atmospheric pressure chart is shown in Figure 5.4. This chart shows a similar increase in NO_x as the ambient pressure is increased from 91 kPa up to 102 kPa (sea level = 101.3 kPa).

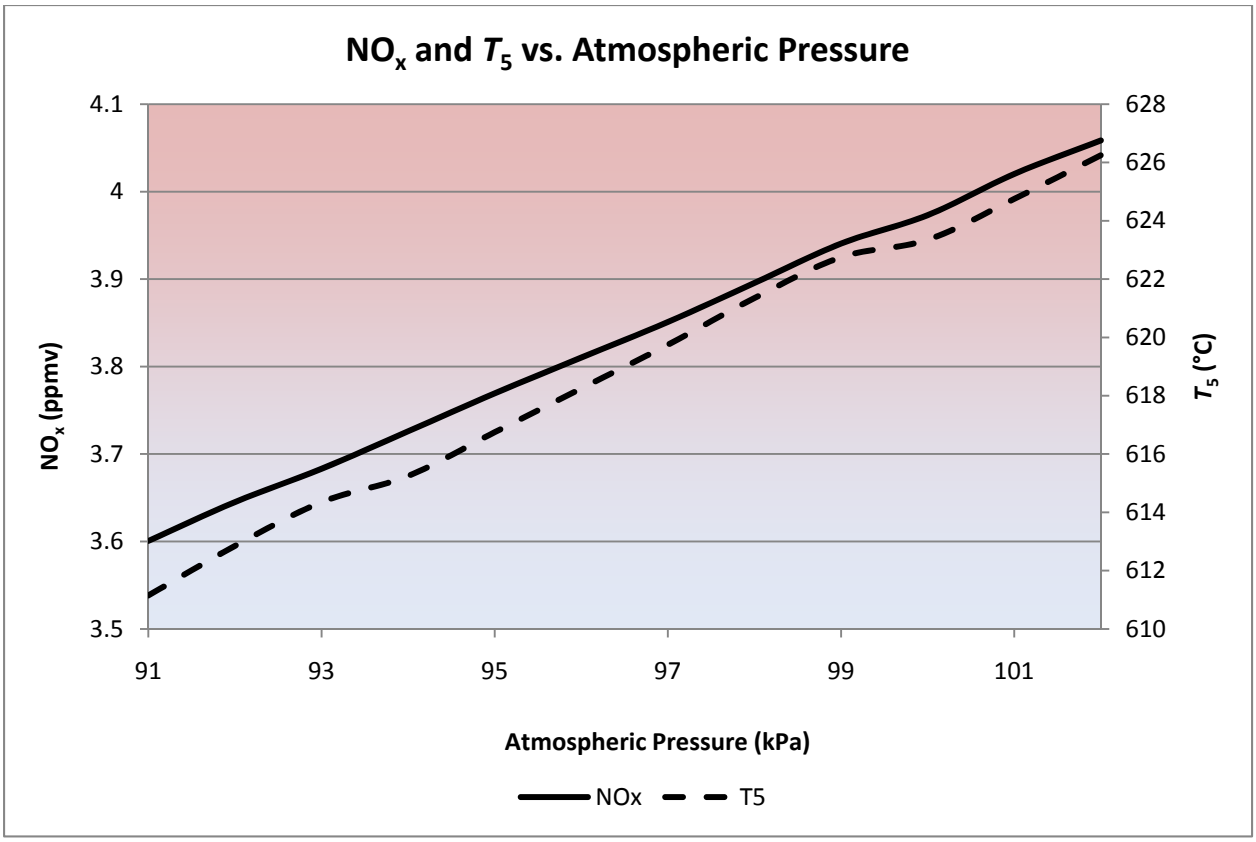

Figure 5.4 Kombust NO_x and T_5 vs. Ambient Atmospheric Pressure

The NO_x effect over this studied range is less than that of the previous analyses. However, because the variables adjusted are mutually exclusive, comparing the absolute change in NO_x over the parameter range is not beneficial. To review the relative contribution a change in combustion temperature has on the change in NO_x, it was determined that a change in T_5 relative to the change in NO_x would be a more useful comparison. A summary of this comparison is presented in Table 5.2.

Table 5.2 NO_x Concentration Change per Change in T_5

PARAMETER STUDY	$dT_5/d[NO_x]$
NO_x vs. Ambient Temperature	8.3 kmol/m^3-C
NO_x vs. Ambient Relative Humidity	N/A
NO_x vs. Ambient Atmospheric Pressure	33.0 kmol/m^3-C
NO_x vs. Combustion to Cooling Air Ratio	68.6 kmol/m^3-C
NO_x vs. Compressor Pressure Ratio	8.7 kmol/m^3-C

The variable $dT_5/d[NO_x]$ represents the change in gas-generator turbine exit temperature relative to a change in NO_x as the parameter in question is varied. As this variable decreases, the relative amount of thermal NO_x change contributing to the overall NO_x change increases, thus the contribution from other sources decreases. In other words, when a greater change in T_5 is required for a given change in NO_x concentration, other sources besides thermal NO_x must be contributing to the NO_x concentration change.

Of the three parametric studies reviewed thus far, the atmospheric pressure analysis has a lesser influence by change in thermal NO_x than does the ambient temperature analysis. The ambient relative humidity term is not applicable because T_5 was constant throughout. This difference is partly because of the constant compressor pressure ratio used, which results in combustion air density changes corresponding to the density changes of the incoming atmospheric air. This causes subsequent concentration changes of the species used in the NO_x concentration calculation.

The parameters studied thus far are ambient conditions, thus they are independent of engine's design. The remaining parameters studied are design and/or operating parameters.

NO_x vs. Combustion Air to Cooling Air Ratio

As defined by equation (39), the combustion air to cooling air ratio, r, represents the split of the incoming compressor air. This variable was changed from 0.85 to 1.15 and plotted against NO_x and T_5.

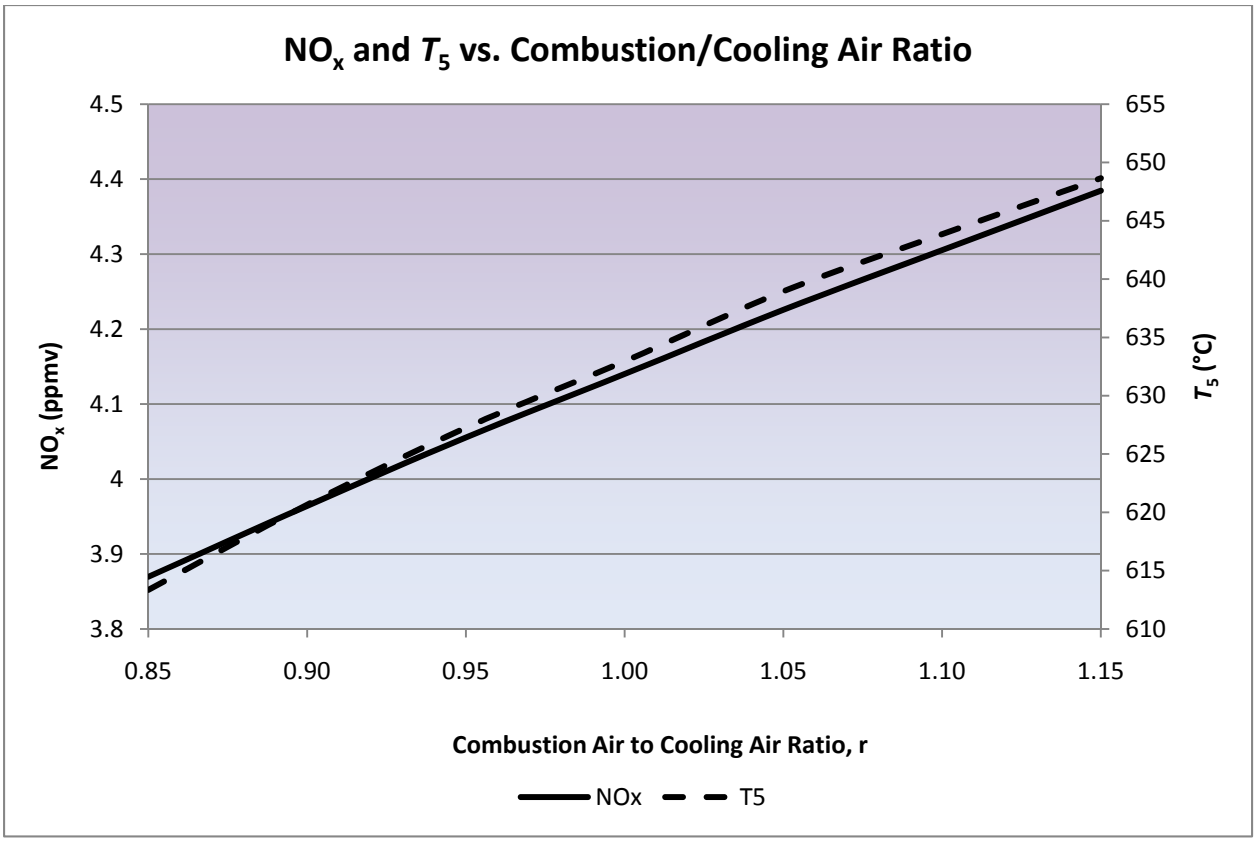

Figure 5.5 Kombust NO_x and T_5 vs. Combustion to Cooling Air Ratio

The design value for *r* is 0.94. The plot shows another near-linear influence with a very high $dT_5/d[NO_x]$ per Table 5.2. Because the cooling air acts to absorb heat from the combustion process, as more cooling air is used the average combustion air temperature decreases. However, adjusting this ratio does not affect the combustion process immediately. Only the lower temperature downstream NO_x formation is affected, hence the very high $dT_5/d[NO_x]$. It is also important to note that the equivalence ratio, and thus the fuel-air ratio, remains constant as *r* is adjusted, so the only effect is from differences in cooling air.

The final parameter reviewed is also engine-specific.

NO_x vs. Compressor Pressure Ratio

The design compressor pressure ratio is 11.7, so the parameter was ranged from 10 to 12 with more margin on the low-end in anticipation of compressor degradation. Figure 5.6 plots NO_x, T_5, and T_3 vs. *PR*.

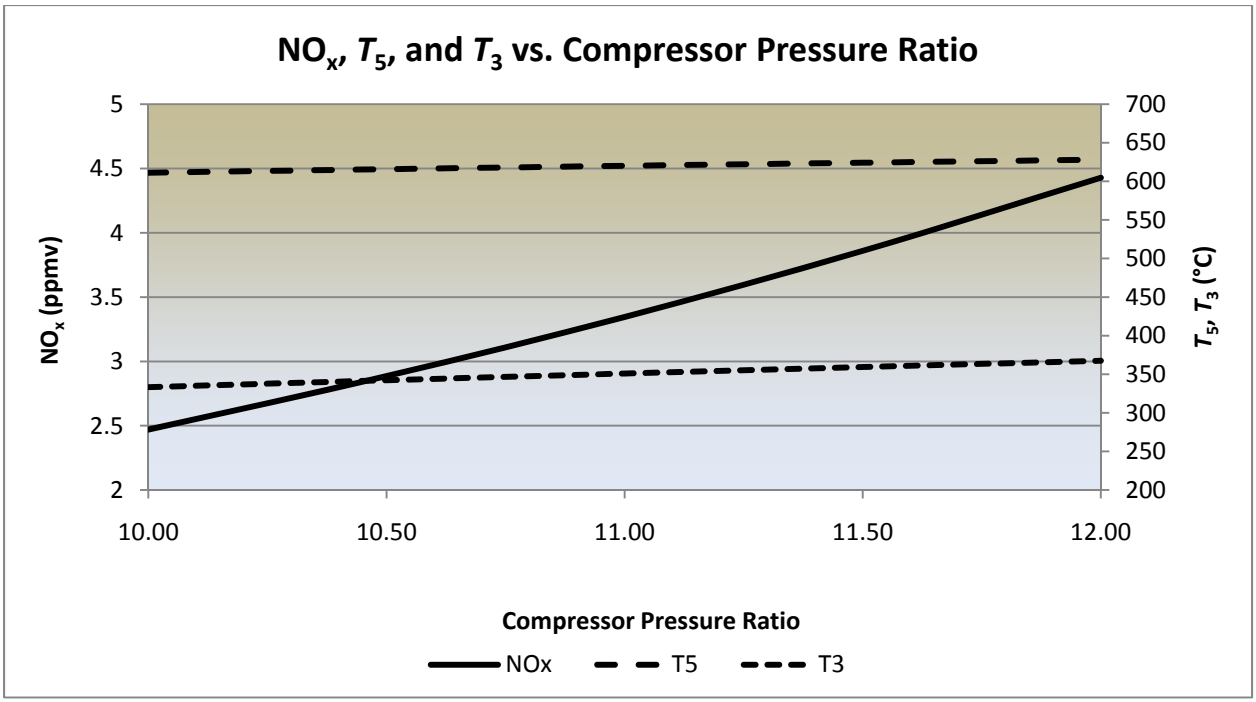

Figure 5.6 Kombust NO_x and T_5 vs. Compressor Pressure Ratio

An increase in the compressor pressure ratio results directly in an increase in combustion temperature, as the more compression done on the air creates a larger temperature increase across the compressor. This is shown directly by the T_3 line, with the parallel T_5 line indicating that all the temperature increase through the engine is a direct result of an increase in compressor exit temperature.

These studies show that the Kombust program is capable of accounting for a number of ambient and design parameters corresponding to the overall operating conditions of the combustion turbine.

CHAPTER 6 - Conclusion

The premise for this research was to investigate methods for less expensive NO_x emission monitoring that could be used on a wide-variety of combustion turbines. Specifically, the goal was to use first-principle engineering to calculate emissions from operating parameters. The expansion of this simple idea was necessitated by the complexity of the engineering principles involved with the NO_x formation and control process, as well as the significant preceding work involving similar topics.

It was ultimately determined that a mathematical combustor model based on lean-premixed combustion would be used to facilitate these goals. The modeling equations and principles were developed and transcribed into a FORTRAN computer program deemed Kombust.

The Kombust program showed valid trends and reasonable accuracy compared to the field test data when considering its limitations. There are a number of refinement opportunities suggested beyond the scope of the present research, including:

- Modeling of the pilot flame system.
- Including the chemical process for the nitrous-oxide NO_x mechanism.
- Adding the ability to model additional fuels beyond methane.
- Validation and/or modification of the heat transfer model through laboratory testing.
- Refinement of the airflow calculations to allow for part-load modeling.
- Refinement of the reactor scheme to represent recirculation.

The goal of these model refinements would be to approach an appropriate accuracy, when compared to a CEMS, such that the program could be integrated a PEMS. Further field test data and program comparisons would be necessary to establish confidence in the program; first on a specific gas turbine model, and ultimately on a family of models with similar design characteristics.

The integration of the model into a PEMS has also been briefly reviewed. As discussed in Chapter 2, the prior PEMS development was focused on primarily statistical techniques to

map the emissions over operating parameters for future prediction. The fundamental problem with this is that the emission-mapping process takes place at a certain condition of the engine that will change over time and affect its operation, including emissions. The best way to account for this is to model the turbine using first-principle concepts that will capture the effects of degradation; this was precisely the goal of this research, and the Kombust program.

The basis for potential integration of the Kombust program into a PEMS is to separate the "base" operating parameters from the "adjusting" operating parameters. The base operating parameters can initially be used to calculate a "new and clean" NO_x concentration. This "new and clean" concentration represents the NO_x produced by the engine shortly after commissioning. However, as run hours progress on the turbine, the remaining parameters may indicate deviation from the new and clean condition, and thus the calculated NO_x should be adjusted accordingly.

A potential scheme for integrating Kombust into a PEMS is shown in Figure 6.1.

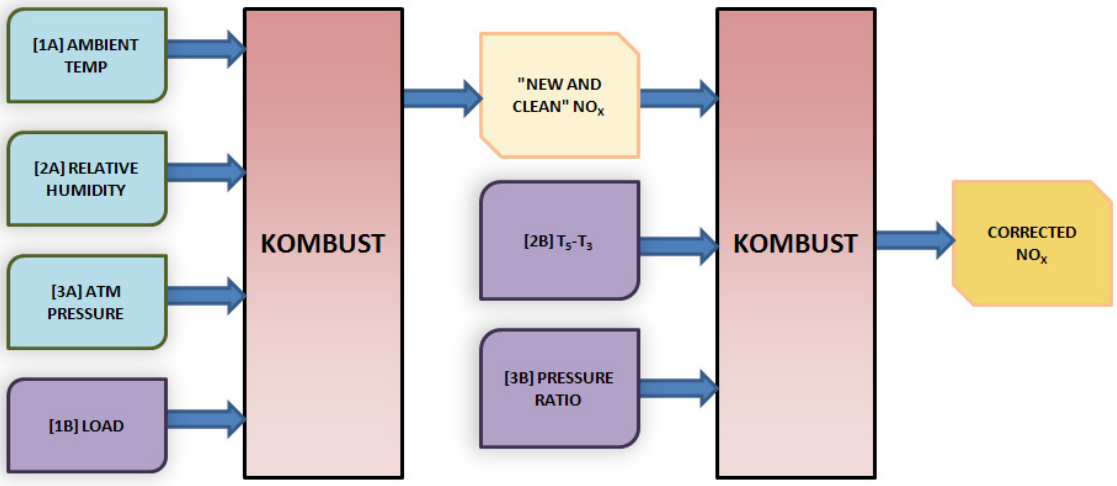

Figure 6.1 Kombust-PEMS Integration Flowchart

The input boxes labeled 1A through 3A represent ambient conditions while boxes labeled 1B through 3B represent operating parameters. The diagram represents calculating a "new and clean" NO_x value based on the ambient conditions and load. This calculation would be corrected by the T_5-T_3 and PR variables to account for component degradation and give a final, corrected

concentration of NO_x. It is in such a manner as this that the NO_x calculated by a PEMS could closely match the actual NO_x and/or that analyzed by a CEMS.

References

Bakken, L.E. and Skogly, L., "Parametric Modelling of Exhaust Gas Emission from Natural Gas Fired Turbines," ASME Paper 95-GT-399, 1995.

AirNova, 2011, www.airnova.com (05 Apr 2011)

Becker, T., and Perkavec, M.A., "The Capability of Different Semianalytical Equations for Estimation of NO_x Emissions of Gas Turbines," ASME Paper 94-GT-282, 1994.

Boyns, M. (Siemens), 2004, Personal Correspondence, Kansas State University, Manhattan, KS.

Corr, R.A., Malte, P.C., and Marinov, N.M., "Evaluation of NO_x Mechanisms for Lean Premixed Combustion," ASME Paper 91-GT-257, 1991.

Correa, S.M. and Smooke, M.D., "NO_x in Parametrically Varied Methane Flames," *Twenty-Third Symposium (International) on Combustion,* paper 51, Orleans, France, 1990.

Correa, S.M., "A Review of NO_x Formation under Gas-Turbine Combustion Conditions," *Combustion Science and Technology,* Vol. 87, pp. 329-362, 1992.

Correa, S.M., "Lean Premixed Combustion for Gas-Turbines: Review and Required Research," *Fossil Fuel Combustion*, presented at the 14th Annual Energy Sources Technology Conference and Exhibition, Houston, TX, Jan. 20-23, 1991.

Environmental Protection Agency, 2011, http://www.epa.gov/air/nitrogenoxides/ (04 Apr 2011).

Fenimore, C.P., "Formation of Nitric Oxide in Premixed Hydrocarbon Flames," *Proceedings of the 13th Symposium (International) on Combustion,* pp. 373-380, The Combustion Institute, Pittsburg, PA, 1971.

Heywood, J., *Internal Combustion Engine Fundamentals,* McGraw-Hill Science, New York, NY, 1988.

Hilt, M.B. and Waslo, J., "Evolution of NO_x Abatement Techniques Through Combustor Design for Heavy-Duty Gas Turbines," *Journal of Engineering for Gas Turbines and Power,* Vol. 106, pp.825-832, 1984.

Hung, W.S. and Langenbacher, F., "PEMS: Monitoring NO_x Emissions From Gas Turbines," ASME Paper 95-GT-415, 1995.

Hung, W.S.Y., "A Predictive Monitoring System for Gas Turbines," ASME Paper 91-GT-306, 1991.

Hung, W.S.Y., "An Experimentally Verified NO_x Emission Model for Gas Turbine Combustors," ASME Paper 75-GT-71, 1975.

Hung, W.S.Y., "PEMS: Monitoring NO_x Emissions from Gas Turbines," ASME Paper 95-GT-415, 1995.

Hung, W.S.Y., "The Reduction of NO_x Emissions from Industrial Gas Turbines," *The Eleventh International Congress on Combustion Engines,* Barcelona, Spain, Vol. 3, pp. 161-181, 1975.

Iowa State University, 2011, http://orion.math.iastate.edu/burkardt/f_src/steam/steam.f90 (14 Jan 2011).

Lefebvre, A.H., *Gas Turbine Combustion – 2nd Edition,* Taylor and Francis, Philadelphia, PA, 1999.

Leonard, G.L. and Correa, S.M., "NO_x Formation in Lean Premixed High-Pressure Methane Flames," *2nd ASME Fossil Fuel Combustion Symposium,* Vol. 30, pp. 69-75, New Orleans, LA, Jan. 14-18, 1990.

Lewis, G.D., "Prediction of NO_x Emissions", ASME Paper 81-GT-119, 1981.

Marshall, A.M., Bautista, P., "Continuous Parametric Monitoring Systems for Gas Turbines," For Presentation at the Air & Waste Management Association's 90th Annual Conference & Exhibition, Toronto, Ontario, Canada, June 8-13, 1997.

Miller, J.A. and Bowman, C.T., "Mechanism and Modeling of Nitrogen Chemistry in Combustion," *Prog. Energy Comb. Sci.,* Vol. 15, pp. 287-338, 1989.

Moran, M.J. and Shapiro, H.N., *Fundamentals of Engineering Thermodynamics – 4th Edition,* Wiley, New York, New York, 1999.

National Institute of Environmental Health Sciences, 2011, http://www.niehs.nih.gov/ (04 Apr 2011)

Nicol, D.G., Steele, R.C., Marinov, N.M., and Malte, P.C., "The Importance of the Nitrous Oxide Pathway to NO_x in Lean-Premixed Combustion," *Journal of Engineering for Gas Turbines and Power,* Vol. 117, pp. 100-111, 1995.

Pletcher, R., *Computational Fluid Mechanics and Heat Transfer – 2nd Edition,* Taylor & Francis, London, UK, 1997.

Pulkrabek, W.W., 1997, *Engineering Fundamentals of the Internal Combustion Engine*, Prentice-Hall Incorporated, Upper Saddle River, New Jersey.

Rizk, N.K. and Mongia, H.C., "Evaluation of Emission Model for Diffusion Flame, Rich/Lean, and Premixed Lean Combustors," ASME Paper 93-GT-165, 1993.

Siemens Energy, 2011, http://www.energy.siemens.com/br/en/power-generation/gas-turbines/sgt-200.htm (02 March 2011).

Toof, J.L., "A Model for the Prediction of Thermal, Prompt, and Fuel NO_x Emissions from Combustion Turbines," ASME Paper 85-GT-29, 1985.

Turns, S.R., *An Introduction to Combustion – 2nd Edition,* McGraw Hill, New York, NY, 2000.

Welty, J., *Fundamentals of Momentum, Heat, and Mass Transfer – 4th Edition,* Wiley, Hoboken, NJ, 2000.

Appendix A - Kombust Combustion Modeling Program

The following pages present the input file, primary subroutines, and output file of the Kombust program.

INPUT FILE

```
0.5      equivrat    equivalence ratio
25       tamb        ambient temperature (C)
101.325  patm        atmospheric pressure (kPa)
0.5      rh          relative humidity
11.66    pratio      compressor pressure ratio (pout/pin)
0.837    comp_eff    isentropic compressor efficiency
0.850    turb_eff    isentropic turbine efficiency
0.938    r           ratio of combustion air to cooling air
2000     tguess      temperature guess (K)
0.1      tinc        temperature increment used in iterations (K)
1.0e-4   timestp     timestep (s)
5        nmrg        number of combustion regions
1.0      comfrac     fuel fraction burnt in each region (must add to 1)
0
0
0
0
0.086    dia         diameter of each region (m)
0.086
0.165
0.165
0.165
0.13     lnth        length of each region (m)
0.13
0.1
0.1
0.0869
0.0012   t_w         liner wall thickness of each region (m)
0.0012
0.0012
0.0012
0.0012
35       vel         average air velocity in each region (m/s)
35
12
12
12
0.7      e_w         emissivity of liner wall
0.4      e_c         emissivity of casing
26       k_w         thermal conductivity of liner (W/m*k)
8.33     h_perc      hydrogen content of fuel (%-mass)
0.03     an_gap      annulus air gap between liner and casing
1.0      dia_case    casing diameter
```

```
program main
include 'var.i'


call input
call chemsetup
call adflame
call t4calc
call eq_nox
call t5calc
call output




end
```

INPUT

```
      subroutine input
      include 'var.i'



      open(10,file='komin.inp')


!-------------------------------------------------------------------------------------------
      !READ STATEMENTS

      read(10,*) equivrat
      read(10,*) tamb
      read(10,*) patm
      read(10,*) rh
      read(10,*) pratio
      read(10,*) comp_eff
      read(10,*) turb_eff
      read(10,*) r
      read(10,*) tguess
      read(10,*) tinc
      read(10,*) timestep
      read(10,*) nmrg

      do j=1, nmrg
      read(10,*) comfrac(j)
      enddo

      do j=1, nmrg
      read(10,*) dia(j)
      enddo

      do j=1, nmrg
      read(10,*) lnth(j)
      enddo

      do j=1, nmrg
      read(10,*) t_w(j)
      enddo

      do j=1, nmrg
      read(10,*) vel(j)
      enddo

      read(10,*) e_w
      read(10,*) e_c
      read(10,*) k_w
      read(10,*) h_perc
      read(10,*) an_gap
      read(10,*) dia_case



!-------------------------------------------------------------------------------------------
      !WRITE STATEMENTS

      write(*,*) equivrat,
     1  'equivrat, Equivalence ratio'
      write(*,*) tamb,
     1  'tamb, Ambient temperature, C'
      write(*,*) patm,
     1  'patm, Ambient pressure, kPa'
      write(*,*) rh,
     1  'rh, Ambient relative humidity'
      write(*,*) pratio,
     1  'pratio, Compressor pressure ratio'
      write(*,*) comp_eff,
     1  'comp_eff, Isentropic compressor efficiency'
      write(*,*) turb_eff,
```

```
     1  'turb_eff, Isentropic turbine efficiency'
      write(*,*) r,
     1  'r, Combustion air to cooling air ratio'
      write(*,*) tguess,
     1  'tguess, Initial adiabatic flame temperature guess, K'
      write(*,*) tinc,
     1  'tinc, Temperature increment for temp calcs'
      write(*,*) timestep,
     1  'timestep, Timestep for NOx calculation, s'
      write(*,100) nmrg
100   format(i5, t26, 'numreg, Number of modeling regions')

      write(*,*) 'comfrac, Combustion fraction in each zone'
      do j=1, nmrg
      write(*,*) j, comfrac(j)
      enddo

      write(*,*) 'dia, Combustion zone diameter'
      do j=1, nmrg
      write(*,*) j, dia(j)
      enddo

      write(*,*) 'lnth, Combustion zone length'
      do j=1, nmrg
      write(*,*) j, lnth(j)
      enddo

      write(*,*) 't_w, Liner wall thickness'
      do j=1, nmrg
      write(*,*) j, t_w(j)
      enddo

      write(*,*) 'vel, Air velocity in each zone'
      do j=1, nmrg
      write(*,*) j, vel(j)
      enddo

      write(*,*) e_w,
     1  'e_w, Liner emissivity'
      write(*,*) e_c,
     1  'e_c, Casing emissivity'
      write(*,*) k_w,
     1  'k_w, Liner thermal conductivity, W/m*k'
      write(*,*) h_perc,
     1  'h_perc, Hydrogen content of fuel, %-mass'
      write(*,*) an_gap,
     1  'an_gap, Annulus air gap, m'
      write(*,*) dia_case,
     1  'dia_case, Casing diameter, m'




      return
      end
```

```
subroutine chemsetup
!CHEMSETUP DETERMINES CHEMICAL EQUATION COEFFICIENTS BASED ON COMBUSTION
!WITH MOIST AIR AND EQUIVALENCE RATIO
include 'var.i'

!zr*FUEL + a*O2 + a3*N2 + a1*H2O + a2*CO2 -> b*CO2 + c*H2O + d*N2 + e*O2 + zp*FUEL

zr(1) = 1
zp(nmrg)=0

do i=1, nmrg-1
zp(i)=zr(i) - comfrac(i)
zr(i+1)=zp(i)
enddo

!CONVERT AMBIENT TEMPERATURE TO KELVIN
tamb=tamb + 273.15

!DETERMINE SATURATION PRESSURE, CONVERT TO kPa
call psat(tamb, psatu, rhol, rhov)
psatu=psatu*1000

!HUMIDITY MOLE RATIO AND AIR MOLE FRACTION FROM REL. HUMIDITY AND SAT. PRESSURE
humr=1.608*(0.622/((patm/(rh*psatu)) - 1))
xa=1.0/(1.0 + humr)

!FUEL MOLECULAR WEIGHT (METHANE FUEL ONLY (CH4))
fuelmw=ch4mw

!STOICHIOMETRIC AIR COEFFICIENT (METHANE FUEL ONLY)
a_st=2

!STOICHIOMETRIC FUEL-AIR RATIO
fstoi=(1.0*fuelmw)/(4.76*a_st*airmw)

!ACTUAL FUEL-AIR RATIO BASED ON EQUIVALENCE RATIO
fact=equivrat*fstoi

!ACTUAL AIR COEFFICIENTS FOR INITIAL ZONE
a(1)=(1.0*fuelmw)/(fact*4.76*airmw)
a1(1)=a(1)/xa - a(1)
a2(1)=0
a3(1)=3.76*a(1)

!CALCULATE ACTUAL COEFFICENTS OF PRODUCTS (METHANE FUEL ONLY)
do i=1, nmrg

b(i)=zr(i) + a2(i) - zp(i)                          !CARBON BALANCE
c(i)=2*zr(i) + a1(i) - 2*zp(i)                      !HYDROGEN BALANCE
d(i)=a3(i)                                          !NITROGEN BALANCE
e(i)=(2*a(i) + a1(i) + 2*a2(i) - 2*b(i) - c(i))/2   !OXYGEN BALANCE

if(i .lt. nmrg)then
!PRODUCTS CARRIED OVER AS REACTANTS TO NEXT ZONE
a(i+1)=e(i)
a3(i+1)=d(i)
a1(i+1)=c(i)
a2(i+1)=b(i)
endif

enddo
```

```
!NUMBER OF MOLES OF MOIST COOLING AIR BASED ON r
a_coola=a(1)/r
a1_coola=a_coola/xa - a_coola

do i=1, nmrg
!MOLE FRACTIONS IN COMBUSTION ZONES
co2frac(i)=b(i)/(b(i) + c(i) + d(i) + e(i) + zp(i))
h2ofrac(i)=c(i)/(b(i) + c(i) + d(i) + e(i) + zp(i))
n2frac(i) =d(i)/(b(i) + c(i) + d(i) + e(i) + zp(i))
o2frac(i) =e(i)/(b(i) + c(i) + d(i) + e(i) + zp(i))
enddo

!AIR MOLE FRACTIONS
 o2frac_a=     a_coola/(a_coola + 3.76*a_coola + a1_coola)
 n2frac_a=3.76*a_coola/(a_coola + 3.76*a_coola + a1_coola)
h2ofrac_a=    a1_coola/(a_coola + 3.76*a_coola + a1_coola)




return
end
```

```
      subroutine adflame
      include 'var.i'

      !GET CONVECTIVE HEAT TRANSFER COEFFICIENT FROM CASING TO AMBIENT FROM extern_heatxfer SUBROUTINE
      call extern_heatxfer

      !CALCULATE COMBUSTOR INLET TEMPERATURE BASED ON COMPRESSOR PRESSURE RATIO,
      !ISENTROPIC IDEAL GAS RELATIONSHIP, AND COMPRESSOR EFFICIENCY ASSUMING
      !CONSTANT Cp
      p=pratio*patm
      tin_s=tamb*((pratio)**((air_k - 1)/air_k))
      tin(1)=tamb + (tin_s - tamb)/comp_eff
      tca(1)=tin(1)

      !COMBUSTION AIR MASS FLOW RATE
      mcomba=((p*airmw)/(rbar*tin(1)))*vel(1)*0.25*pi*dia(1)**2
      !COOLING AIR MASS FLOW RATE
      do i=1, nmrg
      mca(i)=mcomba/r
      enddo
      !FUEL MOLAR FLOW RATE
      nf=(mcomba*fact)/fuelmw

      !=====================================================================

        do 1000 i=1, nmrg
        zz1 = 0
        zz2 = 0
        xx1 = 0
        xx2 = 0

      if(i .gt. 1) tin(i) = t(i-1)

      area(i) = lnth(i)*pi*dia(i)

      !H_RHS = DELTAH(REACTANTS) + ENT_FORMATION(REACTANTS) - ENT_FORMATION(PRODUCTS)
      !LHS = DELTAH(PRODUCTS)
      h_rhs(i) = zr(i)*delh_ch4(tin(i)) + a(i)*delh_o2(tin(i)) +
     1  a3(i)*delh_n2(tin(i)) + a1(i)*delh_h2o(tin(i)) +
     2  a2(i)*delh_co2(tin(i)) + zr(i)*hf_ch4 + a1(i)*hf_h2o +
     3  a2(i)*hf_co2 - b(i)*hf_co2 - c(i)*hf_h2o - zp(i)*hf_ch4

      if(i .eq. 1)then
      t(i)=tguess
      else
      t(i) = t(i-1)
      endif

      !---------------------------------------------------------------------
          do 500 j=1, maxit
          if(j .eq. maxit)then
          write(*,*) 'Combustion temp calc not converged'
          write(15,*) 'Combustion temp calc not converged'
          call exit(0)
          endif

      if(i .gt. 1 .and. j .eq. 1) tca(i) = tca(i-1)
      if(i .eq. 1)then
      qn(i) = 0
      goto 400
      endif

      call heatxfer
      !qn(i) = (( -(r_1(i) + c_1(i))*area(i) ) /nf ) /8
      qn(i) = 0

  400 if(b(i)*delh_co2(t(i)) + c(i)*delh_h2o(t(i)) +
     1   d(i)*delh_n2(t(i)) + e(i)*delh_o2(t(i)) +
     2   zp(i)*delh_ch4(t(i)) - qn(i)
     3   .gt. h_rhs(i))
     4then
         t(i)=t(i) - tinc
         zz1=zz1+1
```

```
      else
        t(i)=t(i) + tinc
        zz2=zz2+1
      endif
      if(zz1 .gt. 0 .and. zz2 .gt. 0) exit


500       continue

      !---------------------------------------------------------------------

      if(i.eq.1)then
      call TPEQUIL(equivrat,t(i),p,h_mofc(i),o_mofc(i),n_mofc(i),h2_mofc(i),
     1oh_mofc(i),co_mofc(i),no_mofc(i),o2_mofc(i),h2o_mofc(i),co2_mofc(i),
     2n2_mofc(i),zr(i),zp(i),a1(i),a(i),i)
      endif

      !COOLING AIR ZONES TEMPERATURE CALCULATION
      if(i .gt. 1)then

      !---------------------------------------------------------------------

          do 600 j=1, maxit
          if(j .eq. maxit)then
          write(*,*) 'Cooling air temp calc not converged'
          call exit(0)
          endif

      q_amb(i) = h_amb*pi*dia_case*lnth(i)*((tca(i)-0.6*tca(i)) - tamb)

      if( (mca(i-1)*(delh_air(tca(i-1))/airmw) -
     1    qn(i-1)*nf - q_amb(i)) / mca(i)
     2   .gt. delh_air(tca(i))/airmw)
     3then
        tca(i)=tca(i) + tinc
        xx1=xx1 + 1
      else
        tca(i)=tca(i) - tinc
        xx2=xx2 + 1
      endif

      if(xx1 .gt. 0 .and. xx2 .gt. 0) exit


600       continue

      !---------------------------------------------------------------------
      endif


        write(*,*) i, t(i), tca(i)
1000    continue

      !=====================================================================

      return


      end
```

EXTERN_HEATXFER

```
      subroutine extern_heatxfer
      include 'var.i'

      double precision k_atm, nud

      !EXTERNAL HEAT TRANSFER CALC


      Pr = 0.71       !PRANDTL NUMBER
      v = 3           !ASSUME AIR SPEED OF 3 m/s
      u_atm = ( 2.27e-8*( (1.8*(tamb))**1.5/(1.8*(tamb)+198.6) ) )*47.88
      k_atm = 2.495e-3*tamb**1.5/(tamb+194)

      !REYNOLDS NUMBER
      Red = ( ((patm*airmw)/(rbar*(tamb)))*v*dia_case ) / u_atm


      !EXPERIMENTAL NUSSELT NUMBER CORRELATION FOR A SINGLE CYLINDER WITH FORCED CONVECTION
      !FROM WELTY, "FUNDAMENTALS OF MOMENTUM, HEAT, AND MASS TRANSFER, 4TH ED, PP. 328
      nud = 0.3+((0.62*Red**0.5*Pr**(1/3))/(1 + (0.4/Pr)**(2/3))**0.25)*
     1      (1 + (Red/282000)**(5/8))**(4/5)

      h_amb = (nud*k_atm)/dia_case


      return

      end
```

```
      subroutine heatxfer
      include 'var.i'

      k=1

      !LUMINOSITY, BEAM LENGTH, AND COMBUSTION GAS EMISSIVITY
      lum = 336/h_perc**2
      l_b = 0.8*dia(1)
      e_g(i) = 1 - exp(-290*p*lum*(fact*l_b)**0.5*t(i)**-1.5)

      !DYNAMIC VISCOSITY OF AIR FROM SUTHERLAND'S FORMULA
      !THERMAL CONDUCTIVITY OF AIR FROM:
      !COMPUTATIONAL FLUID MECHANICS AND HEAT TRANSFER TAYLOR AND FRANCIS, 1997, p. 259.

      u_g = ( 2.27e-8*( (1.8*t(i))**1.5/(1.8*t(i)+198.6) ) )*47.88
      k_g = 2.495e-3*t(i)**1.5/(t(i)+194) !0.157
      u_a = ( 2.27e-8*( (1.8*tca(i))**1.5/(1.8*tca(i)+198.6) ) )*47.88
      k_a = 2.495e-3*tca(i)**1.5/(tca(i)+194)!0.0553

      !RADIATION BETWEEN COMBUSTION GASES AND LINER WALL
      !R1 = r1c1 - r1c2*Tw1**2.5
      r1c2 = 0.5*sig*(1 + e_w)*e_g(i)*t(i)**1.5
      r1c1 = r1c2*t(i)**2.5

      !RADIATION BETWEEN LINER WALL AND CASING
      !R2 = r2c1*Tw2**4 - r2c2
      r2c1 = 0.5*sig
      r2c2 = r2c1*tca(i)**4

      !CONVECTION BETWEEN COMBUSTION GASES AND LINER WALL
      !C1 = c1c2 - c1c1*Tw1
      c1c1 = 0.02*(k_g/dia(i)**0.2)*(mcomba/(0.25*pi*dia(i)**2*u_g))**0.8
      c1c2 = c1c1*t(i)

      !CONVECTION BETWEEN LINER WALL AND COOLING AIR
      !C2 = c2c1*Tw2 - c2c2
      !ASSUME LINER AND CASING ARE CONCENTRIC CYLINDERS
      ca_dia = dia(i) + 2*an_gap              !CASING DIAMETER
      a_an = 0.25*pi*(ca_dia**2 - dia(i)**2)  !ANNULUS AREA
      c2c1 = 0.02*(k_a/(2*an_gap)**0.2)*
     1       (mca(i)/(a_an*u_a))**0.8
      c2c2 = c2c1*tca(i)

      !INITIAL GUESS FOR Tw2
      tw2(i) = t(i) - 500

      zx1 = 0
      zx2 = 0

      !LOOP TO SOLVE FOR Tw1 and Tw2
      !-------------------------------------------------------------------------
      do 100 k=1, maxit
       if(k .eq. maxit)then
       write(*,*) 'Heat transfer calc not converged'
       write(17,*) k, 'Heat transfer calc not converged'
       call exit(0)
       endif

      !CALCULATE R2 and C2 based on Tw2 guess
      r_2(i) = r2c1*tw2(i)**4 - r2c2
      c_2(i) = c2c1*tw2(i) - c2c2
      !CALCULATE Tw1
      tw1(i) = (t_w(i)/k_w)*(r_2(i) + c_2(i)) + tw2(i)
      !CALCULATE R1 and C1 based on Tw1
```

```
      r_1(i) = r1c1 - r1c2*tw1(i)**2.5
      c_1(i) = c1c2 - c1c1*tw1(i)

      zz1 = r_1(i) + c_1(i)
      zz2 = r_2(i) + c_2(i)


      if(r_1(i) + c_1(i) .gt. r_2(i) + c_2(i)) then
      tw2(i) = tw2(i) + tinc
      zx1 = zx1 + 1
      endif
      if(r_1(i) + c_1(i) .lt. r_2(i) + c_2(i)) then
      tw2(i) = tw2(i) - tinc
      zx2 = zx2 + 1
      endif

      if(zx1 .gt. 0 .and. zx2 .gt. 0) exit



  100 continue

      !------------------------------------------------------------------------------




      return
      end
```

```
 double precision function delh_ch4(tmpfc)

 include 'var.i'

 double precision tta,ttaref,tmpfc
 tta=tmpfc/100
 ttaref=tref/100

 delh_ch4=100*(
1                                alp_ch4*(tta - ttaref) +
2         (bet_ch4/(betx_ch4 + 1))*
3          (tta**(betx_ch4 + 1) - ttaref**(betx_ch4 + 1)) +
4         (gam_ch4/(gamx_ch4 + 1))*
5          (tta**(gamx_ch4 + 1) - ttaref**(gamx_ch4 + 1)) +
6         (del_ch4/(delx_ch4 + 1))*
7          (tta**(delx_ch4 + 1) - ttaref**(delx_ch4 + 1))
8             )

 end

 !-------------------------------------------------------------------------------!

 double precision function delh_o2(tmpfc)

 include 'var.i'

 double precision tta,ttaref,tmpfc
 tta=tmpfc/100
 ttaref=tref/100

 delh_o2=100*(
1                                alp_o2 *(tta - ttaref) +
2         (bet_o2 /(betx_o2  + 1))*
3          (tta**(betx_o2  + 1) - ttaref**(betx_o2  + 1)) +
4         (gam_o2 /(gamx_o2  + 1))*
5          (tta**(gamx_o2  + 1) - ttaref**(gamx_o2  + 1)) +
6         (del_o2 /(delx_o2  + 1))*
7          (tta**(delx_o2  + 1) - ttaref**(delx_o2  + 1))
8            )

 end

 !-------------------------------------------------------------------------------!

 double precision function delh_n2(tmpfc)

 include 'var.i'

 double precision tta,ttaref,tmpfc
 tta=tmpfc/100
 ttaref=tref/100

 delh_n2=100*(
1                                alp_n2 *(tta - ttaref) +
2         (bet_n2 /(betx_n2  + 1))*
3          (tta**(betx_n2  + 1) - ttaref**(betx_n2  + 1)) +
4         (gam_n2 /(gamx_n2  + 1))*
5          (tta**(gamx_n2  + 1) - ttaref**(gamx_n2  + 1)) +
6         (del_n2 /(delx_n2  + 1))*
7          (tta**(delx_n2  + 1) - ttaref**(delx_n2  + 1))
8            )

 end

 !-------------------------------------------------------------------------------!

 double precision function delh_h2o(tmpfc)
```

```
 include 'var.i'

 double precision tta,ttaref,tmpfc
 tta=tmpfc/100
 ttaref=tref/100

 delh_h2o=100*(
1                                 alp_h2o *(tta - ttaref) +
2         (bet_h2o /(betx_h2o  + 1))*
3          (tta**(betx_h2o  + 1) - ttaref**(betx_h2o  + 1)) +
4         (gam_h2o /(gamx_h2o  + 1))*
5          (tta**(gamx_h2o  + 1) - ttaref**(gamx_h2o  + 1)) +
6         (del_h2o /(delx_h2o  + 1))*
7          (tta**(delx_h2o  + 1) - ttaref**(delx_h2o  + 1))
8             )

 end

 !------------------------------------------------------------------------------------!

 double precision function delh_co2(tmpfc)

 include 'var.i'

 double precision tta,ttaref,tmpfc
 tta=tmpfc/100
 ttaref=tref/100

 delh_co2=100*(
1                                 alp_co2 *(tta - ttaref) +
2         (bet_co2 /(betx_co2  + 1))*
3          (tta**(betx_co2  + 1) - ttaref**(betx_co2  + 1)) +
4         (gam_co2 /(gamx_co2  + 1))*
5          (tta**(gamx_co2  + 1) - ttaref**(gamx_co2  + 1)) +
6         (del_co2 /(delx_co2  + 1))*
7          (tta**(delx_co2  + 1) - ttaref**(delx_co2  + 1))
8             )

 end

 !------------------------------------------------------------------------------------!

 double precision function delh_air(tmpfc)

 include 'var.i'

 double precision tta,ttaref,tmpfc
 tta=tmpfc/100
 ttaref=tref/100

 delh_air=o2frac_a*100*(
1                                 alp_o2 *(tta - ttaref) +
2         (bet_o2 /(betx_o2  + 1))*
3          (tta**(betx_o2  + 1) - ttaref**(betx_o2  + 1)) +
4         (gam_co2 /(gamx_co2  + 1))*
5          (tta**(gamx_o2  + 1) - ttaref**(gamx_o2  + 1)) +
6         (del_co2 /(delx_co2  + 1))*
7          (tta**(delx_o2  + 1) - ttaref**(delx_o2  + 1))
8                       ) +
9         n2frac_a*100*(
1                                 alp_n2 *(tta - ttaref) +
2         (bet_n2 /(betx_n2  + 1))*
3          (tta**(betx_n2  + 1) - ttaref**(betx_n2  + 1)) +
4         (gam_n2 /(gamx_n2  + 1))*
5          (tta**(gamx_n2  + 1) - ttaref**(gamx_n2  + 1)) +
6         (del_n2 /(delx_n2  + 1))*
```

```
         (tta**(delx_n2  + 1) - ttaref**(delx_n2  + 1))
                    )

 end

 !--------------------------------------------------------------------------------------!
```

```
      subroutine eq_nox

      include 'var.i'

      double precision r1, r2, r3, k1_f, k2_f, k3_f, nmixwet_15,
     1nmixdry_15, fraco2_wet, fraco2_dry, nmixwet_act, nmixdry_act, tmp
      dimension r1(mxrg), r2(mxrg), r3(mxrg)



      do i=1, nmrg


      k1_f=1.8e11*exp(-38370/t(i))
      k2_f=1.8e7*exp(-4680/t(i))
      k3_f=7.1e10*exp(-450/t(i))

      timetot(i)=lnth(i)/vel(i)
      numit(i)=int(timetot(i)/timestep)

      !MOLAR CONCENTRATIONS IN COMBUSTION ZONE BASED ON TURNS EQUILIBRIUM CODE (kmol/m^3)
      o_con(i)  =((o_mofc(1)*p)/(rbar*t(i)))
      n_con(i)  =((n_mofc(1)*p)/(rbar*t(i)))
      h2_con(i) =((h2_mofc(1)*p)/(rbar*t(i)))
      oh_con(i) =((oh_mofc(1)*p)/(rbar*t(i)))
      co_con(i) =((co_mofc(1)*p)/(rbar*t(i)))
      no_con(i) =((no_mofc(1)*p)/(rbar*t(i)))
      o2_con(i) =((o2_mofc(1)*p)/(rbar*t(i)))
      h2o_con(i)=((h2o_mofc(1)*p)/(rbar*t(i)))
      co2_con(i)=((co2_mofc(1)*p)/(rbar*t(i)))
      n2_con(i) =((n2_mofc(1)*p)/(rbar*t(i)))

      r1(i)=k1_f*o_con(i)*n2_con(i)
      r2(i)=k2_f*n_con(i)*o2_con(i)
      r3(i)=k3_f*n_con(i)*oh_con(i)

          do j=1, numit(i)

      !HEYWOOD NOX CORRELATION PG. 574
      nocon=nocon+
     1      (
     2      (2*r1(i)*(1 - (nocon/no_con(i))**2)) /
     3      (1 + ((nocon/no_con(i))*r1(i))/(r2(i)+r3(i)))
     4      ) * timestep



          enddo

      enddo


      !NOX CONCENTRATION IN COMBUSTION ZONE (ppmv = noxfrac * 10^6)
      noxppmv_cma_wt = ( ((nocon)*rbar*t(nmrg))/p ) * 10**6
      noxppmv_tot_wt = noxppmv_cma_wt/(1+(1/r)+((airmw*fact)/fuelmw))

      !RECALCULATE COMPLETE COMBUSTION COEFFICIENTS TO ACCOUNT FOR COOLING AIR DILUTION
      !zr*FUEL + a*O2 + a3*N2 + a1*H2O + a2*CO2 -> b*CO2 + c*H2O + d*N2 + e*O2 + zp*FUEL
      ftot = fact + r*fact

      atot = (1.0*fuelmw)/(ftot*4.76*airmw)
      a1tot = atot/xa - atot
      a2tot = 0
      a3tot = 3.76*atot
```

```
 btot = 1
 ctot = a1tot + 2
 dtot = a3tot
 etot = atot - 1

 !CORRECT NOX TO 15% O2
 !SEE TURNS, PG. 556

 !ACTUAL O2 FRACTIONS, WET AND DRY BASIS
 fraco2_wet = etot / (btot+ctot+dtot+etot)
 fraco2_dry = etot / (btot+dtot+etot)

 !TOTAL NUMBER OF MOLES AT 15% O2, WET AND DRY BASIS
 nmixwet_15 = 4.76* ( (btot + (1+0.15))/(1 - 4.76*0.15) ) + 1
 nmixdry_15 = 4.76* ( (btot + (1-0.15))/(1 - 4.76*0.15) ) - 1

 !ACTUAL TOTAL NUMBER OF MOLES, WET AND DRY BASIS
 nmixwet_act = 4.76*
1              ( (btot + (1+fraco2_wet))/(1 - 4.76*fraco2_wet) )
2               + 1
 nmixdry_act = 4.76*
1              ( (btot + (1-fraco2_dry))/(1 - 4.76*fraco2_dry) )
2               - 1


 !CORRECT ACTUAL NOX TO DRY BASIS
 noxppmvact_dry = noxppmv_tot_wt * (nmixwet_act/nmixdry_act)

 !NOX CONCENTRATION CORRECTED TO 15% O2, WET AND DRY BASIS
 noxppmv15_wet = noxppmv_tot_wt*(nmixwet_act/nmixwet_15)
 noxppmv15_dry = noxppmvact_dry*(nmixdry_act/nmixdry_15)


 end
```

```
      subroutine t4calc
      include 'var.i'


      !ENERGY BALANCE AT COMBUSTOR EXIT (ENTHALPYS ARE PER UNIT MASS)
      !(1 + fact)hcombp_m + (1/r)ha_m = (1 + 1/r + fact)he_m
      !r = comba/coola
      !ENTHALPY PER MASS IS ENTHALPY PER MOLE DIVIDED BY MOLEULAR WEIGHT
      !h = h_/M

      !ADD MOLES OF MOIST COOLING AIR TO COMBUSTION PRODUCTS
      c_tot=c(nmrg) + a1_coola
      d_tot=d(nmrg) + 3.76*a_coola
      e_tot=e(nmrg) + a_coola

      !ADDITIONAL MOLE FRACTIONS
      co2frac_e=   b(nmrg)/(b(nmrg) + c_tot + d_tot + e_tot)
      h2ofrac_e=     c_tot/(b(nmrg) + c_tot + d_tot + e_tot)
       n2frac_e=     d_tot/(b(nmrg) + c_tot + d_tot + e_tot)
       o2frac_e=     e_tot/(b(nmrg) + c_tot + d_tot + e_tot)

      !MOLECULAR WEIGHT OF MIXES
      mw_combp=co2frac(nmrg)*co2mw + h2ofrac(nmrg)*h2omw +
     2         n2frac(nmrg)*n2mw + o2frac(nmrg)*o2mw
      mw_e=co2frac_e*co2mw + h2ofrac_e*h2omw + n2frac_e*n2mw
     1     + o2frac_e*o2mw

      !ENTHALPY CALCULATIONS
      ha=o2frac_a*delh_o2(tca(nmrg)) + n2frac_a*delh_n2(tca(nmrg)) +
     1   h2ofrac_a*delh_h2o(tca(nmrg)) + h2ofrac_a*hf_h2o
      hcombp=co2frac(nmrg)*delh_co2(t(nmrg)) +
     1       h2ofrac(nmrg)*delh_h2o(t(nmrg)) +
     2       n2frac(nmrg)*delh_n2(t(nmrg)) +
     3       o2frac(nmrg)*delh_o2(t(nmrg)) +
     4       h2ofrac(nmrg)*hf_h2o + co2frac(nmrg)*hf_co2
      he=(((1.0 + fact)*(hcombp/mw_combp) + (1.0/r)*(ha/airmw))*mw_e)/
     1   (1 + 1.0/r + fact)
      he_i=he - h2ofrac_e*hf_h2o - co2frac_e*hf_co2


      t4=tguess
      xxy1 = 0
      xxy2 = 0

      do j=1, maxit
      if(co2frac_e*delh_co2(t4) + h2ofrac_e*delh_h2o(t4) +
     1   n2frac_e*delh_n2(t4) + o2frac_e*delh_o2(t4) .gt. he_i)
     2then
        t4=t4 - tinc
        xxy1 = xxy1 + 1
      else
        t4=t4 + tinc
        xxy2 = xxy2 + 1
      endif

      if(xxy1 .gt. 0 .and. xxy2 .gt. 0) exit

      enddo



      return
      end
```

```
      subroutine t5calc
      include 'var.i'


      !WORK OF COMPRESSOR = WORK OF GAS GENERATOR TURBINE
      !nt(h3-h2) = (1+f)(h4-h5), h4=he from t4calc
      !ENTHALPY PER MASS IS ENTHALPY PER MOLE DIVIDED BY MOLEULAR WEIGHT
      !h = h_/M
      !h2, h3, and h5 all enthalpy per mole
      h2=o2frac_a*delh_o2(tamb) + n2frac_a*delh_n2(tamb) +
     1   h2ofrac_a*delh_h2o(tamb) + h2ofrac_a*hf_h2o
      h3=o2frac_a*delh_o2(tin(1)) + n2frac_a*delh_n2(tin(1)) +
     1   h2ofrac_a*delh_h2o(tin(1)) + h2ofrac_a*hf_h2o
      h5=(he/mw_e - (turb_eff*((h3/airmw) - (h2/airmw))/(1+fact)))*mw_e

      h5_i=h5 - h2ofrac_e*hf_h2o - co2frac_e*hf_co2


      t5=tguess
      xyy1 = 0
      xyy2 = 0

      do j=1, maxit
      if(co2frac_e*delh_co2(t5) + h2ofrac_e*delh_h2o(t5) +
     1   n2frac_e*delh_n2(t5) + o2frac_e*delh_o2(t5) .gt. h5_i)
     2then
        t5=t5 - tinc
        xyy1 = xyy1 + 1
      else
        t5=t5 + tinc
        xyy2 = xyy2 + 1
      endif

      if(xyy1 .gt. 0 .and. xyy2 .gt. 0) exit

      enddo



      return
      end
```

```
subroutine output
include 'var.i'

open(11,file='komout.out')


write(11,100) equivrat
write(11,101) tamb-273.15
write(11,102) patm
write(11,103) rh
write(11,104) pratio
write(11,105) comp_eff
write(11,106) turb_eff
write(11,107) tguess
write(11,109) tinc
write(11,110) timestep
write(11,111) nmrg

do j=1, nmrg
write(11,112) j, comfrac(j)
enddo

do j=1, nmrg
write(11,113) j, dia(j)
enddo

do j=1, nmrg
write(11,114) j, lnth(j)
enddo

do j=1, nmrg
write(11,156) j, t_w(j)
enddo

do j=1, nmrg
write(11,115) j, vel(j)
enddo

write(11,118) e_w
write(11,119) e_c
write(11,157) k_w
write(11,158) h_perc
write(11,159) an_gap
write(11,161) dia_case


write(11,117)
write(11,150) fact
write(11,151) tin(1)-273.15
write(11,152) t4-273.15
write(11,153) t5-273.15
write(11,154) t5-tin(1)
write(11,162) t5-tamb
write(11,155) noxppmv_tot_wt
write(11,163) noxppmvact_dry
write(11,164) noxppmv15_wet
write(11,165) noxppmv15_dry
do j=1, nmrg
write(11,200) j, t(j)
enddo
```

```
100 FORMAT('Equivalence Ratio                          = ',F12.4)
101 FORMAT('Ambient Temperature                  (C) = ',F12.4)
102 FORMAT('Ambient Pressure                   (kPa) = ',F12.4)
103 FORMAT('Relative Humidity                    (%) = ',F12.4)
104 FORMAT('Compressor Pressure Ratio                = ',F12.4)
105 FORMAT('Compressor Efficiency                    = ',F12.4)
106 FORMAT('Turbine Efficiency                       = ',F12.4)
107 FORMAT('Initial Temperature Guess            (K) = ',F12.4)
108 FORMAT('Max Error for Enthalpy Iteration         = ',F12.4)
109 FORMAT('Temp. Increment for Iteration            = ',F12.4)
110 FORMAT('Timestep for NO Calc                     = ',F12.4)
111 FORMAT('Number of Combustion Regions             = ',I7)
112 FORMAT('Combustion Fraction in Region ',I2,'          = ',F12.4)
113 FORMAT('Diameter of Region ',I2,'                (m) = ',F12.4)
114 FORMAT('Length of Region ',I2,'                  (m) = ',F12.4)
115 FORMAT('Gas Velocity in Region ',I2,'          (m/s) = ',F12.4)
117 FORMAT(//'***KOMBUST OUTPUT***'//)
118 FORMAT('Emissivity of liner                      = ',F12.4)
119 FORMAT('Emissivity of casing                     = ',F12.4)
150 FORMAT('Fuel/air Ratio                           = ',F12.4)
151 FORMAT('T3                                   (C) = ',F12.4)
152 FORMAT('T4                                   (C) = ',F12.4)
153 FORMAT('T5                                   (C) = ',F12.4)
154 FORMAT('T5-T3                                (C) = ',F12.4)
155 FORMAT('Actual NOx concentration, wet      (ppmv) = ',F12.4)
156 FORMAT('Liner wall thickness of region ',I2,'      (m) = ',F12.4)
157 FORMAT('Thermal conductivity of liner    (W/m*K) = ',F12.4)
158 FORMAT('Hydrogen content of fuel        (%-mass) = ',F12.4)
159 FORMAT('Annulus air gap                      (m) = ',F12.4)
160 FORMAT('Max Error for Temp. Iteration            = ',F12.4)
161 FORMAT('Casing Diameter                      (m) = ',F12.4)
162 FORMAT('T5-T1                                (C) = ',F12.4)
163 FORMAT('Actual NOx concentration, dry      (ppmv) = ',F12.4)
164 FORMAT('NOx concentration @ 15% O2, wet    (ppmv) = ',F12.4)
165 FORMAT('NOx concentration @ 15% O2, dry    (ppmv) = ',F12.4)
200 FORMAT('Temperature of region ',I2,'             (K) = ',F12.4)

    return
    end
```

OUTPUT FILE

```
Equivalence Ratio                          =       0.5000
Ambient Temperature                  (C) =      25.0000
Ambient Pressure                   (kPa) =     101.3250
Relative Humidity                    (%) =       0.5000
Compressor Pressure Ratio                =      11.6600
Compressor Efficiency                    =       0.8370
Turbine Efficiency                       =       0.8500
Initial Temperature Guess            (K) =    2000.0000
Temp. Increment for Iteration            =       0.1000
Timestep for NO Calc                     =       0.0001
Number of Combustion Regions             =       5
Combustion Fraction in Region  1         =       1.0000
Combustion Fraction in Region  2         =       0.0000
Combustion Fraction in Region  3         =       0.0000
Combustion Fraction in Region  4         =       0.0000
Combustion Fraction in Region  5         =       0.0000
Diameter of Region  1                (m) =       0.0860
Diameter of Region  2                (m) =       0.0860
Diameter of Region  3                (m) =       0.1650
Diameter of Region  4                (m) =       0.1650
Diameter of Region  5                (m) =       0.1650
Length of Region  1                  (m) =       0.1300
Length of Region  2                  (m) =       0.1300
Length of Region  3                  (m) =       0.1000
Length of Region  4                  (m) =       0.1000
Length of Region  5                  (m) =       0.0869
Liner wall thickness of region  1    (m) =       0.0012
Liner wall thickness of region  2    (m) =       0.0012
Liner wall thickness of region  3    (m) =       0.0012
Liner wall thickness of region  4    (m) =       0.0012
Liner wall thickness of region  5    (m) =       0.0012
Gas Velocity in Region  1          (m/s) =      35.0000
Gas Velocity in Region  2          (m/s) =      35.0000
Gas Velocity in Region  3          (m/s) =      12.0000
Gas Velocity in Region  4          (m/s) =      12.0000
Gas Velocity in Region  5          (m/s) =      12.0000
Emissivity of liner                      =       0.7000
Emissivity of casing                     =       0.4000
Thermal conductivity of liner    (W/m*K) =      26.0000
Hydrogen content of fuel        (%-mass) =       8.3300
Annulus air gap                      (m) =       0.0300
Casing Diameter                      (m) =       1.0000


***KOMBUST OUTPUT***


Fuel/air Ratio                           =       0.0291
T3                                   (C) =     387.3760
T4                                   (C) =    1004.0500
T5                                   (C) =     751.3500
T5-T3                                (C) =     363.9740
T5-T1                                (C) =     726.3500
Actual NOx concentration, wet     (ppmv) =       1.0263
Actual NOx concentration, dry     (ppmv) =       1.0718
NOx concentration @ 15% O2, wet   (ppmv) =       0.5124
NOx concentration @ 15% O2, dry   (ppmv) =       0.6327
Temperature of region  1             (K) =    1770.6000
Temperature of region  2             (K) =    1770.6000
Temperature of region  3             (K) =    1770.6000
Temperature of region  4             (K) =    1770.6000
Temperature of region  5             (K) =    1770.6000
```